APPROVED UGC CARE

ISSN - 2348 - 2397

SHODH SARITA

JOURNAL OF ARTS, HUMANITIES AND SOCIAL SCIENCES

AN INTERNATIONAL MULTIDISCIPILANARY QUARTERLY BILINGUAL
PEER REVIEWED REFERED RESEARCH JOURNAL

Certificate of Publication

Jasmeet Kaur
Dept. of Economics
Govt. MRPD College, Talwara

TITLE OF RESEARCH PAPER

POVERTY AND HUMAN DEVELOPMENT : AN INTER COUNTRY ANALYSIS

This is certified that your research paper will be published in
Shodh Sarita, Volume 6 Issue 24 October to December 2019

Date : 17-09-2019

SHODH SARITA
Editor in Chief

CHIEF EDITORIAL OFFICE

448 /119/76, KALYANPURI THAKURGANJ, CHOWK, LUCKNOW -226003 U.P.,
Cell.: 09415578129, 09415141368, 09161456922 | E-mail : dr.vinaysharma123@gmail.com
Website : http://www.seresearchfoundation.in | http://www.seresearchfoundation.in/shodhsarita

ISSN - 2348-2397
APPROVED UGC CARE

SHODH SARITA

SHODH SARITA
Vol. 6, Issue 24, October-December, 2019
Page Nos. 258-263

AN INTERNATIONAL BILINGUAL PEER REVIEWED REFEREED RESEARCH JOURNAL

POVERTY AND HUMAN DEVELOPMENT : AN INTER COUNTRY ANALYSIS

Jasmeet Kaur*

ABSTRACT

The aim of the present study is to compute HPI 2010 and to analyse the position of various countries on the basis of their HDI and HPI. The HDI shows a country's achievements in human capabilities whereas the HPI examines human development from the angle of deprivation. The study shows that positions of various countries are different in terms of both HPI and HDI. Findings show that poverty may be defined in a better manner by HPI which is based on the lack of access to basic services such as health and education rather than by the HDI which is based on human capabilities and achievement of basic services.

Keywords : Human Development Index (HDI), Human Poverty Index (HPI), Depreviation Indicators, Ranking, Inter Country Analysis

INTRODUCTION

Poverty is not a self-defining concept. Experts and academics have suggested many definitions over time. Poverty could be lack of command over commodities in general (Watts 1968) alternatively it could be lack of command over some basic goods (e.g. food and housing) Sen 1985 agreed that poverty is lack of "capabilities" to function in a given society.

The United Nations High Commission for Refugees (UNHCR) defines "poverty" as human condition characterized by the sustained or chronic deprivation of resources, capabilities choices, security and power necessary for an adequate standard of living and civil, cultural, economic, political as well as social rights (UNHCR 2004) Thus poverty can be described as the state of being without the necessities of daily living often associated with need hardship and lack of resources across a wide range of circumstances.

United Nations thought its Human development Reports since 1990 have brought into focus that the objective of development is to increase the capabilities of people to lead full productive and satisfying what is of basic concern is the ability of people to lead a long and healthy life, to have access to knowledge and sufficient income to buy adequate amounts of food, clothing, shelters and other basic amenities. Human development reports have identified three areas of social concern via education health and material wellbeing. Adult literacy rate for education, life expectancy at birth for health and per capita income for material well being are the indicators used in arriving at the deprivation of the masses.

These HDR's have advocated the use of the HDI (Human Development Index) to measure a country's achievements in human capabilities. The parameters constituting HDI are life expectancy at birth adult literacy rate and the per capita gross domestic product. While the Human Poverty Index (HPI) in human development report (1997) was an attempt to examine human development from the angle of deprivation. The aim of the present study is to compute the Human Poverty Index (HPI) for which Secondary data were needed. Various publication of World Bank, WHO and UNDP like Core Health Indicators, Human development indicators, world

*Lecturer, MRPD Government College, Talwara

development Indicators were consulted. Efforts were made to list maximum number of variables on Education, Health, Sanitation, Nutrition and Economic dimensions for maximum number of countries. The analysis was carried 110 countries in the year 2010 as per availability of data. The aim of the present study is to compute the Human Poverty Index (HPI) for the year 2010. The overall objective of the study is to analyze the position of various countries on the basis of HDI and HPI in the light of the experience of different countries in the past decade.

METHODOLOGY

A simple technique of ratio, percentages and ranking along with tabular analysis were applied to analyze the data for achieving desired objectives.

HUMAN POVERTY INDEX

For constructing the HPI, deprivation in health, knowledge and economic dimensions have been calculated on the basis of different variables.

The under mentioned 9 variables were used in the study for analysis and construction of HPI for the year 2010. These variables are

1. Adult mortality rate (per thousand population)
2. Infant mortality rate (per thousand live births)
3. Adult illiteracy rate (percent)
4. Non enrollment ratio (percent)
5. Population without sustainable access to improved drinking water (percent)
6. Population without sustainable access to improved sanitation (percent)
7. One year-olds not immunized with MCV.
8. One year olds not immunized with DPT
9. Rate of unemployment (percent of labour force)

Longevity Deprivation (P_1): Longevity Deprivation (P_1) has been captured by using infant mortality rate and Adult mortality rate has been calculated as

$$P_1 = \frac{(IMR + Adult\ Mortality\ Rate)}{2}$$

Knowledge Deprivation (P_2): Knowledge or educational deprivation (P_2) has been calculated by using illiteracy rate and non-enrollment ratio, Thus, P_2 has been calculated by giving 35% weight age to illiteracy rate and 65% weight age has been given to combined non enrollment in education. The formula for calculating (P_2) is as follows:

P_2 = (illiteracy rate x 0.35) + (non-enrollment ratio x 0.65)

Economic Deprivation (P_3): Economic Deprivation (P_3) has been calculated by using the following indicators :

- Proportion of population without sustainable access to improved drinking water (P_{31})
- Proportion of population without access to improved sanitation (P_{32})
- One year olds not immunized with MCV(P_{33})
- One year olds not immunized with DPT(P_{34})
- Unemployment Rate (P_{35})

$$P_3 = \frac{1}{5} \times \sum_{i=1}^{5} P_{3i}$$

In order to construct Human poverty index (HPI) all the three deprivations viz: (P_1) (P_2) and (P_3) were given equal weight age. Thus, HPI was constructed by using UNDP's formula.

$$HPI_j = \left[\frac{1}{3} \sum_{i=0}^{3} P_i \right]^{1/3}$$

Where HPI is for the jth country and P_i goes from 1 to 3 refers to the deprivations in the three above identified dimensions.

The ranking of HDI and HPI of 101 countries for the year 2010 is shown in Table No.1. Table shows that Canada, Iceland, Spain, Italy, and Luxemburg were the top performers in HDI but their ranking in HPI was 4th, 1st, 51st, 3rd, 16th respectively. Worst performers in HDI were Congo, Nigeria, Mozambique, Burkina Faso, and Chad but their ranking in HPI was 83rd, 99th, 96th, 91st and 101st respectively.

Table No-1, Ranking of Countries (2010), Human Poverty Index (HPI) & Human Development Index (HDI)

Countries	HPI	Rank	HDI	Rank
Albania	8.357245	32	0.746	31
Algeria	8.745722	34	0.71	46
Argentina	4.953798	8	0.805	16
Armenia	8.144901	30	0.722	40
Azerbaijan	14.84789	61	0.734	35
Bahamas	14.0208	59	0.79	18
Bangladesh	15.5494	64	0.508	76
Belarus	7.061289	19	0.785	20
Benin	25.50469	90	0.432	89
Bhutan	15.62454	65	0.525	72
Bolivia	16.27991	67	0.668	54
Botswana	15.78667	66	0.663	56
Brazil	7.266654	21	0.726	39
Bulgaria	6.64285	17	0.778	23
Burkina Faso	25.52954	91	0.334	98
Burundi	19.17287	74	0.348	95
Cameroon	20.83568	81	0.488	78
Canada	4.08518	4	0.909	1
Cape Verde	10.5565	50	0.581	66
Chad	38.12801	101	0.336	97
Chile	4.994618	9	0.813	13
China	9.214759	40	0.689	49
Colombia	9.565861	42	0.714	44
Cambodia	18.46634	72	0.532	71
Comoros	18.663	73	0.426	90
Congo	21.5763	83	0.295	101
Costa Rica	8.2304	31	0.768	28
Croatia	5.624772	11	0.804	17
Cuba	4.22707	5	0.775	25
Cyprus	4.262362	6	0.849	8
Czech Republic	5.847524	14	0.871	6
Egypt	10.1975	48	0.663	55
Ecuador	8.793067	36	0.719	42
Estonia	5.7204	13	0.839	10
Ethiopia	30.42404	98	0.387	94
Georgia	8.141249	29	0.735	34
Ghana	19.19531	76	0.54	68
Greece	3.156311	2	0.866	7
Honduras	9.801395	45	0.629	59
Hungary	5.571451	10	0.829	11
Iceland	2.992296	1	0.901	2

Indonesia	18.1312	71	0.62	60
Italy	3.54004	3	0.881	4
Jamaica	8.81881	37	0.721	41
Kazakhstan	8.94427	38	0.744	32
Kenya	22.47666	85	0.511	75
Kyrgyzstan	16.8595	68	0.615	61
L P Demo.	19.84182	77	0.534	69
Latvia	7.365898	22	0.805	15
Lebanon	7.513547	25	0.743	33
Lesotho	27.06514	93	0.452	87
Libya	5.9385	15	0.773	26
Lithuania	8.717858	33	0.81	14
Luxembourg	6.461976	16	0.875	5
Madagascar	26.7087	92	0.484	79
Malawi	17.61461	70	0.413	92
Malaysia	8.051007	28	0.763	29
Maldives	6.654912	18	0.683	51
Mali	29.68444	95	0.344	96
Malta	8.755523	35	0.844	9
Mauritania	32.67895	100	0.464	83
Mauritius	8.039092	27	0.732	37
Mexico	7.437881	24	0.77	27
Morocco	15.5383	63	0.586	65
Mozambique	29.74417	96	0.318	99
Myanmar	13.81613	58	0.49	77
Namibia	20.52268	79	0.604	63
Nepal	19.17405	75	0.458	85
Niger	32.67124	99	0.298	100
Nigeria	30.3468	97	0.462	84
Nicaragua	12.65598	56	0.593	64
Oman	7.5886	26	0.728	38
Pakistan	20.8152	80	0.512	74
Paraguay	11.53668	53	0.668	52
Peru	9.383837	41	0.733	36
Philippines	12.81581	57	0.649	57
Qatar	10.19609	47	0.827	12
Romania	7.192639	20	0.783	21
Russian Republic	9.604824	43	0.782	22
Rwanda	15.0259	62	0.425	91
Salvador	12.03643	55	0.668	53
Samoa	10.31846	49	0.699	48
Sao Tome Principe	14.58476	60	0.522	73
Saudi Arabia	5.633166	12	0.777	24

Senegal	21.5493	82	0.47	80
Spain	10.637	51	0.884	3
Sri Lanka	10.12249	46	0.705	47
Sudan	25.361	89	0.411	93
Swaziland	21.58344	84	0.532	70
Tanzania	23.44864	87	0.466	82
Thailand	11.718	54	0.686	50
Togo	27.42311	94	0.452	86
Trinidad And Tobago	17.40414	69	0.752	30
Tunisia	11.04337	52	0.71	45
Turkey	7.409881	23	0.715	43
Uganda	22.76719	86	0.45	88
Uruguay	4.799927	7	0.785	19
Uzbekistan	8.955824	39	0.644	58
Vietnam	9.748446	44	0.611	62
Yemen	23.51983	88	0.466	81

Source: UNDP, Human Development Report

Iceland, Greece, Italy, Canada, Cuba were the best performing countries in terms of HPI but their ranking in HDI was 2nd, 7th, 4th, 1st and 25th respectively. On the other hand the worst performers in terms of HPI were Chad, Mauritania, Niger, Ethiopia and Nigeria, but their ranking in HDI was 97th, 83rd, 100th, 94th, 84th, respectively.

It is further found that there were 54 countries where rank improved and in 46 countries ranks deteriorated but Philippines was the only country where the rank remained the same.

Of the 54 countries, Malawi, Maldives, Rwanda, and Burundi were the countries where ranks improved by more than 20 points. The ranks improved between 10 to 20 points in Algeria, Armenia, Bangladesh, Brazil, Cuba, Honduras, Mauritius, Myanmar, Nepal, Sao Tome Principe, Saudi Arabia, Uruguay, Uzbekistan, Vietnam, Oman, Libya, Cape Verde, Comoros and Congo. There were 13 countries where ranks improved by 5 to 9 points namely Argentina, Bhutan, Bulgaria, Burkina Faso, China, Croatia, Ecuador, Georgia, Greece, Lebanon, Nicaragua and Egypt. Ranks improved by less than 5 points in Belarus, Chile, Colombia, Cyprus, Hungry, Italy, Iceland, Jamaica, Malaysia, Mali, Mexico, Morocco, Mozambique, Niger, Romania, Sri Lanka Uganda and Sudan.

Of the 46 countries where ranks deteriorated by more than 20 points were Azerbaijan, Bahamas, Malta, Qatar, Russia, Spain, Trinidad & Tobago. Ranks improved by 10 to 20 points in Bolivia, Botswana, India, Indonesia, Kenya, Lithuania, Luxembourg, Mauritania, Namibia, Nigeria, Swaziland and Madagascar. Czech Republic, Ghana, Kazakhstan, Kyrgyzstan, L.P. Demo, Latvia, Lesotho, Peru, Togo, Tunisia, Tanzania, Yemen and Pakistan were the 13 other countries where the ranks improved by 5 to 9 points. The remaining 14 countries where the ranks deteriorated by less than 5 points were Albania, Cambodia, Chad, Cameroon, EL Salvador, Estonia, Ethiopia, Paraguay, Samoa, Thailand, Canada, Benin, Costs Rica, Senegal.

Maximum improvement was found in Maldives by 33 points whereas minimum improvement was found in the case of Belarus, Hungary, Iceland, Italy, Malaysia, Mali, Romania and Sri Lanka by only one point.

On the other hand, the study found maximum deterioration in the ranks of Trinidad & Tobago and minimum deterioration in the case of Albania, Cambodia, Samoa and Benin.

CONCLUSION :

By using HPI as a measure vis-à-vis HDI, study found that in the year 2010 there was an improvement in the ranks of 53.46 percent countries, deterioration in the ranks of 45.54 percent countries and in 0.99 percent countries ranks remained the same. Maximum improvement was seen in the ranks of Maldives and maximum deterioration was seen in the case of Trinidad and Tobago.

The analysis based on poverty shows that HPI is an alternative for countries to measure poverty based on the indicators of human welfare that aid in understanding the impact of economic investments on human development and poverty alleviation so HPI gives more people centered indicators to measure the depth of depreviation across the countries.

References :

1. Alkire Sabina (2007) "Choosing Dimensions: The Capabilities Approach and Multi dimensional Poverty Chronic Poverty Research Centre W.P. No. 88.
2. Atkinson, A.B, "On Measurement of Poverty, " Econometrical, Vol 55 n4 794-764 July 1987
3. Brooks Thom (2006), "Is Global poverty a Crime". www.ssrn.com/abstract=943762
4. Deaton Angus (2003); Measuring Poverty in Growing World. NBER WP No. 9822. JE No.01 Princeton University.
5. Dessalien R.L. (2000) Review of Poverty Concepts and Indicators.
6. Sen Amartya (1985), Commodities and Capabilities. New York Oxford University Press.
7. UNDP ,Human development Reports New York oxford University Press Various Issues.
8. UNDP International Human development Indicators http//hrd.UNDP.org
9. WHO Statistical Information Systems (WHOSIS), Case Health Indicators http://www.who.int/whosis/

International Journal of Advanced Engineering, Management and Science (IJAEMS)
Peer-Reviewed Journal
ISSN: 2454-1311 | Vol-9, Issue-8; Aug, 2023
Journal Home Page: https://ijaems.com/
Article DOI: https://dx.doi.org/10.22161/ijaems.98.6

Data Mining Framework for Network Intrusion Detection using Efficient Techniques

Inderjit Kaur[1], Dr. Pardeep Saini[2]

[1]Research Scholar, Sunrise University, Alwar, Rajasthan, India
[2]Professor, Sunrise University, Alwar, Rajasthan, India

Received: 06 Jul 2023; Received in revised form: 07 Aug 2023; Accepted: 20 Aug 2023; Available online: 26 Aug 2023

Abstract— *The implementation measures the classification accuracy on benchmark datasets after combining SIS and ANNs. In order to put a number on the gains made by using SIS as a strategic tool in data mining, extensive experiments and analyses are carried out. The predicted results of this investigation will have implications for both theoretical and applied settings. Predictive models in a wide variety of disciplines may benefit from the enhanced classification accuracy enabled by SIS inside ANNs. An invaluable resource for scholars and practitioners in the fields of AI and data mining, this study adds to the continuing conversation about how to maximize the efficacy of machine learning methods.*

Keywords— ***Data Mining, Techniques, SIS, ANNs***

I. INTRODUCTION

Data mining, which "mines" knowledge from data, has recently attracted attention from the information industry and society due to the availability of massive amounts of data and the need to turn it into meaningful information/knowledge. Market research, factory administration, basic research, and even customer retention might all benefit from this data. In order to glean even the most fundamental insights from massive datasets, data mining employs a set of fundamental algorithms. Statistics, machine learning, database systems, and pattern recognition are just few of the areas of study that are included within this multidisciplinary field. System security procedures must be built to prevent Organization access to resources/data, and because data mining enables data analysis applications, this is a need. Protecting applications and networks against intrusion in highly interconnected systems is the job of an intrusion detection system.

Password/biometric user authentication, avoiding programming errors like buffer overflow, and encrypting sensitive data on computers are all initial lines of defense. When systems get complex, intrusion prevention alone isn't enough to keep them safe. As the number of people with access to the internet grows, the number of cyber threats faced by businesses also grows.

II. LITERATURE REVIEW

Kumar et al. (2016) The neural network approach has also been shown for automatic tumor detection in liver CT scans. Because the input may include noise introduced during acquisition, the CT input image is first pre-processed using a Median Filter based on expert opinion. The next step involves using first-order statistics and the gray-level matrix to extract local and textural features. Pixels in the gathered data sets are used to determine whether they are associated with the liver or not using a neural network. Tumor boundary detection using an active contour model of the targeted region 32 is possible, and the study's findings are both effective and timely.

J. Peter Campbell (2020) To provide an introduction to contemporary techniques of machine learning, with a focus on selected machine-learning methodologies, best practice, and deep learning, and their application in medical research. The literature on artificial intelligence techniques in medicine, particularly ophthalmology, was searched extensively in PubMed.a summary of machine learning for those who aren't familiar with the ins and outs of programming. However, there are still several obstacles that must be overcome before AI may be widely used in the medical field. This review article aims to provide an accessible overview of current machine learning

applications in healthcare for readers who are not experts in the field. The goal is to help readers understand the potential and challenges of AI in healthcare.

Jonathan Schmidt (2019) There have been many fascinating new additions to the materials science toolset in recent years, but machine learning ranks among the highest. Previous research has shown that this statistical toolkit may significantly speed up both basic and applied research. Studies focusing on applying machine learning to solid-state electronics have recently proliferated. Here, we survey and evaluate the most recent studies addressing this topic. Here, we lay out the foundations of machine learning by introducing key concepts including algorithms, descriptors, and databases for the study of materials science. We proceed to detail further methods in which machine learning may be used to locate stable materials and predict their crystal structure. Here, we provide findings from studies investigating various strategies for using machine learning to supplant first principles in design, as well as quantitative relationships between structures and their attributes. Using examples from the fields of rational design and related applications, we investigate how active learning and surgical optimization may be used to improve the process. There are always major issues with the interpretability and physical understanding of machine learning models. For this reason, we discuss the different facets of interpretability and their importance in the study of materials. In conclusion, we provide solutions to a variety of computational materials science problems and suggest directions for further study.

Pita Jarupunphol (2022) In order to find the most reliable classification model for predicting dengue illness, this research investigates a wide variety of feature selection and classification combinations. Dengue fever prediction parameters based on association patterns were investigated. In order to get the most effective classification model, several feature selection procedures have been categorized and studied with the use of popular classifiers. Many models' measurements were compared graphically. The three-layer neural network model is the most effective. One hundred ReLu-enabled nodes make up each tier. Accuracy of 64.9%, F-measure of 71.8, accuracy of 65.7%, accuracy of 66.0%, and recall of 79.0% were achieved in the identification of five qualities. In addition to the Naive and information gain combination, the Naive and Relief neural network combination, and the Naive and FCBF combination are all competing machine learning approaches with fairly equivalent efficiency. However, if specific feature selection procedures are investigated, SVM is seen as the weaker model.

Saima Anwar Lashari (2018) In this research, we investigate how medical data is currently being categorized and where future prospects may lie by applying data mining techniques. It explains major modern approaches to classification that have been shown to significantly raise the bar for classification precision. Past research has provided literature on the subject of medical data classification through data mining techniques. Extensive research shows that data mining methods excel at the task of classification. This article evaluated and contrasted the current state of medical data classification. The study's findings suggested that the current system for classifying medical data had room for improvement. However, further research is needed to identify and eliminate the uncertainties associated with classification in order to increase precision.

III. DATA MINING ALGORITHM

Without a priori knowledge of the structure of the data points, clustering labels and distributes them to groups of similar objects. The instances of a cluster are unique, but its members are consistent. Organizationa's clustering techniques include the partition algorithm, the hierarchical algorithm, the grid algorithm, and the density algorithm.

Recursively separating cases, hierarchical methods produce clusters from the top down or the bottom up. The following may be further broken down into:

Clusters are initially items, according to agglomerative hierarchical clustering. Once a suitable cluster architecture has been reached, more clusters are fused.

Distinctive hierarchical clustering - Initially, all data points are assigned to a single cluster. After then, a cluster is divided into even smaller clusters. This process is repeated until the cluster is properly structured.

KDD99 DATASET

Third International Competition for Knowledge Discovery and Data Mining Tools produced the data mining technique known as the KDD99 data detection data set. A data set may be thought of as a collection of inferred characteristics of a network link. When it comes to intrusion detection datasets for data mining, the KDD99 IDS dataset has been widely used. Connection records for each link in the Annie George network are among the 42 primary features that make up the KDD99 dataset benchmark.

The KDD 99 is based on five million logs representing seven weeks of network activity, extracted from four gigabytes (GB) of compressed TCP binary dump data. Two million connection records were gathered from two weeks of test data. Using three servers housing computers belonging to the victims, the network mimicked a military

network, revealing several attacks and routine network activity.

There are a total of 65 features in the training and testing data sets, with 24 types of assaults used in training and 14 in testing. Here are a few examples of names for attributes:

- Duration: continuous,
- protocol_type: symbolic,
- Service: symbolic,
- Flag: symbolic,
- src_bytes: continuous,
- dst_bytes: continuous,
- Land: symbolic,
- wrong_fragment: continuous,
- Urgent: continuous,
- Hot: continuous,
- num_failed_logins:continuous,
- logged_in: symbolic,

I Bayes (Nb)

In the simplest type of Bayesian network, I Bayes (NB), all characteristics are treated as unrelated to the value of the class variable. Conditional autonomy describes this situation. In practice, conditional independence almost never holds. Adding the ability to represent attribute dependency is a simple method for expanding Bayes beyond its naive restrictions.

The class node in an Augmented I Bay expands the original I Bay by pointing out direct nodes with links between attribute nodes. I Bayes classification does this by assuming conditional independence to drastically reduce the number of modeling parameters.

$PX|Y$, from original to just 2n

$$PX|Y^{22nl}$$

In real-world settings, including as text categorization, medical diagnosis, and system performance monitoring, I Bayes has been shown to be useful. It works well when there are interdependencies between features because... The quality of the fit to a probability distribution (the suitability of the independence assumption) is unrelated to the optimality of a zero-one loss (classification error). Certain deterministic or low-entropy dependencies result in strong performance on I Bayes, as shown by the effect of distribution entropy on classification error. As entropy decreases toward zero, the I Bayes error disappears. NB is easy to understand and compute.

$$argmax\left(p(c_i)\prod_{j=1}^{n}p(a_j|c_i)\right)$$

NB classifies I by selecting

Random Tree

The decision-making bodies in the random decision tree classification are selected at random. When classifying a test instance, the posterior probability is calculated as the sum of the weighted probability outputs of the individual trees. Generating a random tree has less memory requirements and reduces training time. There are two primary settings to adjust in this ensemble method:

(i) height h of each random tree, and

(ii) number N of base classifiers.

Database analysis, computer science search methods, and even biological models (evolutionary family trees) all make use of random trees in some capacity. As the number of vertices increases indefinitely, the spectrable distributions of the neighboring matrices of the random trees converge on the line of deterministic probability measures, demonstrating a topology of weak convergence.

The average height and average diameter of a random tree is the subject of a large body of literature. The height/diameter enumeration dilemma holds true for both labelled and unlabeled trees, with the anticipated height of a randomly labelled rooted tree being 1 2n. There is a large but scattered body of work on exact/asymptotic results for various models, and many other random tree models have emerged to meet the needs of certain applications. Deep searching in a particular random treeline pattern is reflected here: the "uniform ordered trees" combinatorial model is the model CBP(n) with a shifted geometric (1/2) offspring distribution. When you build on n nodes, you get a random Tn tree. It is easy to calculate the center of the star graph t with vertex 1.

Neural Network

In mathematics and computers, an Artificial Neural Network (ANN), often known as a "Neural Network" (NN), is a model inspired by biological NNs. Information is processed utilizing a network of artificial neurons and a connectionist approach to computing. During the training phase, an ANN adapts its structure in response to information from the network and the outside world. A NN is a widely dispersed, massively parallel processor with easy access to stored accumulated wisdom. In two aspects, it resembles a brain:

1. One acquires information by way of a networked learning procedure.

2. Synaptic weight information is stored as intensities of connections between neurons.

An algorithm for learning describes the method used to carry out the learning process. Neuro-computers (NNs) are a kind of a distributed parallel processor also known as a neuro-network or a connection network.

Advantages:

- In contrast to linear programs, neural networks are able to.
- When an element of a NN fails, the network as a whole keeps running because to its parallel design.
- It is not necessary to retrain a neural network since it is self-learning.
- It's adaptable enough to use in any scenario.
- Its implementation poses no difficulties.

Disadvantages:

- NN needs training to operate.
- Since NN architecture varies from that of microprocessors, the latter needs to be modeled after the former.
- Significant time for processing is required for rganiz.

IV. INVESTIGATION OF FEATURE SELECTION TECHNIQUES FOR INTRUSION DETECTION SYSTEM

One common method for streamlining businesses is called Feature Selection (FS). It improves learning performance (higher classification accuracy), reduces computational costs, and enhances model interpretability by selecting a small subset of relevant features from the original, based on predefined relevance evaluation criteria. Based on whether or not a training set is labeled, FS algorithms are categorized as supervised, unattended, or semi-supervised. FS is a method for identifying, within a collection of data, the subset of features that is optimal for processing according to a certain set of criteria. The method through which an FS may to find a subset ${}^{A}opt^{a}1,opt^{a}2,opt^{\cdots,a}m,opt_{\text{of A,which guarantees}}$ accomplishment of a processing goal by reducing a defined FS criterion ${}_{JfeatureAfeature\_subset}$. Optimal FS solutions are not need to be unique. The faster computation speed and more accurate predictions are made possible by using fewer characteristics in the learning process. Filters and wrappers are two types of FS procedures. First, there is agnostic classification, which does not include any specific methods of categorization. Instead, the wrappers evaluate the quality of a set of features and, from a statistical and computational standpoint, create an efficient filter based on the performance of a classifier type. The relevance of qualities is analyzed using filter techniques by looking just at the data's fundamental properties. The importance of each item is assigned a value, and those with low scores are omitted. Several FS methods are used in this data gathering process. accuracy values depend on the base rates of different classes, therefore in practice, the percentage of accuracy is not preferred for classification. The accuracy of a predictor may be evaluated by calculating its ROC or F-Measure value. Feature ratings evaluate the importance of an individual trait while disregarding the effects of other traits. The output functions of classifiers or statistical methods provide the basis for many ranking systems.

IDS has the potential to mitigate or prevent attacks in the event of updated signatures or improved attack recognition/response capabilities. Intruder detection systems are now distributed real-time component networks rather than batch-oriented monolithic systems. Monolithic IDS either combines all these features into a single system or splits them out into several procedures and applications.

Feature Selection Techniques For Ids

FS is an essential and popular tool for IDS data pre-processing. It has direct repercussions on IDS because of the decreased functionality and the elimination of irrelevant/redundant/noisy data. Many experts recommend using wrapper, filter, or hybrid methods for feature detection in feature selection. In order to evaluate the features' (or feature set's) quality, the wrapper method employs a learning algorithm. The Filter method relies on the central characteristics of the training data to evaluate the relevance of features and feature sets using objective metrics like distance, correlation, and consistency rather than any machine learning methodology.

Feature Selection Based On Correlation (Cfs)

CFS is an efficient FS method, and it selects, using gene expression data, a set of properties that are important to some class. It often reduces the dimensionality of data by over 60% without sacrificing precision.

On the other hand, CFS is able to establish a link between features and classes, as well as features. CFS is a correlation-based rapid filter used in continuous/discrete circumstances. The CFS algorithm ranks a collection of criteria based on their worth or quality. CFS takes use of the best search by using a correlation measure to evaluate a subset's quality, with each feature's predictive power and inter-feature correlation taken into account.

Analysis Of Independent Components (Ica)

Since many ICA features are predetermined at the primary data processing component analysis (PCA) stage, the ICA approaches do not provide such feature selection opportunities. The only feature selection technique used in

ICA face recognition literature to yet to account for this is the percentage of variance (PoV).

Since the original ICA facial recognition architecture provides local features, we've also been working to determine which of these traits are most useful for identifying specific people. In the ICA method, we know nothing about the mixing matrix or the distribution of sources beyond what is gleaned from the data.

Information Gain (Ig)

Word IG measures the data we learn about a category from the presence/absence of a certain word in a text.

Let me be the class number. The IG of a word t must be defined as

$$IG(t) = -\sum_{i=l}^{m} p(c_i)\, logP(c_i) + P(t)\sum_{i=l}^{m} p(c_i|t) logP(c_i|t) + P(\check{t})\sum_{i=l}^{m} p(c_i|t) logP(c_i|t)$$

The error rate for the test set is substantially higher (13.5 percent) than it is for the training set (for which the stated functions constitute an IG filter). This second discovery suggests that a redundancy reduction approach, such a Markov blanket filter, is necessary for feature selection beyond a simple "relevance check."

This section discussed the feature selection strategies that were put to use in this investigation.

V. CONCLUSION

This research takes a look at how normal/abnormal traffic is currently classified using data mining methods and makes recommendations for improvement. The KDD 99 dataset was mined for UDP data streams, and from there a multi-class dataset was created to emphasize the many threats inherent to UDP data streams. Naive Bayes Algorithm, Random Tree, and NN were all shown to be accurate in classifying the dataset's signatures. The random tree-based methods were 99.88% accurate in their classifications. In this study, we compare PCA to the Fisher Score for dimensionality reduction. PCA is a data-minimization technique for discovering and articulating patterns in order to highlight similarities and differences. Fisher Score is a model-based statistical method that may be used to make distinctions. It's a quick and easy approach to evaluate your ability to distinguish between label and trait.

REFERENCES

[1] Kumar, SN, Lenin Fred, A, Lalitha Kumari, S, Anchalo Bensigerm S M 2016, „Feed Forward Neural Network Based Automatic Detection of Liver in Computer Tomography Images", 2 International Journal of Pharm Tech Research CODEN (USA): IJPRIF, ISSN: 0974-4304, ISSN(Online): 2455-9563, vol. 9, no. 5, pp. 231-239.

[2] J. Peter Campbell 2020," Introduction to Machine Learning, Neural Networks, and Deep Learning," Translational Vision Science & Technology February 2020, Vol.9, 14. doi: https://doi.org/10.1167/tvst.9.2.14

[3] Jonathan Schmidt 2019," Recent advances and applications of machine learning in solid-state materials science," npj Computational Materials volume 5, Article number: 83 (2019)

[4] Pita Jarupunphol 2022," dengue fever; data mining; classification; feature selection; ranking.

[5] Saima Anwar Lashari 2018," Application of Data Mining Techniques for Medical Data Classification: A Review," MATEC Web of Conferences 150, 06003 (2018) https://doi.org/10.1051/matecconf/201815006003 MUCET 2017

[6] Lemnaru C. (2012). Strategies for dealing with Real World Classification Problems, (Unpublished PhD thesis) Faculty of Computer Science and Automation, UniversitateaTechnica, Din Cluj-Napoca. Available at website: http://users.utcluj.ro/~cameliav/documents/TezaFinalLemnaru.pdf

[7] Newsom, I. (2015). Data Analysis II: Logistic Regression. Available at: http://web.pdx.edu/~newsomj/da2/ho_logistic.pdf

[8] Pradeep, K. R. & Naveen, N. C. (2017). A Collective Study of Machine Learning (ML)Algorithms with Big Data Analytics (BDA) for Healthcare Analytics (HcA). International Journal of Computer Trends and Technology (IJCTT) – Volume 47 Number 3, 2017. ISSN: 2231-2803, doi: 10.14445/22312803/IJCTT-V47P121, pp 149 – 155. Available from IJCTT website: http://www.ijcttjournal.org/2017/Volume47/number-3/IJCTT-V47P121.pdf

[9] R. Vijaya Kumar Reddy.et.al 2018," A Review on Classification Techniques in Machine Learning,"InternationalJonroual of Advance Research in Sciences and Engineering Volumn no.7

[10] Anu Sharma.et.al. 2017," Literature Review and Challenges of Data Mining Techniques for Social Network Analysis," Advances in Computational Sciences and Technology ISSN 0973-6107 Volume 10, Number 5 (2017) pp. 1337-1354

[11] Zain Anwar Ali 2018," Role of Machine Learning and Data Mining in Internet Security: Standing State with Future Directions," Review Article | Open Access Volume 2018 |Article ID 6383145 | https://doi.org/10.1155/2018/6383145

[12] AJAY SHRESTHA 2019," Review of Deep Learning Algorithms and Architectures," Department of Computer Science and Engineering, University of Bridgeport, Bridgeport, CT 06604, USA

[13] statistical learning theory; optimisation theory; financial econometrics; support vector machine; SVM; kernel methods. DOI: 10.1504/IJBIDM.2019.10019195

[14] Dharmender Kumar 2017," Classification Using ANN: A Review," International Journal of Computational Intelligence Research ISSN 0973-1873 Volume 13, Number 7 (2017), pp. 1811-1820

[15] Networks: A Review," (IJCSIS) International Journal of Computer Science and Information Security, Vol. 14, No. 7, July 2016

International Journal of Advanced Engineering, Management and Science (IJAEMS)
Peer-Reviewed Journal
ISSN: 2454-1311 | Vol-9, Issue-8; Aug, 2023
Journal Home Page: https://ijaems.com/
Article DOI: https://dx.doi.org/10.22161/ijaems.98.6

Data Mining Framework for Network Intrusion Detection using Efficient Techniques

Inderjit Kaur[1], Dr. Pardeep Saini[2]

[1]Research Scholar, Sunrise University, Alwar, Rajasthan, India
[2]Professor, Sunrise University, Alwar, Rajasthan, India

Received: 06 Jul 2023; Received in revised form: 07 Aug 2023; Accepted: 20 Aug 2023; Available online: 26 Aug 2023

Abstract— *The implementation measures the classification accuracy on benchmark datasets after combining SIS and ANNs. In order to put a number on the gains made by using SIS as a strategic tool in data mining, extensive experiments and analyses are carried out. The predicted results of this investigation will have implications for both theoretical and applied settings. Predictive models in a wide variety of disciplines may benefit from the enhanced classification accuracy enabled by SIS inside ANNs. An invaluable resource for scholars and practitioners in the fields of AI and data mining, this study adds to the continuing conversation about how to maximize the efficacy of machine learning methods.*

Keywords— ***Data Mining, Techniques, SIS, ANNs***

I. INTRODUCTION

Data mining, which "mines" knowledge from data, has recently attracted attention from the information industry and society due to the availability of massive amounts of data and the need to turn it into meaningful information/knowledge. Market research, factory administration, basic research, and even customer retention might all benefit from this data. In order to glean even the most fundamental insights from massive datasets, data mining employs a set of fundamental algorithms. Statistics, machine learning, database systems, and pattern recognition are just few of the areas of study that are included within this multidisciplinary field. System security procedures must be built to prevent Organization access to resources/data, and because data mining enables data analysis applications, this is a need. Protecting applications and networks against intrusion in highly interconnected systems is the job of an intrusion detection system.

Password/biometric user authentication, avoiding programming errors like buffer overflow, and encrypting sensitive data on computers are all initial lines of defense. When systems get complex, intrusion prevention alone isn't enough to keep them safe. As the number of people with access to the internet grows, the number of cyber threats faced by businesses also grows.

II. LITERATURE REVIEW

Kumar et al. (2016) The neural network approach has also been shown for automatic tumor detection in liver CT scans. Because the input may include noise introduced during acquisition, the CT input image is first pre-processed using a Median Filter based on expert opinion. The next step involves using first-order statistics and the gray-level matrix to extract local and textural features. Pixels in the gathered data sets are used to determine whether they are associated with the liver or not using a neural network. Tumor boundary detection using an active contour model of the targeted region 32 is possible, and the study's findings are both effective and timely.

J. Peter Campbell (2020) To provide an introduction to contemporary techniques of machine learning, with a focus on selected machine-learning methodologies, best practice, and deep learning, and their application in medical research. The literature on artificial intelligence techniques in medicine, particularly ophthalmology, was searched extensively in PubMed.a summary of machine learning for those who aren't familiar with the ins and outs of programming. However, there are still several obstacles that must be overcome before AI may be widely used in the medical field. This review article aims to provide an accessible overview of current machine learning

applications in healthcare for readers who are not experts in the field. The goal is to help readers understand the potential and challenges of AI in healthcare.

Jonathan Schmidt (2019) There have been many fascinating new additions to the materials science toolset in recent years, but machine learning ranks among the highest. Previous research has shown that this statistical toolkit may significantly speed up both basic and applied research. Studies focusing on applying machine learning to solid-state electronics have recently proliferated. Here, we survey and evaluate the most recent studies addressing this topic. Here, we lay out the foundations of machine learning by introducing key concepts including algorithms, descriptors, and databases for the study of materials science. We proceed to detail further methods in which machine learning may be used to locate stable materials and predict their crystal structure. Here, we provide findings from studies investigating various strategies for using machine learning to supplant first principles in design, as well as quantitative relationships between structures and their attributes. Using examples from the fields of rational design and related applications, we investigate how active learning and surgical optimization may be used to improve the process. There are always major issues with the interpretability and physical understanding of machine learning models. For this reason, we discuss the different facets of interpretability and their importance in the study of materials. In conclusion, we provide solutions to a variety of computational materials science problems and suggest directions for further study.

Pita Jarupunphol (2022) In order to find the most reliable classification model for predicting dengue illness, this research investigates a wide variety of feature selection and classification combinations. Dengue fever prediction parameters based on association patterns were investigated. In order to get the most effective classification model, several feature selection procedures have been categorized and studied with the use of popular classifiers. Many models' measurements were compared graphically. The three-layer neural network model is the most effective. One hundred ReLu-enabled nodes make up each tier. Accuracy of 64.9%, F-measure of 71.8, accuracy of 65.7%, accuracy of 66.0%, and recall of 79.0% were achieved in the identification of five qualities. In addition to the Naive and information gain combination, the Naive and Relief neural network combination, and the Naive and FCBF combination are all competing machine learning approaches with fairly equivalent efficiency. However, if specific feature selection procedures are investigated, SVM is seen as the weaker model.

Saima Anwar Lashari (2018) In this research, we investigate how medical data is currently being categorized and where future prospects may lie by applying data mining techniques. It explains major modern approaches to classification that have been shown to significantly raise the bar for classification precision. Past research has provided literature on the subject of medical data classification through data mining techniques. Extensive research shows that data mining methods excel at the task of classification. This article evaluated and contrasted the current state of medical data classification. The study's findings suggested that the current system for classifying medical data had room for improvement. However, further research is needed to identify and eliminate the uncertainties associated with classification in order to increase precision.

III. DATA MINING ALGORITHM

Without a priori knowledge of the structure of the data points, clustering labels and distributes them to groups of similar objects. The instances of a cluster are unique, but its members are consistent. Organizationa's clustering techniques include the partition algorithm, the hierarchical algorithm, the grid algorithm, and the density algorithm.

Recursively separating cases, hierarchical methods produce clusters from the top down or the bottom up. The following may be further broken down into:

Clusters are initially items, according to agglomerative hierarchical clustering. Once a suitable cluster architecture has been reached, more clusters are fused.

Distinctive hierarchical clustering - Initially, all data points are assigned to a single cluster. After then, a cluster is divided into even smaller clusters. This process is repeated until the cluster is properly structured.

KDD99 DATASET

Third International Competition for Knowledge Discovery and Data Mining Tools produced the data mining technique known as the KDD99 data detection data set. A data set may be thought of as a collection of inferred characteristics of a network link. When it comes to intrusion detection datasets for data mining, the KDD99 IDS dataset has been widely used. Connection records for each link in the Annie George network are among the 42 primary features that make up the KDD99 dataset benchmark.

The KDD 99 is based on five million logs representing seven weeks of network activity, extracted from four gigabytes (GB) of compressed TCP binary dump data. Two million connection records were gathered from two weeks of test data. Using three servers housing computers belonging to the victims, the network mimicked a military

network, revealing several attacks and routine network activity.

There are a total of 65 features in the training and testing data sets, with 24 types of assaults used in training and 14 in testing. Here are a few examples of names for attributes:

- Duration: continuous,
- protocol_type: symbolic,
- Service: symbolic,
- Flag: symbolic,
- src_bytes: continuous,
- dst_bytes: continuous,
- Land: symbolic,
- wrong_fragment: continuous,
- Urgent: continuous,
- Hot: continuous,
- num_failed_logins:continuous,
- logged_in: symbolic,

I Bayes (Nb)

In the simplest type of Bayesian network, I Bayes (NB), all characteristics are treated as unrelated to the value of the class variable. Conditional autonomy describes this situation. In practice, conditional independence almost never holds. Adding the ability to represent attribute dependency is a simple method for expanding Bayes beyond its naive restrictions.

The class node in an Augmented I Bay expands the original I Bay by pointing out direct nodes with links between attribute nodes. I Bayes classification does this by assuming conditional independence to drastically reduce the number of modeling parameters.

$PX|Y$, from original to just 2n

$$PX|Y^{22nl}$$

In real-world settings, including as text categorization, medical diagnosis, and system performance monitoring, I Bayes has been shown to be useful. It works well when there are interdependencies between features because... The quality of the fit to a probability distribution (the suitability of the independence assumption) is unrelated to the optimality of a zero-one loss (classification error). Certain deterministic or low-entropy dependencies result in strong performance on I Bayes, as shown by the effect of distribution entropy on classification error. As entropy decreases toward zero, the I Bayes error disappears. NB is easy to understand and compute.

$$argmax\left(p(c_i)\prod_{j=1}^{n}p(a_j|c_i)\right)$$

NB classifies I by selecting

Random Tree

The decision-making bodies in the random decision tree classification are selected at random. When classifying a test instance, the posterior probability is calculated as the sum of the weighted probability outputs of the individual trees. Generating a random tree has less memory requirements and reduces training time. There are two primary settings to adjust in this ensemble method:

(i) height h of each random tree, and

(ii) number N of base classifiers.

Database analysis, computer science search methods, and even biological models (evolutionary family trees) all make use of random trees in some capacity. As the number of vertices increases indefinitely, the spectrable distributions of the neighboring matrices of the random trees converge on the line of deterministic probability measures, demonstrating a topology of weak convergence.

The average height and average diameter of a random tree is the subject of a large body of literature. The height/diameter enumeration dilemma holds true for both labelled and unlabeled trees, with the anticipated height of a randomly labelled rooted tree being 1 2n. There is a large but scattered body of work on exact/asymptotic results for various models, and many other random tree models have emerged to meet the needs of certain applications. Deep searching in a particular random treeline pattern is reflected here: the "uniform ordered trees" combinatorial model is the model CBP(n) with a shifted geometric (1/2) offspring distribution. When you build on n nodes, you get a random Tn tree. It is easy to calculate the center of the star graph t with vertex 1.

Neural Network

In mathematics and computers, an Artificial Neural Network (ANN), often known as a "Neural Network" (NN), is a model inspired by biological NNs. Information is processed utilizing a network of artificial neurons and a connectionist approach to computing. During the training phase, an ANN adapts its structure in response to information from the network and the outside world. A NN is a widely dispersed, massively parallel processor with easy access to stored accumulated wisdom. In two aspects, it resembles a brain:

1. One acquires information by way of a networked learning procedure.

2. Synaptic weight information is stored as intensities of connections between neurons.

An algorithm for learning describes the method used to carry out the learning process. Neuro-computers (NNs) are a kind of a distributed parallel processor also known as a neuro-network or a connection network.

Advantages:

- In contrast to linear programs, neural networks are able to.
- When an element of a NN fails, the network as a whole keeps running because to its parallel design.
- It is not necessary to retrain a neural network since it is self-learning.
- It's adaptable enough to use in any scenario.
- Its implementation poses no difficulties.

Disadvantages:

- NN needs training to operate.
- Since NN architecture varies from that of microprocessors, the latter needs to be modeled after the former.
- Significant time for processing is required for rganiz.

IV. INVESTIGATION OF FEATURE SELECTION TECHNIQUES FOR INTRUSION DETECTION SYSTEM

One common method for streamlining businesses is called Feature Selection (FS). It improves learning performance (higher classification accuracy), reduces computational costs, and enhances model interpretability by selecting a small subset of relevant features from the original, based on predefined relevance evaluation criteria. Based on whether or not a training set is labeled, FS algorithms are categorized as supervised, unattended, or semi-supervised. FS is a method for identifying, within a collection of data, the subset of features that is optimal for processing according to a certain set of criteria. The method through which an FS may to find a subset ${}^{A}opt^{a}1,opt^{a}2,opt^{\cdots,a}m,opt_{\text{of A,which guarantees}}$ accomplishment of a processing goal by reducing a defined FS criterion ${}_{JfeatureAfeature\_subset}$. Optimal FS solutions are not need to be unique. The faster computation speed and more accurate predictions are made possible by using fewer characteristics in the learning process. Filters and wrappers are two types of FS procedures. First, there is agnostic classification, which does not include any specific methods of categorization. Instead, the wrappers evaluate the quality of a set of features and, from a statistical and computational standpoint, create an efficient filter based on the performance of a classifier type. The relevance of qualities is analyzed using filter techniques by looking just at the data's fundamental properties. The importance of each item is assigned a value, and those with low scores are omitted. Several FS methods are used in this data gathering process. accuracy values depend on the base rates of different classes, therefore in practice, the percentage of accuracy is not preferred for classification. The accuracy of a predictor may be evaluated by calculating its ROC or F-Measure value. Feature ratings evaluate the importance of an individual trait while disregarding the effects of other traits. The output functions of classifiers or statistical methods provide the basis for many ranking systems.

IDS has the potential to mitigate or prevent attacks in the event of updated signatures or improved attack recognition/response capabilities. Intruder detection systems are now distributed real-time component networks rather than batch-oriented monolithic systems. Monolithic IDS either combines all these features into a single system or splits them out into several procedures and applications.

Feature Selection Techniques For Ids

FS is an essential and popular tool for IDS data pre-processing. It has direct repercussions on IDS because of the decreased functionality and the elimination of irrelevant/redundant/noisy data. Many experts recommend using wrapper, filter, or hybrid methods for feature detection in feature selection. In order to evaluate the features' (or feature set's) quality, the wrapper method employs a learning algorithm. The Filter method relies on the central characteristics of the training data to evaluate the relevance of features and feature sets using objective metrics like distance, correlation, and consistency rather than any machine learning methodology.

Feature Selection Based On Correlation (Cfs)

CFS is an efficient FS method, and it selects, using gene expression data, a set of properties that are important to some class. It often reduces the dimensionality of data by over 60% without sacrificing precision.

On the other hand, CFS is able to establish a link between features and classes, as well as features. CFS is a correlation-based rapid filter used in continuous/discrete circumstances. The CFS algorithm ranks a collection of criteria based on their worth or quality. CFS takes use of the best search by using a correlation measure to evaluate a subset's quality, with each feature's predictive power and inter-feature correlation taken into account.

Analysis Of Independent Components (Ica)

Since many ICA features are predetermined at the primary data processing component analysis (PCA) stage, the ICA approaches do not provide such feature selection opportunities. The only feature selection technique used in

ICA face recognition literature to yet to account for this is the percentage of variance (PoV).

Since the original ICA facial recognition architecture provides local features, we've also been working to determine which of these traits are most useful for identifying specific people. In the ICA method, we know nothing about the mixing matrix or the distribution of sources beyond what is gleaned from the data.

Information Gain (Ig)

Word IG measures the data we learn about a category from the presence/absence of a certain word in a text.

Let me be the class number. The IG of a word t must be defined as

$$IG(t) = -\sum_{i=l}^{m} p(c_i)\, logP(c_i) + P(t)\sum_{i=l}^{m} p(c_i|t) logP(c_i|t) + P(\check{t})\sum_{i=l}^{m} p(c_i|t) logP(c_i|t)$$

The error rate for the test set is substantially higher (13.5 percent) than it is for the training set (for which the stated functions constitute an IG filter). This second discovery suggests that a redundancy reduction approach, such a Markov blanket filter, is necessary for feature selection beyond a simple "relevance check."

This section discussed the feature selection strategies that were put to use in this investigation.

V. CONCLUSION

This research takes a look at how normal/abnormal traffic is currently classified using data mining methods and makes recommendations for improvement. The KDD 99 dataset was mined for UDP data streams, and from there a multi-class dataset was created to emphasize the many threats inherent to UDP data streams. Naive Bayes Algorithm, Random Tree, and NN were all shown to be accurate in classifying the dataset's signatures. The random tree-based methods were 99.88% accurate in their classifications. In this study, we compare PCA to the Fisher Score for dimensionality reduction. PCA is a data-minimization technique for discovering and articulating patterns in order to highlight similarities and differences. Fisher Score is a model-based statistical method that may be used to make distinctions. It's a quick and easy approach to evaluate your ability to distinguish between label and trait.

REFERENCES

[1] Kumar, SN, Lenin Fred, A, Lalitha Kumari, S, Anchalo Bensigerm S M 2016, „Feed Forward Neural Network Based Automatic Detection of Liver in Computer Tomography Images", 2 International Journal of Pharm Tech Research CODEN (USA): IJPRIF, ISSN: 0974-4304, ISSN(Online): 2455-9563, vol. 9, no. 5, pp. 231-239.

[2] J. Peter Campbell 2020," Introduction to Machine Learning, Neural Networks, and Deep Learning," Translational Vision Science & Technology February 2020, Vol.9, 14. doi: https://doi.org/10.1167/tvst.9.2.14

[3] Jonathan Schmidt 2019," Recent advances and applications of machine learning in solid-state materials science," npj Computational Materials volume 5, Article number: 83 (2019)

[4] Pita Jarupunphol 2022," dengue fever; data mining; classification; feature selection; ranking.

[5] Saima Anwar Lashari 2018," Application of Data Mining Techniques for Medical Data Classification: A Review," MATEC Web of Conferences 150, 06003 (2018) https://doi.org/10.1051/matecconf/201815006003 MUCET 2017

[6] Lemnaru C. (2012). Strategies for dealing with Real World Classification Problems, (Unpublished PhD thesis) Faculty of Computer Science and Automation, UniversitateaTechnica, Din Cluj-Napoca. Available at website: http://users.utcluj.ro/~cameliav/documents/TezaFinalLemnaru.pdf

[7] Newsom, I. (2015). Data Analysis II: Logistic Regression. Available at: http://web.pdx.edu/~newsomj/da2/ho_logistic.pdf

[8] Pradeep, K. R. & Naveen, N. C. (2017). A Collective Study of Machine Learning (ML)Algorithms with Big Data Analytics (BDA) for Healthcare Analytics (HcA). International Journal of Computer Trends and Technology (IJCTT) – Volume 47 Number 3, 2017. ISSN: 2231-2803, doi: 10.14445/22312803/IJCTT-V47P121, pp 149 – 155. Available from IJCTT website: http://www.ijcttjournal.org/2017/Volume47/number-3/IJCTT-V47P121.pdf

[9] R. Vijaya Kumar Reddy.et.al 2018," A Review on Classification Techniques in Machine Learning,"InternationalJonroual of Advance Research in Sciences and Engineering Volumn no.7

[10] Anu Sharma.et.al. 2017," Literature Review and Challenges of Data Mining Techniques for Social Network Analysis," Advances in Computational Sciences and Technology ISSN 0973-6107 Volume 10, Number 5 (2017) pp. 1337-1354

[11] Zain Anwar Ali 2018," Role of Machine Learning and Data Mining in Internet Security: Standing State with Future Directions," Review Article | Open Access Volume 2018 |Article ID 6383145 | https://doi.org/10.1155/2018/6383145

[12] AJAY SHRESTHA 2019," Review of Deep Learning Algorithms and Architectures," Department of Computer Science and Engineering, University of Bridgeport, Bridgeport, CT 06604, USA

[13] statistical learning theory; optimisation theory; financial econometrics; support vector machine; SVM; kernel methods. DOI: 10.1504/IJBIDM.2019.10019195

[14] Dharmender Kumar 2017," Classification Using ANN: A Review," International Journal of Computational Intelligence Research ISSN 0973-1873 Volume 13, Number 7 (2017), pp. 1811-1820

[15] Networks: A Review," (IJCSIS) International Journal of Computer Science and Information Security, Vol. 14, No. 7, July 2016

ISSN 2561-9594

ਜੁਲਾਈ-ਦਸੰਬਰ, 2019

ਪੰਜਾਬੀ ਕਲਮ

Punjabi Kalm

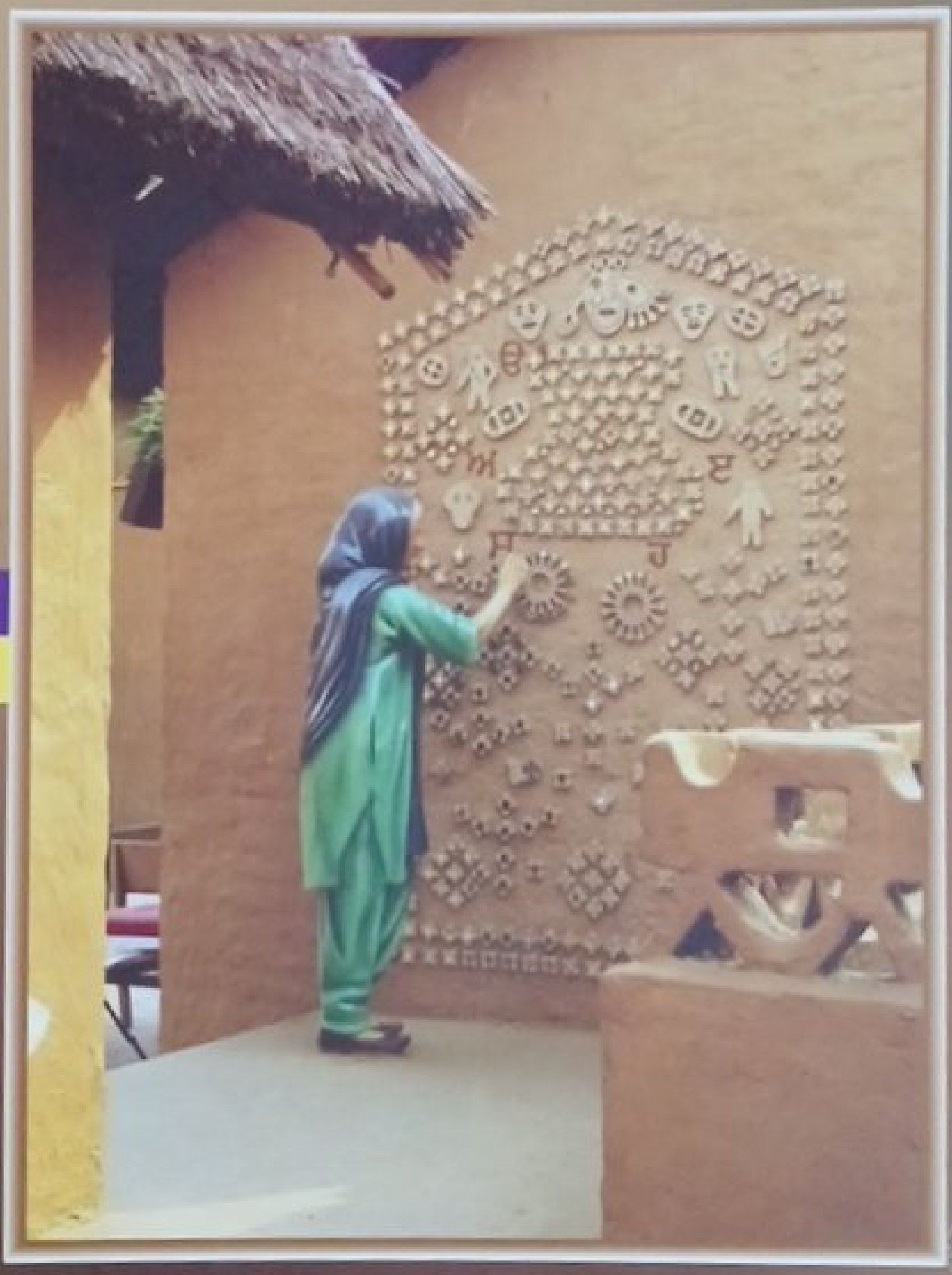

ਰੁਪਏ 75

ਡਾਲਰ 5

ਅੰਕ 2

ਪੰਜਾਬੀ ਬਿਜ਼ਨਸ ਪ੍ਰੋਫੈਸ਼ਨਲ ਐਸੋਸੀਏਸ਼ਨ ਕੈਨੇਡਾ ਦਾ ਸਾਹਿਤਕ ਮੈਗਜ਼ੀਨ

ਪੰਜਾਬੀ ਬਿਜ਼ਨਸ ਪ੍ਰੋਫੈਸ਼ਨਲ ਐਸੋਸੀਏਸ਼ਨ, ਕੈਨੇਡਾ ਦਾ

ਸਾਹਿਤਕ ਮੈਗਜ਼ੀਨ

ਪੰਜਾਬੀ ਕਲਮ
Punjabi Kalm

ਜੁਲਾਈ-ਦਸੰਬਰ, 2019 ISSN 2561-9594 ਅੰਕ : 2

— ਕੈਨੇਡੀਅਨ ਪਤਾ —

ASEEM PUBLICATION INC.
Punjabi Business Professional Association,
45 Ray Lawson Blvd. Brampton, On. LY 3L4, CANADA
e-mail:punjabikalm2018@gmail.com M. 0016474031299

—ਸ਼ਬਦ ਸੰਸ਼ੋਧਨ—
H.S. Computers, NABHA
98760-57400

ਤਰਤੀਬ

—ਵਿਸ਼ੇਸ਼ ਲੇਖ—

—ਕਹਾਣੀਆਂ—

—ਕਵਿਤਾਵਾਂ—

—ਅਲੋਚਨਾ ਨਿਬੰਧ—

—ਪੁਸਤਕ ਰੀਵਿਊ—

ਪੰਜਾਬੀ ਕਲਮ ਦੇ ਸੰਪਾਦਕ ਅਤੇ ਸਾਰੇ ਸਹਿਯੋਗੀ ਆਨਰੇਰੀ ਹਨ।
ਪੰਜਾਬੀ ਕਲਮ ਦਾ ਪ੍ਰਕਾਸ਼ਨ ਨਿਰੋਲ ਗੈਰ ਵਪਾਰਕ ਹੈ।

ਸਤਿ ਸ਼ਿਵ ਅਤੇ ਸੁੰਦਰ ਵਰਗੇ ਸਰੋਕਾਰਾਂ ਨੂੰ ਤਲਾਸ਼ਦਾ ਪਰਮਿੰਦਰ ਸੋਢੀ ਦਾ ਕਾਵਿ-ਸੰਗ੍ਰਹਿ

'ਇੱਕ ਚਿੜੀ ਤੇ ਮਹਾਂਨਗਰ'

—ਅਜੈ ਕੁਮਾਰ ਅਰਸ਼

ਆਧੁਨਿਕ ਪੰਜਾਬੀ ਕਵਿਤਾ ਵਿਸ਼ਵ ਪੱਧਰ ਦੇ ਸਾਹਿਤ ਦੀ ਹਾਣੀ ਬਣਦੀ ਵਿਭਿੰਨ ਸਰੋਕਾਰਾਂ ਨੂੰ ਆਪਣੇ ਕਲਾਵੇ ਵਿਚ ਸਮੇਟਦੀ ਸੰਦਲੀ ਪੈੜਾਂ ਪਾ ਰਹੀ ਹੈ। ਆਬਾਦੀ ਦੀ ਬਹੁਤਾਂਤ, ਆਰਥਿਕ ਸਹੂਲਤਾਂ ਦੀ ਘਾਟ ਤੇ ਕਾਣੀ-ਵੰਡ, ਉਪਜਾਊ ਜ਼ਮੀਨਾਂ ਦਾ ਘਟਣਾ ਤੇ ਗਰੀਬੀ-ਗਰੀਬਾਂ ਦਾ ਨਿਰੰਤਰ ਵਧਣਾ ਵਰਗੇ ਕਾਰਨਾਂ ਕਰਕੇ ਭਾਰਤ ਖਾਸ ਕਰਕੇ ਪੰਜਾਬ ਦੀ ਨੌਜਵਾਨ ਪੀੜ੍ਹੀ ਆਪਣੀ ਜੱਦੀ ਪੁਸ਼ਤੀ ਜਾਇਦਾਦ ਤੇ ਮਾਪਿਆਂ ਨੂੰ ਛੱਡ ਕੇ ਚੰਗੇਰੇ ਭਵਿੱਖ ਦੀ ਆਸ ਵਿਚ ਬਾਹਰਲੇ ਮੁਲਕਾਂ ਦੀ ਖ਼ਾਕ ਛਾਣ ਰਹੀ ਹੈ। ਇਹ ਭਟਕਣਾ ਕੋਈ ਅੱਜ ਦੀ ਨਹੀਂ ਸਗੋਂ ਸਦੀਆਂ ਪੁਰਾਣੀ ਹੈ। ਜਿੱਥੇ ਪਹਿਲਾਂ-ਪਹਿਲ ਅਨਪੜ੍ਹ, ਅੱਧਪੜ੍ਹੇ ਲੋਕ ਆਵਾਸ ਕਰਦੇ ਸਨ, ਉੱਥੇ ਰਾਜਨੀਤਿਕ, ਸਮਾਜਿਕ, ਧਾਰਮਿਕ ਤੇ ਖਾਸ ਕਰ ਆਰਥਿਕ ਹਾਲਤਾਂ ਦੇ ਮੱਦੇਨਜ਼ਰ ਅਜੋਕੇ ਸਮੇਂ ਵਿੱਚ ਪੜ੍ਹੇ-ਲਿਖੇ ਡਾਕਟਰ, ਪ੍ਰੋਫੈਸਰ, ਅਧਿਆਪਕ ਅਤੇ ਵਿਦਿਆਰਥੀ ਵੀ ਆਵਾਸ ਕਰਦੇ ਨਜ਼ਰ ਆ ਰਹੇ ਹਨ। ਇਹਨਾਂ ਪਰਵਾਸ ਕਰਨ ਵਾਲਿਆਂ ਵਿਚ ਕੇਵਲ ਪੈਸੇ ਦੀ ਚਾਹਤ ਹੀ ਨਹੀਂ ਸਗੋਂ ਆਪਣਾ ਜੀਵਨ ਪੱਧਰ ਉੱਚਾ ਚੁੱਕਣਾ ਤੇ ਆਪਣੇ ਮੁਲਕ ਨਾਲੋਂ ਵਧੇਰੇ ਚੰਗੇਰੀਆਂ ਸਹੂਲਤਾਂ ਨੂੰ ਪ੍ਰਾਪਤ ਕਰਨਾ ਵੀ ਆਵਾਸ ਕਰਨ ਦਾ ਇੱਕ ਕਾਰਨ ਹੈ। ਮੁੱਢਲੇ ਦੌਰ ਸਮੇਂ ਪੰਜਾਬੀਆਂ ਵਿਚ ਪਰਵਾਸ ਕਰਨ ਦੀ ਰੁੱਚੀ ਵਧੇਰੇ ਕਰਕੇ ਆਪਣੇ ਗੁਲਾਮ ਹਿੰਦੋਸਤਾਨ ਨੂੰ ਆਜ਼ਾਦ ਕਰਵਾਉਣ ਲਈ ਹੀ ਸੀ। ਜਿਸਦੇ ਸਦਕੇ ਪਰਵਾਸੀਆਂ ਨੇ ਦੇਸ਼ ਦੀ ਆਜ਼ਾਦੀ ਲਈ ਗ਼ਦਰ ਲਹਿਰ ਦੇ ਰੂਪ ਵਿਚ ਵੀਹਵੀਂ ਸਦੀ ਦੇ ਦੂਸਰੇ ਦਹਾਕੇ ਵਿੱਚ ਸੰਘਰਸ਼ ਸ਼ੁਰੂ ਕੀਤਾ। ਇਸੇ ਲਹਿਰ ਨੇ ਪਰਵਾਸੀਆਂ ਨੂੰ ਇੱਕ -ਜੁਟ ਕਰਨ, ਦੇਸ਼ ਭਾਵਨਾ ਪੈਦਾ ਕਰਨ ਲਈ ਮੁੱਢਲੇ ਪਰਵਾਸੀ ਸਾਹਿਤ ਦੀ ਰਚਨਾ ਕੀਤੀ ਤੇ ਆਪਣੇ ਉਦੇਸ਼ ਦੇ ਪ੍ਰਚਾਰ ਲਈ 'ਗਦਰ ਗੂੰਜ' ਦੀ ਪਹਿਲੀ ਪੱਤ੍ਰਿਕਾ ਆਰੰਭ ਕੀਤੀ। ਇਸੇ ਨੂੰ ਹੀ ਪਰਵਾਸੀ ਸਾਹਿਤ ਦਾ ਆਰੰਭ ਕਿਹਾ ਜਾਸਕਦਾ ਹੈ। ਪਰਵਾਸੀ ਕਵਿਤਾ ਕੋਈ ਮੁੱਖ ਧਾਰਾ ਨਹੀਂ ਸਗੋਂ ਪੰਜਾਬੀ ਕਵਿਤਾ ਅੰਦਰ ਵਿਚਰਦੀਆਂ ਧਾਰਾਵਾਂ ਵਿਚੋਂ ਹੀ ਇੱਕ ਕਹੀ ਜਾਸਕਦੀ ਹੈ। ਪਰਵਾਸੀ ਕਵਿਤਾ, ਵਿਦੇਸ਼ਾਂ ਵਿੱਚ ਰਹਿੰਦੇ ਅਰਥਾਤ ਪਰਵਾਸ ਕਰ ਰਹੇ ਲੇਖਕਾਂ ਦੁਆਰਾ ਲਿਖੀ ਕਵਿਤਾ ਹੈ, ਜਿਸਦੀਆਂ ਆਪਣੀਆਂ ਸਮੱਸਿਆਵਾਂ, ਪ੍ਰਾਪਤੀਆਂ ਤੇ ਸੰਭਾਵਨਾਵਾਂ ਹਨ, ਜੋ ਉੱਥੇ ਰਹਿੰਦੇ ਕਵੀਆਂ ਨੇ ਉੱਥੋਂ ਦੇ ਮੁਲਕਾਂ ਦੇ ਹਾਲਾਤਾਂ, ਪਰਸਥਿਤੀਆਂ ਤੇ ਪਿਛੇ 'ਤੇ ਹੰਢਾਏ ਸੱਚ ਨੂੰ ਸਾਕਾਰ ਕਰਦੀਆਂ ਹਨ ਅਤੇ ਉੱਥੋਂ ਦੇ ਲੋਕਾਂ ਨਾਲ ਰੁਆਰਫ਼ ਕਰਵਾਉਣ ਦੇ ਨਾਲ-ਨਾਲ ਰਚੇ ਜਾ ਰਹੇ ਨਵੇਕਲੇ ਸਾਹਿਤ ਨਾਲ ਵੀ ਜਾਣ-ਪਹਿਚਾਣ ਕਰਵਾਉਂਦੀ ਹੈ।

ਪਰਵਾਸੀ ਪੰਜਾਬੀ ਸਾਹਿਤ ਜਾਂ ਕਵਿਤਾ ਕੇਵਲ ਪਰਵਾਸੀ ਜੀਵਨ ਨੂੰ ਹੀ ਵਿਅਕਤ ਨਹੀਂ ਕਰਦੀ ਸਗੋਂ ਬੇਗਾਨੇ ਮੁਲਕਾਂ ਵਿੱਚ ਰਹਿ ਕੇ ਕੀਤੀਆਂ ਆਰਥਿਕ ਉਪਲੱਬਧੀਆਂ ਤੇ ਮਾਨਸਿਕ ਸੰਤੁਸ਼ਟੀ ਨੂੰ ਵੀ ਜੱਗ ਜਾਹਰ ਕਰਦੀ ਹੈ। ਇਸੇ ਸਾਹਿਤ ਸਿਰਜਣਾ ਦੇ ਖੇਤਰ ਵਿਚ ਕਵਿਤਾ, ਨਾਵਲ, ਨਾਟਕ, ਕਹਾਣੀਆਂ ਅਤੇ ਵਾਰਤਕ ਵਧੇਰੇ ਉਲਾਘਾਂ ਪੁੱਟ ਰਹੀ ਹੈ। ਦੂਸਰੇ ਦੌਰ ਸਮੇਂ ਪਰਾਏ ਸੱਭਿਆਚਾਰ, ਪਰਾਏ ਲੋਕ, ਪਰਾਈ ਧਰਤੀ ਅਤੇ ਆਪਣੀ ਭੂਮੀ ਦੇ ਮੋਹ ਨੇ ਪਰਵਾਸੀ ਕਵਿਤਾ ਵਿੱਚ ਪ੍ਰਮੁੱਖ ਸਥਾਨ ਬਣਾਇਆ ਹੈ। ਸਾਹਿਤ ਸਿਰਜਣਾ ਦੇ ਅੰਤਰਗਤ ਪਰਵਾਸੀ ਪੰਜਾਬੀਆਂ ਦਾ ਅਨੁਭਵ ਆਪੋ- ਆਪਣੇ ਖਿੱਤੇ ਅਨੁਸਾਰ ਭਿੰਨ-ਭਿੰਨ ਹੈ। ਇਸੇ ਕਰਕੇ ਇਨ੍ਹਾਂ ਖਿੱਤਿਆਂ ਵਿੱਚ ਰਚੇ ਗਏ ਸਾਹਿਤ ਵਿਚ ਵੀ ਵੱਖਰਤਾ ਪ੍ਰਾਪਤ ਹੁੰਦੀ ਹੈ। ਪਰੰਤੂ ਪਰਵਾਸ ਦੌਰਾਨ ਪਰਵਾਸੀ ਆਪਣਾ ਮੁਲਕ, ਸਮਾਜ, ਸੱਭਿਆਚਾਰ, ਸੰਸਕ੍ਰਿਤੀ ਨੂੰ ਛੱਡ ਕੇ ਜਦੋਂ ਦੂਸਰੇ ਮੁਲਕ ਵਿਚ ਵੱਸਣ ਦੇ ਇਰਾਦੇ ਨਾਲ ਪ੍ਰਵੇਸ਼ ਕਰਦਾ ਹੈ ਤਾਂ ਉਹ ਨਵੇਂ ਮੁਲਕ ਦੇ ਸਮਾਜਿਕ, ਆਰਥਿਕ, ਰਾਜਨੀਤਿਕ, ਧਾਰਮਿਕ, ਨੈਤਿਕ ਅਤੇ ਸੰਸਕ੍ਰਿਤਕ ਪ੍ਰਬੰਧ ਵਿੱਚ ਵਖਰੇਵੇਂ ਕਾਰਨ ਕਈ ਪ੍ਰਕਾਰ ਦੀਆਂ ਜਟਿਲ ਸਮੱਸਿਆਵਾਂ ਵਿੱਚ ਪੈ ਜਾਂਦਾ ਹੈ। ਇਨ੍ਹਾਂ ਸਮੱਸਿਆਵਾਂ ਨਾਲ ਜੂਝਦਿਆਂ ਪਰਵਾਸੀ ਨੂੰ ਆਪਣੀ ਚੇਤਨਾ ਵਿਚੋਂ ਕਈ ਕੁੱਝ ਮਨਫ਼ੀ ਕਰਨਾ ਪੈਂਦਾ ਹੈ ਤੇ ਕਈ ਕੁੱਝ ਨਵਾਂ ਗ੍ਰਹਿਣ ਕਰਨਾ ਪੈਂਦਾ ਹੈ। ਚੇਤਨਾ ਦੇ ਇਸ ਪੱਧਰ ਉਹ ਇੱਕ ਨਿਰੰਤਰ ਪਰਿਵਰਤਨ ਦੀ ਸਥਿਤੀ ਵਿਚ ਰਹਿੰਦਾ ਹੈ, ਜਿਸ

ਵਿਚਲੀ ਬੌਧਿਕਤਾ ਪਾਠਕ ਨੂੰ ਥਕਾਵਟ ਜਾਂ ਨਿਰਾਸ਼ਾ ਪ੍ਰਦਾਨ ਨਹੀਂ ਕਰਦੀ ਸਗੋਂ ਸਧਾਰਨਤਾ ਇਖ਼ਤਿਆਰ ਕਰਦੀ ਪਾਠਕ ਦੇ ਹਿਰਦੇ ਨੂੰ ਟੁੰਬਦੀ ਹੈ। ਸਹਿਜ ਮਾਨਸਿਕਤਾ ਇਸ ਕਾਵਿ ਸੰਗ੍ਰਹਿ ਵਿਚਲੀਆਂ ਕਵਿਤਾਵਾਂ ਦਾ ਪਹਿਰਾਵਾ ਹੈ। ਵਿਚਾਰਧਾਰਕ ਸਥਿਰਤਾ ਨੂੰ ਤੋੜਦੀਆਂ ਇਹ ਨਜ਼ਮਾਂ ਇੱਕ ਖਿੜਕੀ ਵਾਂਗ ਖੁੱਲ੍ਹਦੀਆਂ ਹਨ ਤੇ ਪਾਠਕ ਨੂੰ ਮਾਨਸਿਕ ਸੰਤੁਸ਼ਟੀ ਦੀ ਅਨੁਭੂਤੀ ਕਰਵਾਉਂਦੀਆਂ ਹਨ। ਇੱਕ ਚਿੜੀ, ਮਹਾਂਨਗਰ, ਬੁੱਧ ਨਗਰ, ਸੁੱਕਾ ਪੱਤਾ, ਪਲ, ਮਹਾਂਕਾਲ, ਮੰਗਲ ਦੀ ਚੁੱਪ ਵਰਗੇ ਲਛਜ਼ ਬਹੁਰੂਪਤਾ ਤੇ ਵਿਸ਼ਾਲਤਾ ਨੂੰ ਧਾਰਨ ਕਰਦੇ ਸੋਢੀ ਦੀ ਸ਼ਾਇਰੀ ਦਾ ਅੰਗ ਬਣਦੇ ਹਨ। ਸ਼ਬਦ ਨੂੰ ਉਸਦੀ ਬਹੁਰੂਪਤਾ ਵਿੱਚ ਚਿਤਰਿਤ ਕਰਕੇ ਪਰਮਿੰਦਰ ਨੇ ਆਪਣਾ ਕਾਵਿਕ ਮੁਹਾਂਦਰਾ ਸਿਰਜਣ ਵਿਚ ਇੱਕ ਵੱਡੀ ਪੁਲਾਂਘ ਭਰੀ ਹੈ। ਪਰਤੱਖ ਯਥਾਰਥ ਨੂੰ ਵੀ ਭਾਵ ਬੋਧ ਤੇ ਅਨੁਭਵ ਬੋਧ ਵਿਚ ਪ੍ਰਗਟਾਉ'ਦਿਆਂ ਇਹ ਕਵਿਤਾਵਾਂ ਪਾਠਕ ਦੀ ਸੰਵੇਦਨਸ਼ੀਲਤਾ ਨੂੰ ਅਸਲੋਂ ਨਵੇਂ ਧਰਾਤਲ ਤੇ ਲੈ ਆਉਂਦੀਆਂ ਹਨ। ਇਹਨਾਂ ਕਵਿਤਾਵਾਂ ਦੇ ਪਾਣੀਆਂ ਵਿਚ ਡੂੰਘੀ ਤੇਹ ਦਾ ਸਿਰਨਾਵੇਂ ਹਨ।' ਜਪਾਨੀ ਕਾਵਿ-ਵਿਧਾ ਹਾਇਕੂ ਨੂੰ ਆਪਣੀ ਕਾਵਿ-ਰਚਨਾ ਦਾ ਅੰਗ ਬਣਾ ਕੇ ਪਰਮਿੰਦਰ ਸੋਢੀ ਨੇ ਪੰਜਾਬੀ ਸਾਹਿਤ ਵਿਚ ਪਲੇਠੀ ਸੰਦਲੀ ਪੈੜ ਪਾਈ ਹੈ:—

ਮੱਛੀ ਛਲਾਂਗ

ਪਾਣੀ ਛਪਾਕ

ਮੇਰਾ ਜੀਵਨ (ਛਿਣ ਭੰਗਰ)

ਅਤੀਤ ਨੂੰ ਨਵੀਂ ਰੰਗਤ ਦੇਣੀ, ਔਰਤ ਦੇ ਅਸਤਿੱਤਵ ਨੂੰ ਸਧਾਰਨਤਾ ਤੋਂ ਉੱਚਤਤਾ ਵੱਲ ਲਿਜਾ ਕੇ ਕਾਵਿ ਦਾ ਹਿੱਸਾ ਬਣਾਉਣਾ ਪਰਵਾਸ ਨੂੰ ਭੂ-ਹੇਰਵੇ ਵਾਲੀ ਤੜਪ ਜਾਂ ਸਧਾਰਨ ਮਾਨਸਿਕਤਾ ਵਿਚੋਂ ਕੱਢ ਕੇ ਨਵੇਂ ਤੇ ਨਰੋਏ ਅਰਥ ਪ੍ਰਦਾਨ ਕਰਨਾ, ਧਰਮ, ਧਰਮ ਗ੍ਰੰਥਾਂ ਅਤੇ ਧਾਰਮਿਕਤਾ ਤੇ ਅਧਿਆਤਮ ਨੂੰ ਸਾਧਾਰਨ ਦ੍ਰਿਸ਼ਟੀ ਤੋਂ ਉੱਚਤਮ ਨਜ਼ਰੀਆ ਪ੍ਰਦਾਨ ਕਰਕੇ ਨਿੱਜ ਦੀ ਬਜਾਇ ਸਮੂਹ ਤੇ ਮਨੁੱਖਤਾਨੂੰ ਕਾਵਿ-ਪ੍ਰੇਮ ਦਾ ਹਿੱਸਾ ਬਣਾਉਣਾ ਅਤੇ ਜਪਾਨੀ ਕਾਵਿ-ਵਿਧਾ 'ਹਾਇਕੂ' ਨੂੰ ਪੰਜਾਬੀ ਕਵਿਤਾ ਦਾ ਅੰਗ ਬਣਾਉਣਾ, ਸਕੀਨਨ ਪਰਮਿੰਦਰਸੋਢੀ ਦੀ ਡੂੰਘੀ ਅਨੁਭਵੀ ਦ੍ਰਿਸ਼ਟੀ ਦੀ ਵਿਲੱਖਣਤਾ ਹੈ। ਪਰਮਿੰਦਰ ਸੋਢੀ ਦੀ ਸ਼ਾਇਰੀ ਦੀ ਆਮਦ ਨਾਲ ਜਿੱਥੇ ਪਰਵਾਸੀ ਕਵਿਤਾ/ਪੰਜਾਬੀ ਸ਼ਾਇਰੀ ਨੂੰ ਵੱਖਰੀ ਪਹਿਚਾਣ ਮਿਲੀ ਹੈ, ਉੱਥੇ ਉਸਦੀ ਸ਼ਾਇਰੀ ਕਈ ਪ੍ਰਾਪਤੀਆਂ ਦੀ ਮਾਲਕ ਤੇ ਆਪਣੇ ਅੰਦਰ ਭਵਿੱਖਤ ਸੰਭਾਵਨਾਵਾਂ ਸਮੋਈ ਬੈਠੀ ਹੈ।

●

ਹਵਾਲੇ ਤੇ ਟਿੱਪਣੀਆਂ

1. ਅੰਮ੍ਰਿਤਪਾਲ ਕੌਰ (ਡਾ.), ਬਾਲ ਵਿਸ਼ਵਕੋਸ਼ (ਭਾਸ਼ਾ, ਸਾਹਿਤ ਅਤੇ ਸੱਭਿਆਚਾਰ), ਪਬਲੀਕੇਸ਼ਨ ਬਿਊਰੋ, ਪੰਜਾਬੀ ਯੂਨੀਵਰਸਿਟੀ, ਪਟਿਆਲਾ।
2. ਢਾਅ, ਸਤਨਾਮ ਸਿੰਘ, ਵਿਸ਼ੇਸ਼ ਮੁਲਾਕਾਤ, 'ਜਾਪਾਨ ਵਿਚ ਪੰਜਾਬੀ ਸਾਹਿਤ ਦਾ ਝੰਡਾ ਬਰਦਾਰ : ਪਰਮਿੰਦਰ ਸੋਢੀ'
3. ਢਾਅ, ਸਤਨਾਮ ਸਿੰਘ, ਵਿਸ਼ੇਸ਼ ਮੁਲਾਕਾਤ, 'ਜਾਪਾਨ ਵਿਚ ਪੰਜਾਬੀ ਸਾਹਿਤ ਦਾ ਝੰਡਾ ਬਰਦਾਰ : ਪਰਮਿੰਦਰ ਸੋਢੀ'
4. ਢਾਅ, ਸਤਨਾਮ ਸਿੰਘ, ਵਿਸ਼ੇਸ਼ ਮੁਲਾਕਾਤ, 'ਜਾਪਾਨ ਵਿਚ ਪੰਜਾਬੀ ਸਾਹਿਤ ਦਾ ਝੰਡਾ ਬਰਦਾਰ : ਪਰਮਿੰਦਰ ਸੋਢੀ'
5. ਪ੍ਰਮਿੰਦਰਜੀਤ, ਇੱਕ ਚਿੜੀ ਤੇ ਮਹਾਂਨਗਰ, ਚੇਤਨਾ ਪ੍ਰਕਾਸ਼ਨ ਪੰਜਾਬੀ ਭਵਨ, ਲੁਧਿਆਣਾ-2001, ਪੰਨਾ-7.

ਅਸਿਸਟੈਂਟ ਪ੍ਰੋਫੈਸਰ,
ਪੋਸਟ ਗਰੈਜੂਏਟ ਪੰਜਾਬੀ ਵਿਭਾਗ,
ਸਰਕਾਰੀ ਕਾਲਜ, ਹੁਸ਼ਿਆਰਪੁਰ

Exploration of solute-solvent interactions in aqueous mixtures of monosaccharides and triammonium citrate (TAC) at different temperatures: Volumetric and acoustic approach

Author: Harsh Kumar,Monisha Sharma,Vaneet Kumar

Publication: The Journal of Chemical Thermodynamics

Publisher: Elsevier

Date: December 2019

Welcome to RightsLink

J. Chem. Thermodynamics 119 (2018) 1–12

Contents lists available at ScienceDirect

J. Chem. Thermodynamics

journal homepage: www.elsevier.com/locate/jct

Studies on the interactions behaviour of polyhydroxy solutes D(+)-glucose and D(−)-fructose in aqueous triammonium citrate solutions over temperature range $T = (288.15–318.15)$ K

Harsh Kumar [a,*], Vaneet Kumar [b,c], Monisha Sharma [b,d], Isha Behal [a]

[a] Department of Chemistry, Dr B R Ambedkar National Institute of Technology, Jalandhar 144011, Punjab, India
[b] IKG Punjab Technical University, Kapurthala Road, Jalandhar, Punjab, India
[c] Department of Applied Sciences, CT Group of Institutions (CTIEMT), Shahpur, Jalandhar, Punjab, India
[d] MRPD Govt Arts and Science College, Talwara 144216, Punjab, India

ARTICLE INFO

Article history:
Received 24 August 2017
Received in revised form 1 December 2017
Accepted 4 December 2017
Available online 6 December 2017

Keywords:
D(+)-Glucose
D(−)-Fructose
Triammonium citrate
Apparent molar property
Interaction coefficients
Thermophysical properties

ABSTRACT

The interactions of polyhydroxy solutes D(+)-glucose and D(−)-fructose with aqueous solutions of triammonium citrate (TAC) as a function of temperature have been enquired upon by combination of volumetric and ultrasonic studies. Densities and speed of sound of D(+)-glucose and D(−)-fructose in (0.2, 0.4 and 0.6) mol·kg^{-1} aqueous solutions of triammonium citrate (TAC) are measured at $T = (288.15, 298.15, 308.15$ and $318.15)$ K and experimental pressure $p = 0.1$ MPa. The apparent molar volume, V_ϕ, the partial molar volume V^o_ϕ, and standard partial molar volumes of transfer, ΔV^o_ϕ for D(+)-glucose and D(−)-fructose from water to aqueous solutions of triammonium citrate (TAC) have been calculated from density data. Apparent molar isentropic compression, $K_{\phi,s}$, partial molar isentropic compression $K^o_{\phi,s}$ and partial molar isentropic compression of transfer, $\Delta K^o_{\phi,s}$ have been calculated from ultrasonic speed data. The expansibility parameter $(\partial V\phi^0/\partial T)_p$ and its derivative $(\partial^2 V\phi^0/\partial^2 T)_p$ along with pair (V_{AB}, K_{AB}) and triplet (V_{ABB}, K_{ABB}) interaction coefficients have also been calculated. The results have been interpreted in terms of solute–solute and solute–solvent interactions in these systems.

1. Introduction

Saccharides belongs to the class of compounds which are diversified and shows a dominant presence in natural living systems [1,2]. These classes of compounds when in conjugation with proteins and lipids play an important role in most of biological processes. They are used as energy houses, as building blocks for cofactors and biomolecules, and are in used in the design of biocompatible and bio degradable materials [3–5]. Novel photochemical method of immobilization and patterning of unmodified carbohydrates onto glass substrates to create carbohydrate microarrays which display well-defined antigenic determinants for antibody recognition has been presented [6]. Saccharides play a crucial role in biological recognition phenomenon in the process of exchanging information between the cells like cell–cell interactions and cell death signal transduction, inflammatory processes, cancer metastasis, bacterial and viral infections, thus paving a way for designing of anti-cancer drugs [6,7]. Saccharide based synthetic ion transporters, useful for technological and biomedical applications, have been designed [8]. Saccharides, being polyhydroxy (PHC) compounds, show peculiar hydration characteristics, and the thermodynamic data characterizing the solvation behaviour of polyhydroxy compounds in their aqueous solutions, is very informative for the growth of food and biological industries. Polyhydroxy compounds are characterized by their polar nature and ability to participate in hydrogen bonding, both as donors and acceptors. As a class of chemical compounds they, therefore, display a high affinity for water and other polar solvents. It is to be expected that solute–solvent hydrogen bonding plays some role in determining the structures and conformations of PHCs in solution, and indirectly, also their interactions with one another, perhaps even intramolecular interactions [9]. Binary and ternary mixtures of saccharides such as glucose, fructose, and sucrose upon mixing of glycerols, salts, and ethanol act as immersion medium for the freezing fruits [10,11]. The presence of salt modifies many properties such as water sorption, crystallization rate, viscosity and glass transition temperature of aqueous saccharides mixtures [12,13]. The hydration behaviour of saccharides helps to understand the structural, stereochemical, and functional properties

* Corresponding author.
E-mail address: manchandahi@nitj.ac.in (H. Kumar).

https://doi.org/10.1016/j.jct.2017.12.003
0021-9614/

Journal of chemical & engineering data

Article

pubs.acs.org/jced

Effect of Citrate Salts on the Volumetric and Ultrasonic Properties of Sucrose in Aqueous Solutions at Temperatures T = (288.15−318.15) K

Harsh Kumar,[†,*] Monisha Sharma,[‡,§] and Vaneet Kumar[‡,∥]

[†]Department of Chemistry, Dr. B. R. Ambedkar National Institute of Technology, Jalandhar 144011, Punjab, India

[‡]IKG Punjab Technical University, Kapurthala Road, Jalandhar 144011, Punjab, India

[§]MRPD Govt. Arts and Science College, Talwara 144216, Punjab, India

[∥]Department of Applied Sciences, CT Group of Institutions (CTIEMT), Shahpur, Jalandhar 144011, Punjab, India

ABSTRACT: The volumetric and ultrasonic properties of sucrose in aqueous solutions of citrate salts trisodium citrate (TSC) and tripotassium citrate (TPC) were studied at temperatures T = (288.15−318.15) K and at atmospheric pressure. Apparent molar volumes V_ϕ and apparent molar isentropic compressibilities $K_{\phi,s}$ were calculated from measured density ρ and speed of sound u data. Partial molar volumes V_ϕ° and partial molar isentropic compressibilities $K_{\phi,s}^\circ$ at infinite dilution, transfer parameters ΔV_ϕ° and $\Delta K_{\phi,s}^\circ$ of sucrose from water to aqueous solutions of TSC and TPC, expansion coefficients $(\partial V\phi^0/\partial T)_p$, $(\partial^2 V\phi^0/\partial^2 T)_p$, and interaction coefficients $(V_{AB}, K_{AB})(V_{ABB}, K_{ABB})$ were also evaluated. These parameters are discussed in terms of solute−cosolute interactions to understand the solvation behavior of sucrose in theses salts. Positive and increasing values of ΔV_ϕ° with increasing citrate salt concentrations were obtained. This indicated the dehydration of the sucrose in the presence of the citrate salts due to the predominance of solute−cosolute interactions. Hydration number N_w was also calculated for the mixtures in this study.

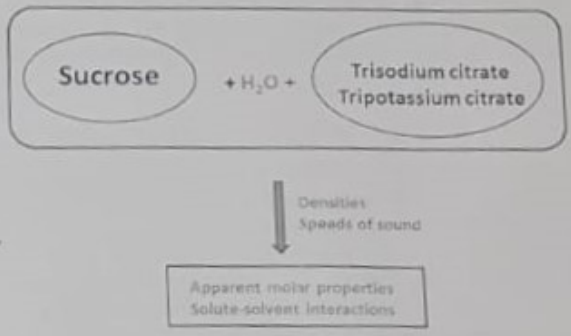

1. INTRODUCTION

Knowledge of thermophysical properties of aqueous systems with citrate anions is of great importance in beverage, cosmetics, chemical industries, and in the colloid synthesis of gold and silver nanoparticles.[1] Saccharides and their derivatives are the most resource-full class of biomolecules, known for versatility and great diversity of their biological functions. Saccharides, polyalcohols, and salt solutions are commonly used in several food industries to adjust the water activity and pH to reduce the growth of contaminating microorganisms.[2−4] Animals tolerate dehydration stress by accumulation of disaccharides.[5] Disaccharides, trehaloses, sucrose and maltose, etc. found their application as the most suitable cryo- or lyoprotective excipient for maintaining the viability of plants and animals under adverse conditions as well as the stability of pharmaceutical products.[6−8] Green and Angell attributed this peculiarity of trehalose to the fact that it has the highest glass transition temperature, T_g, for its aqueous solutions among the homologous disaccharides, which protects desert animals from dehydration and allows them to survive for decades in these drought conditions by producing trehalose intracellularly during desiccation.[9] This has been demonstrated by ultrasonic measurements,[10] Raman scattering,[11] neutron scattering,[12] etc. Sucrose affects the properties of surfactants such as lowering cloud point, increasing hydrophobicity, and changing phase behavior, hence affecting the droplet size of nanoemulsion formation in an aqueous phase/nonionic surfactant/oil system.[13−16] Saccharides have also been exploited in pharmaceuticals, foods, and biomedical applications.[17,18] Binary and ternary aqueous solutions containing saccharides (e.g., sucrose, glucose, and fructose) and additives (ethanol, glycerol, salts, etc.) have been widely used as a suitable immersion media for freezing fruits.[19] The thermochemical methods of energy production from sucrose biomass are gaining interest, and the possibility of hydrogen production from the catalytic reforming of sucrose biomass has been reported.[20]

The hydration behavior of saccharides is a key feature to understand their structural and functional properties. In the past few years, the thermodynamic properties (apparent specific volumes and apparent specific isentropic compressibilities) of different sapid substances (including saccharides) have been studied[21−24] in aqueous and mixed aqueous solutions[25−27] to understand the role of water−solute interactions and the influence of additives on the solute−solvent interactions. Moreover, the role of water in sweet taste chemoreception has

Received: May 8, 2018
Accepted: August 31, 2018

DOI: 10.1021/acs.jced.8b00379
J. Chem. Eng. Data XXXX, XXX, XXX−XXX

International Journal of Advanced Engineering, Management and Science (IJAEMS)
Peer-Reviewed Journal
ISSN: 2454-1311 | Vol-9, Issue-7; Jul, 2023
Journal Home Page: https://ijaems.com/
Article DOI: https://dx.doi.org/10.22161/ijaems.97.1

Characteristics of Murta Bast Fiber Reinforced Epoxy Composites

Muneesh Kashyap[1], Dr. Ranoji K. Shillargol[2]

[1]Research Scholar, Sunrise University, Alwar, Rajasthan, India
[2]Professor, Sunrise University, Alwar, Rajasthan, India

Received: 20 Jun 2023; Received in revised form: 16 Jul 2023; Accepted: 23 Jul 2023; Available online: 31 Jul 2023

Abstract**—** *In daily applications, the composites may also be found. The most prevalent kind of life is concrete. Concrete is a gravel, sand and cement composite material. The main aim of the study is Characteristics of Murta Bast Fiber Reinforced Epoxy Composites. Epoxy resin and HV953U Hardensin from a nearby supplier were purchased and used in accordance with the provision. Bisphénol A diglycidyl ether (BADGE) of the araldite AW106 has an epoxy of the same weight as the eq-1 (203–222 g). Increasing assembly of innovation alone is not enough, especially for composites, to overcome the cost barrier. For composites to be cut through with metals, it is crucial that an integrated application be made in plan, material, measure, tooling, quality verification, production and even programming.*

Keywords**— Composite, Reinforced, Epoxy, Cost, Barrier, programming.**

I. INTRODUCTION

In daily applications, the composites may also be found. The most prevalent kind of life is concrete. Concrete is a gravel, sand and cement composite material. It also creates another kind of composite when used with steel to build structural components. The other is wood, a combination of lignin and cellulose. One of the most sophisticated wooden composites kinds is Plywood. These may be composites with particles bound, or combines wooden boards or blocks with the suitable binding substance. The furnishings and building materials nowadays are extensively utilized.

Muscles are a good example of a natural composite in the human body. The muscles exist in a tiered structure of fibers in various directions and concentrations. The results are extremely powerful, efficient, flexible and adaptive. The muscles give bones strength and vice versa. Both create a distinct structure. The bone itself is a composite structure and includes a substance of a mineral matrix that connects the collagen fibers. The remaining examples are bird wings, fish fins, trees and grass. An example of a composite structure is also a tree leaf. The veins in the leaf not onlycarry food and water, which also provide the leaf its power to keep the leaf stretched over a large surface. This assists the plant in the photosynthesis to obtain more energy from the sun.

1.2 POLYMER COMPOSITES

Synthetic polymers are attractive materials because they have a high strength-to- weight relationship and need little surface treatment. The mechanical characteristics of polymers are lower than the metals and not chosen for structural purposes, althoughthe adding of fillers and fibers may enhance their capabilities. Their comparative easy processing, low density, corrodance resistance, desired electric characteristics and thermal qualities has attracted considerable interest from polymer matrix composites. Thermosetting or thermoplastic may be these polymers. Polymers like epoxy and polyester do not soften when heated, while thermoplastics like polyvinyl and polymides are not softened. Thermoplastics are used in thermoplate. Therefore, they are stronger, tougher, more fragile and more stable thanthermoplastics.

II. LITERATURE REVIEW

Haina (2020) - Haina (2020) - In the context of the cutting-edge sustainable materials, this study effectively addresses the development in the investigation of polymer biocomposites. More recently, curiosity with the bio-composite frameworks was attracted by its potential as a replacement for conventional materials in major assembly

sectors. From late on, it has been a major achievement to prepare biocompatible and biodegradable polymer composites as an alternative for limitless petrochemical products. Instead of included fibers like carbon and orchestrated saps, polyvinyl alcohol, epoxy etc.. Effective manufacture of eco-friendly bio-materials has been achieved using natural fibers such as jute, bamboo, hair, flex, wool, silk and many more products. In addition, natural fibers dispersed within the natural matrix have been produced using biomaterials such as natural elastic or polyester for limitless human uses. Their simple removal and sustainability is attributed to the useof these materials for the well well of mankind. The last but not least, is that bio- unusual composite's mechanical characteristics superior than many other conventionalmaterials. The audit study focuses on novel patterns, mechanical and compound characteristics, summarization and application in the New Year of bio-composites.

Rajak, et al (2019) - Dipen Kumar Rajak. The most encouraging and knowing substance available this century has been found to be composites. Based on current needs for lightweight materials with high strength for specific applications, composites with fiber reinforced from manufactured or natural materials acquire importance. Composite fiber-reinforced polymer provides a high weight to strength ratio but also reveals good characteristics such as high durability, rigidity, damping capabilities, flexural strength and consumption resistance, wear, effect and fire. These broad ranges of features have led to composite materials being found in mechanical, building, aerospace, car, biomedical, marine and many other assembly sectors. Composite materials are largely manufactured by their components and assembling strategies, so practical characteristics, orders and assembly procedures for various fibers worldwide accessible for the production of combined materials should be concentrated to sort out the upgraded standard for the material ideal for use. To find out the improved fiber-reinforced composite material for enormous applications, an overview of a diverse range of fibers, their characteristics, usefulness, group and various fiber composite assembly methods is provided. Their unusual presentation of composite fibers has become a tempting alternative over lonely metals and/or mixtures in many applications.

Prosenjit Ghosh & Narayan Ch. Das (2019) - Tushar Kanti das, Prosenjit Ghosh & Narayan Ch. The superior strength to weight ratio of carbon fibers, above conventional hardwearing materials like steel, has made it an appealing energy savings material. In many strong applications, the high weight steel is being replaced by low weight and consumption safe carbon fiber composites. The PMC has therefore become the frontline material in the field of aircraft, cars, sports goods and other applications requiring high strength and a high module. In addition, its gradual reduction in cost has opened up its market in different building applications since late on in the wide exploratory area of carbohydrate innovation. This study covers a range of polymer matrix composites layered in carbon fibers, where the structural importance of these composites is stressed. The aim of this discussion is to provide information on all types of polymer composites based on carbon fiber. It also includes a short discussion with the processing, manufacturing and structural uses of these carbon fiber-based polymers, on the preparation and characteristics of carbon fibers.

Nagaraju B and Bhanutej B (2019) – Nagaraju J and V Since its inception, Additive Manufacturing is well known for being flexible in materials and easy to utilise with complicated calculations in manufacuring components. The work identified with FFF, explicitly pushed polymer composites and the effects of different operating boundaries on their sustainability, has become a major factor in additive production during recent few years due to the improvements made to advanced materials such as composites. Additive fabrications have acquired a broad importance.

Yubo Tao et al (2019) – Contextual survey on the optimisation of polymer composites by FFF Mechanical Modeling. In this study compression was investigated using restricted component reproductions and compression tests for FDM printed circles, squares and voronoi WPCs cellular structures. The findings demonstrated the enormous variations between leisure and trial outcomes in the circular cell design. Furthermore, the cavity porosity increased as the printing line width was expanded. In addition, cavity porosity is conceived in the cellular buildings while altering the models to enhance the accuracy of the recreations. Square cell models, followed by circular and voronoi models, packed the least after the modification, as might be predicted from exploratory results. Furthermore, it may decrease cavity porosity by reducing the print line width. However, the wider printing line and the smaller the sizeof the wood fibers in fiber are likely to increase production costs and problems.

III. METHODOLOGY

Characteristics of Murta Bast Fiber Reinforced EpoxyComposites

➢ Materials

Epoxy resin and HV953U Hardensin from a nearby supplier were purchased and used in accordance with the provision. Bisphénol A diglycidyl ether (BADGE) of the

araldite AW106 has an epoxy of the same weight as the eq-1 (203–222 g). The HV953U hardener includes 1,3-propylenediamine-N-(3-dimethyaminopropyl). The BADGE and hardener structures are shown. The NaOH grade laboratory reagent has been used for the treatment of fibers (S. D. Fine Chemicals, India).

IV. RESULTS

4.1 CHARACTERISTICS OF MURTA BAST FIBER REINFORCED EPOXY COMPOSITES

In this specific chapter we repeat again the advantages of natural fibers for polymer matrix reinforcement. The increasing global problem of the negative effects of human activities on earth has led to the thought that natural fiber enhanced polymer composites constitute one of the substitutes for earth friendly and cost-effective products for use in various sectors such as the automotive, construction, electricity, sports, packaging, houses etc. It has stimulated the research into polymer composites and scientists are facing the challenge of producing much superior composites. Therefore, several natural fibers for the reinforcement of polymer matrices have been investigated. The use of natural fibers, including easy accessibility, renewability, biodegradability, low density, considerable strength, non-corrosive nature and low- cost reinforcing, offers many advantages. We showed that fibers from centres of the murta (schumannianthus dichotomus) stems may be used for reinforcement and characterization of the mechanical characteristics of murta core polymer enhanced by AW106 epoxy resin and HV953U hardness. polymer enhanced by the murta corefiber (in the ratio of 2:1 by volume).

In West Bengal and Assam India, in North Eastern Bangladesh's, Vietnam's, Thai, Philippine's, Myanmar's, and Malaysia, murta crops were really grown in Chapter Three. Murta fibers are used exclusively to produce various artisanal products, and themat is quite well known for these things in Bangladesh and India. It may be noted thatthe outer-level fibers of murta trunks, which we will call murta bast fiber, are used formanufacturing artisanal solutions. The only thing that the authors have studied is the effect of the talc on the properties of a polyester resin reinforced by murta bast fiber, which is insaturated in a ball.

4.1.1 Characteristics of Fiber and Density

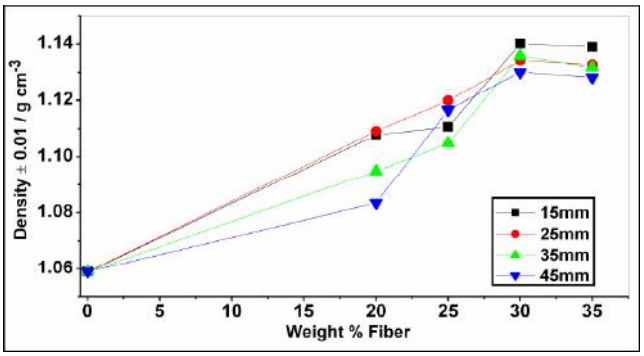

Fig.4.1 Density of the composite as a function of weight % of fiber ofdifferent lengths

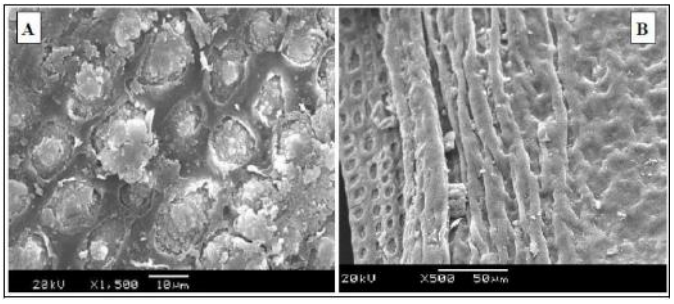

Fig.4.2 SEM images of (A) untreated and (B) treated fiber

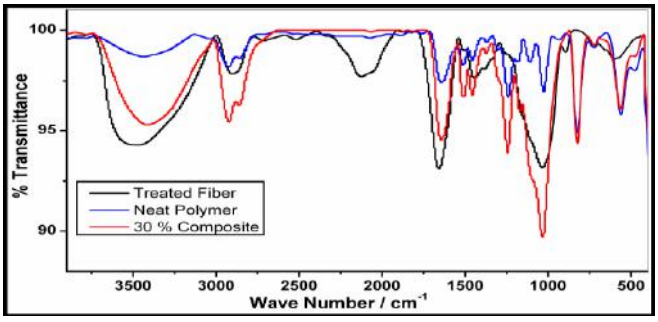

Fig.4.3 FTIR spectra of the fiber, polymer and composite (containing 30 %fiber)

Table 4.1 records the characteristics and the chemistry of murta bast fiber which are contrasting with those of murta primary element and a few other natural fibers. Figure 4.4 presents the experimental density values of the composites. With weight percentage increase, the density of the composites increased. When the fiber load exceeded 20 percent by weight, the composite density was even more than that of the fivers (1,06 g cm-3) which showed a smaller fiber compound with an irrelevant vacancy. The composites had a greater density than polymers (1,06 g cm-3). The smallness of composites indicates thus that fibers and polymers are permanently associated with a chemical treatment that may be

attributed to them. As seen by the SEM image (Figure 4.5), the therapy of the fiber is asymmetrical to the surface and provides for a better union of the fiber and matrix in a specific field. In Figure 4.5, the strong communications between the fiber and the polymer are also apparent from the IR spectra. In the fiber, the IR-band extends at 3490 cm-1, whereas the IR-band extends at 3450 cm-1 with OH and NH-. Increased power and the expansion of the IR band on fiber stacking to 3450 cm-1 of the polymer confirm that hydrogen retaining improvements occur throughout composite growth.

Table 4.1 Composition and properties of murta and other fibers

Fiber	Cellulose (%)	Hemi cellulose (%)	Lignin (%)	Density (g cm^{-3})	TS (MPa)
Murta bast fiber	56	19	16	1.10	378 ± 13
Murta core fiber	38	26	22	0.94	242 ± 24
Jute	71	20	13	1.30	393 - 773
Sisal	65	12	10	1.50	511 - 635
Coir	43	0.3	45	1.20	175
bamboo	26 - 43	30	21 - 31	0.80	140 - 230
Flax	71	21	2	1.50	345 - 1035
Kenaf	72	20	9	1.20	930

4.1.2 Water Absorption

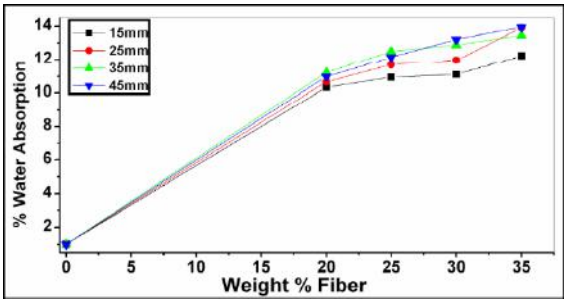

Fig.4.4 Amount of water absorbed by the composites as a function ofweight % of fibers of different lengths

Figure 4.4 shows the conduit of water absorption in composites and the results of themeasurement in percent of the water swallowed are shown in Table 4.6. With weight percent expansion of the fiber and fiber lengths, the measurement of water consumingthe composite will generally increase. The composite with 35% weight of 45mm fiberconsumes approximately 14% of the largest intake. This means that the hydrophilic idea of lignocellulose fibers is not particularly great. For example, jute-reinforced polyester composite has a water absorption of about 25%.

Table 4.2 Amount of water absorbed by the composite as functions of fiber load and fiber length

Weight % Fiber	Fiber length (mm)			
	15	25	35	45
	% Water Absorption (For Neat Polymer = 1.0)			
20	10.3	10.7	11.2	11.0
25	10.9	11.7	12.5	12.2
30	11.1	12.0	12.9	13.2
35	12.2	13.9	13.5	14.0

4.1.3 Thermal Behaviour

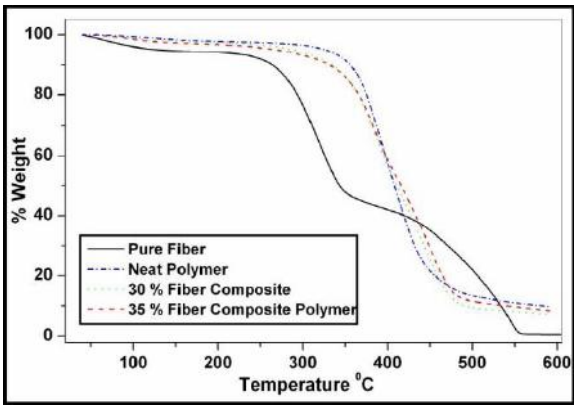

Fig.4.5 Thermograms of the fiber, polymer and composites obtainedfrom the TGA

Figure 4.7 shows thermogram from TGA and illustrates the response to heat energy of the fiber, polymer and composites. Before the initial phase of heat deterioration, thefiber loses approximately 7 percent. This underlying loss of weight is regarded as the evaporation of the fiber surface water, which, due to its hydrophilic nature, is a characteristic element with natural fibers. A weight loss of about 53 percent is the main phase of thermal deterioration of the fibers to around 350 °C. Yang et al. isolated from palm oil spraying samples hemicellulose, cellulose and lignin by their independent TGA pyrolysis turns. Considering these details of the three important components of natural fibers, the aim here is to calculate the total weight loss of murta fibers towards the completion of the first degradation stage. Detailed thermogram results show that hemicellulose, cellulose and lignin weight losses are 63,50 and 25 percent individually at a temperature of 350°C. In view of the nature of murta bast fiber, at 350°C the fiber is anticipated to lose 12, 28 and 4% of weight due to hemicellulose degradation (63% by 19%), cellulose

(50% by 56%) and lignin (25% by 16%). The expected total fiber loss is equal to 51 percent at 350°C (44 percent because of degradation of hemicellulose, cellulose and lignin and 7 weights percent because of water evaporation). Strangely, we have a weight loss at 350°C, which is equal to 53 percent in acceptable competition with the expected value, from the experimental thermograms in the figure4.7. The second phase of thermal fiber breakdown is occurring gradually above 350°C. According to the aftereffects of Yang et al.,26 cellulose in the TG AG, it deteriorates quickly, somewhere within a phase of 315 and 400°C, to a decrease of 95%, from 240°C onwards and to a degree of 220 to 315, followed by a slow decline (<.15% /°C) and a slow degradation of hemicellulose (< 0.1% /°C) Then the lethargic thermal breakdown of murta fiber is due to the slow destruction of hemicellulose and lignin. The thermal degradation characteristics of the polymers and the composites are similar. The polymer is heat stable (epoxy resin to hardness = 1:1), up to 325 °C, which is more than the thermal safety of the epoxy resin polymer to a hardness of 1:2 (293 °C). 24 Although natural fiber support reduces Polymer Matrix's thermostatic stability, the thermal strength of the composites is nearly 300°C with between 30% and 35% fiber weight.

4.1.4 Tensile Strength and Modulus

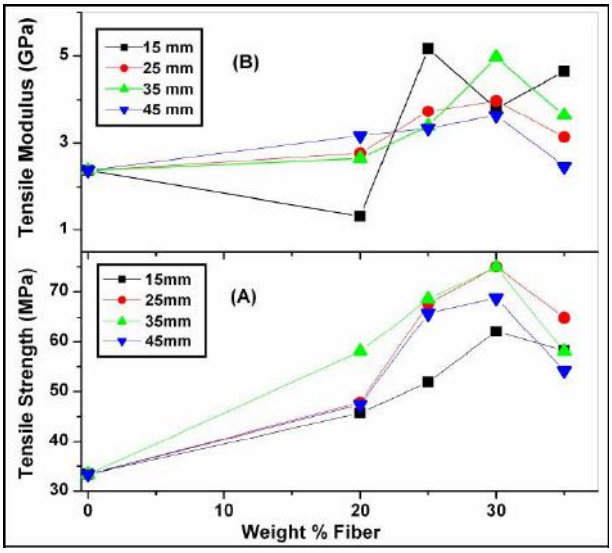

Fig.4.6 Variation of (A) tensile strength and (B) tensile modulus of the compositeas a function of weight % of fiber at fixed fiber lengths

The polymer and composites' purposeful tensile strength (TS) are shown in Table 4.7 in Figure 4.18A. The TS of a composite is administered via a number of variablessuch as fiber length, fiber measurement, matrix orientation of fibers, matrix fiber conveyor, fiber matrix adhesion etc. During the present study, the composites are formed by random fiber orientations and the only variables that may detect the characteristics of the composite are length and measurement of the fiber. The TS ofthe composite is the highest in the basic length and measurement of the fiber. The TS is a characteristic component of natural fiber-enhanced composites with this type of fiber length and sum dependency. The TS is determined to be the most severe at the time where the composite includes 30 percent fiber weight and 74.9 MPa, which adds up to an expansion of 124 percent in comparison to the TS of a clean polyp. The composite with 30 percent by weight of 25 mm fiber has almost the highest TS equal to 74,3 MPa. After 30% weight of fiber stacks, TS is starting to decrease and this is attributed to the fiber trap producing composite and weakening irregularities in fiber – matrix adherence. The SEM images shown in Figure 4.7 show the composite morphological adjustment including 35% fiber by seeing the fiber traps.

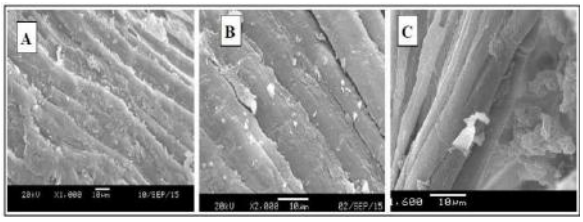

Fig.4.7 SEM images of composites containing (A) 20 %, (B) 25 % and (C)35 %fibers of 35 mm length

V. CONCLUSION

Increasing assembly of innovation alone is not enough, especially for composites, to overcome the cost barrier. For composites to be cut through with metals, it is crucial that an integrated application be made in plan, material, measure, tooling, quality verification, production and even programming. The company Composites hasbecome clear that, because of the sheer scale of the transport sector, the commercial usage of composites offers far more business opportunities than aviation. This means that composite uses have recently changed unmistakably from an aircraft to other companies. The entry of these high-level materials has witnessed a steady growth in employment and volume gradually strengthened by the introduction of more current polymer resin matrix materials and elite support fibers, including glass, carbon, aramid. The increased volume led to a typical cost reduction. In a range currently of uses including composite protection against harmful effects, natural gas fuel chambers, windmill-sharp edges, mechanical drive shafts, light emission connectors and even paper manufacturing rolling machines, the Elite FRP may be found. The use of composites as opposed to metals in particular applications effectively has resulted in both

expenses and weight in reserve funds. Some models include engine bending, bending and bended fillets, metallic replacements, chambers, tubes, pipes, belt controlunits, etc. In addition, composite requirements have placed a high degree of emphasis on the use of innovative and advanced materials that reduce dead weight as well as absorb shock and vibration via personalised micro-structures.

REFERENCES

[1] Haina (2020) - Recent Trends in Preparation and Applications of BiodegradablePolymer Composites. JRM, 2020, vol.8, no.10

[2] Dipen Kumar Rajak, et al (2019) - Fiber-Reinforced Polymer Composites: Manufacturing, Properties, and Applications. Polymers 2019, 11, 1667; doi:10.3390/polym11101667

[3] Das, T.K., Ghosh, P. & Das, N.C. Preparation, development, outcomes, and application versatility of carbon fiber-based polymer composites: a review. Adv Compos Hybrid Mater 2, 214–233 (2019). https://doi.org/10.1007/s42114-018- 0072-z

[4] V Bhanutej J and Nagaraju B (2019) - Polymer Based Composites via Fused Filament Fabrications (FFF) - A Review and Prospective. International Journal of Engineering Research & Technology (IJERT) ISSN: 2278-0181 Published by, www.ijert.org AMDMM - 2019 Conference Proceedings

[5] Yubo Tao, Ling Pan, Dexi Liu, Peng Li ―A Case Study: Mechanical Modeling Optimization of Cellular Structure Fabricated Using Wood Flour-Filled Polylactic Acid Composites with Fused Deposition Modeling‖ Additive Manufacturing, 2019; PII: S2214- 8604(18)30809-1

[6] Athijayamani A, Thiruchitrambalam M, Natarajan U and Pazhanivel B (2009),―Effect of moisture absorption on the mechanical properties of randomly oriented natural fibers/polyester hybrid composite‖, Materials Science and Engineering, 517, pp. 344– 353.

[7] B. Du ―Advances in Thermal Performance of Polymer-Based Composites 33(14):3149-3159 2018

[8] Baptista, Ricardo & Mendão, Ana & Guedes, Mafalda & Marat-Mendes, R.. (2016). An experimental study on mechanical properties of epoxy-matrix composites containing graphite filler. Procedia Structural Integrity. 1. 74-81. 10.1016/j.prostr.2016.02.011.

[9] Barreto A.C.H, Rosa D.S, Fechine P.B.A and Mazzettoa S.E (2011), ―Properties of sisal fibers treated by alkali solution and their application into cardanol-based bio-composites‖ Composites: Part-A, 42, pp.492-500

[10] Colombo, C, Vergani, L & Burman, M 2012, Static and fatigue characterisation of new basalt fiber reinforced composites_, Composite Structures, vol. 94, no. 3, pp. 1165-1174

International Journal of Chemistry, Mathematics and Physics (IJCMP)
[Vol-7, Issue-4, Jul-Aug, 2023]
https://dx.doi.org/10.22161/ijcmp.7.4.3
ISSN: 2456-866X

Effects of Fiber Length and Loading on the Qualities of Fiber Reinforced Epoxy Composites from Schumannianthus Dichotomus (Murta)

Muneesh Kashyap[1], Dr. Ranoji K. Shillargol[2]

[1]Research Scholar, Sunrise University, Alwar, Rajasthan, India
[2]Professor, Sunrise University, Alwar, Rajasthan, India

Received: 19 Jun 2023; Received in revised form: 25 Jul 2023; Accepted: 03 Aug 2023; Available online: 09 Aug 2023

Abstract**—** *Composite isn't a new word, it's a long time around. Due to its usage in several applications, it has risen in prominence over the last four to five decades.* ***T****he main aim of the study is Effects of Fiber Length and Loading on the Qualities of Fiber Reinforced Epoxy Composites from Schumannianthus Dichotomus (Murta)****.*** *The polymer matrix is made of Araldite AW106 epoxy resin and HV953U hardener. Bisphenol A Diglycidyl Ether with the same epoxy weight as 214 – 221 g eq-1 is included in Araldite AW106. The HV953U hardener includes 1,3-propylenediamine N-(3-dimethaminopropyl)-. Composite materials have a very adaptable component lay out above normal materialsdue to their clear strength, strength, and exhaustive characteristics.*

Keywords**— Composite, Fiber, Reinforced, Strength, Adaptable.**

I. INTRODUCTION

Composite isn't a new word, it's a long time around. Due to its usage in a number of applications it has risen in prominence over the last four to five decades. In 10000 BC the pavement brichs had been a prominent building composite material. Fibrous composite material was then used in preparing written materials in Egypt about 4,000 BC, and these papyrus plant laminated written material was produced. In addition, Egyptians made containers and tins from heat softened glass made of raw fibers.

The Mongolians used composites again about 1200 BC. The Mongols have created the so-called contemporary composite arch. The oldest proofs of the presence of composite bows, according to Angara Dating, date from 3000 BC. The bow was constructed of various materials such as wood, horn, sinew (tendon), leather, bamboo and antler. Since horn and antler are very flexible and robust, the primary body of the bow has been made. For connecting and covering the horn with the antler, sinews were employed. Clue is formed of a fish's bladder and serves as a holding unit. Sinew,horse hair, and silk were fashioned of the bow string. It was anticipated that the composite bow would last over a year. The bows were so strong that over 1.5 kilometres from the arrows could be fired. The composite bow was a highly deadly weapon before the discovery of gunpowder since it was short and convenient.

1.1 COMPOSITE MATERIALS

Due to developments in the next generation, the need for technology has risen in recent days. A good product which fulfils customers' requirements should thus be of excellent quality and affordable pricing. The industry now dominates engineering materials such materials, intelligent materials, and materials. In recent years, a multitude of novel materials have developed. Examples of these include polymers, metals, ceramics and composites. In the area of materials science significant progress has been achieved. The latest developments in material technology are composite materials, which show substantial progress. They are regarded highly and have a great influence on industry. Their strength and matrix characteristics are both. A hybrid construction has many more benefits and is lightweight, sturdy, and ecological. Polymers are utilised in a broad variety of applications including aramid fibers, glass, and carbon. The fibers are usually uniformly, bi- and multi-directionally arranged.The main classification of polymers is two kinds. They are plastics for thermoplastics and

plastics for thermoplastics. Thermoplastic materials have been used in various areas because of their significant structural characteristics. Examples include acrylics, nylons, polycarbonates, polyvinylchloride, etc. Examples of such products include polyester, phenolics, polyamides, vinyl esters, bismaleimides, epoxies, etc.

1.1.1 Composites Classification

Composites are ranked based on pure reinforcement geometry, whether inparticles, flakes or fiber materials – polymers, metal, ceramics or carbon, in a matrix type. Particulate composites consist of particles submerged in matrices like metals or ceramics. Due to random particle accumulation, they are typically isotropic. The benefits of certain composites include greater strength, higher working temperature, resistance to oxidation, and so on. Examples include the application of rubber aluminium particles, the use of gravel, sand and cement in aluminium particles and the use of cement. Flake composites consist of flat reinforcements of matrices. The common materials include glass, mica, aluminium and silver. The high outdoor bending module, high strength and cheap cost outcomes of flake composites offer excellent performance. Flakes cannot, however, be organised readily, and only a few elements may be utilised. In fiber composites, matrix reinforcement may be short or long (discontinuous) or long.

II. LITERATURE REVIEW

Mr. Tolessa Berhanu (2020) The industrial methods of reducing carbon emissions and recyclable materials that limit waste play a significant significance in natural fibers. Added flexibility may be achieved in fiber composites by producing hybrid composites, when more than one kind of fiber is used. Cost efficiency may be improved by employing various reinforcing types carefully and selectively to get the greatest strength in highly stressed places and orientations. The cost of hybrid composites may be reduced by decreasing the amount of carbon fiber while optimum positioning or orientation of the fiber maximises performance. As an alternate approach for fiber reinforced composites, natural fibers have lately become interestingfor researchers due to their properties. This study reviewed the uses and different characteristics of natural fibers such as hemp, jute, sisal kenaf and was used for glass fiber replacement.

Bhattacharya Somnath (2020) For researchers in recent years, polymer composites have become one of the most significant fields. It is because polymer composites havea higher resistance to weight ratio than most traditional metals and composites now used for structural purposes. In addition, the researchers are also developing new hybrid composites to attain the mechanical characteristics required. This review of hybrid polymer composites therefore focuses on mechanical properties such as impact, bending and tensile strengths of hybrid polymer composites in order to show that their mechanical behaviour, influenced by crucial factors such as type selection, orientation and the arrangement of reinforcement in polymer matrix composites, is essential. This comprehensive study is an attempt to reveal the key elements of this field as unexplored research gaps. The research indicates that there is a restrictedusage of fillers in hybrid polymer composites (such as red mud and fly ash) and natural fibers (abaca, bamboo, ramie and coir). The study also reveals a lack of research that has been carried out in order to model, forecast and optimise mechanical features such as hardness, bending strength, tensile strength and impact strength of hybrid composites. It also reveals that

Brostow Witold (2020) Although universities and industry concentrate mostly on material characteristics, wear generates losses in the industry at least not less than mechanical deformation fractures. We talk about the significance of polymer based materials for tribology (PBMs). For at least two reasons, traditional tribology initially established for metals could not be used to PBMs. Their characteristics — unlike to metals and ceramics – vary on time, and PBMs are viscoelastic. Second, PBMs readily absorb external liquid lubricants, which are successful for other types of materials; the consequence is swelling. Taking into account viscosity, materials fragility defined in 2006 and the linkages between frailty and recuperation when determining sliding wear, the relation of friction and surface resistance to scratch tension and the impacts of magnetic fields on polymer tribology, both of us develop tribology of PBMs. Traditional wear assessment techniques based on the quantity of debris produced do not work for PBMs since often there is no debris - yet the material movement is considerable (top ridge formation, densification). There is discussion about more suitable test methods. Computer simulations of scratching polymers are also addressed in the results of molecular dynamics. In addition, we explore techniques for improving scratch and wear resistance to PBMs. The above-mentioned techniques include modification of surface pressure, microhybrid creation, forming of nanohybrids and irradiation. Based on the overall findings and ideas and models from experiments and simulations, several suggestions have been given for addressing PBM tribology, both in instructional and industrial as well as research environments.

Huang Ming (2020) - Composites are materials composed of two single components at least. While polymers relate to various materials it will be possible to enhance the characteristics of each polymer, such as the mechanical strength, surface quality and biocompatibility. The

composites are normally used in the aerospace, car, military, and sports industries, and are used in biomedicine gradually in tissue engineering, wound dressings, drug release, regenerative treatment, composites in the dental pitch, and operations. The research topics in this area include specific questions on how best various materials and material characteristics may be coordinated.

Isiaka Oluwole Oladele et al (2020) - Isiaka Oluwole Oladele et al. Polymer materials have directly been found to be helpful for many purposes from the earliest days, but their usage has not been fully understood. Nevertheless, polymer materials havegradually dislodged other materials in a number of applications by adjusting this pattern. Polymer-based materials are the best choice for a few applications recently, thanks to better inspection and information, and are now supplying various materials rapidly. Even in areas where polymers have been deemed not to be suitable inprevious times, more materials from polymers are cultivated each day as a replacement for other materials. Most of the time in industries like building, aircraft, cars and medical, polymers are used to substitute metals and ceramics. It is no doubt that due of the innate characteristics of polymers and the management capacity, this pattern will continue. Today, in the composite materials strategy, most of the limitations of polymers are addressed. Researchers and analysts are also responsible for the transition to positive ecological effect. This study now unlocks the areas in which polymer-based composites are used and the significance of these materials for human progress.

III. METHODOLOGY

PROPOSED METHODOLOGY

The study has been divided into following sections:

Part A - Impact of Fiber Length and Loading on the Properties of Schumannianthus Dichotomus (Murta) Fiber Reinforced Epoxy Composites

- **Materials**

The polymer matrix is made of Araldite AW106 epoxy resin and HV953U hardener. Bisphenol A Diglycidyl Ether with the same epoxy weight as 214 – 221 g eq-1 is included in Araldite AW106. The HV953U hardener includes 1,3-propylenediamine N-(3-dimethaminopropyl)-. Figure 3.1 shows BADGE's molecular structures and hardeners. The resin and hardener were purchased and used as required by a local supplier. The NaOH grade laboratory reagent has been used for the treatment of fibers(S. D. Fine Chemicals, India).

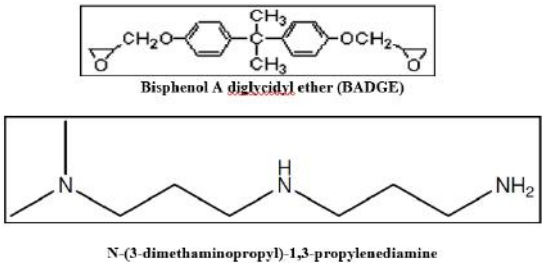

Fig.3.1 Molecular structures of BADGE (top) and the hardener (bottom)

IV. RESULTS

4.1 DATA ANALYSIS ON PART A

Natural fiber reinforced polymer composites are being discovered as a result of the increasing environmental impact, energy shocks and production pricing issues as increasing uses in most manufacturing industries such as automotive components, sports systems, electrical components and packaging materials. The most utilised natural polymer enhancement fibers, such as bamboo, wood, cotton, coir, sisal, flax, kenaf, hemp and jute. Other natural Lignocellulosic Fibers were alsoutilised, such as curaua, nettle, aloevera, abaca, palm oil, wheat straw, banana, bagasse, pine aple, rice husk, olive shell, henequen, etc. The research has continuously being evaluated to enhance the quality of natural fiber-reinforced polymer composites. Natural fibers gain from the easy accessibility of their components, the renewability of them, their biodegradability, their light density, their considerable strength (force/density ratio), their minimum cost and their non- corrosive nature. The main disadvantage in the usage of natural fibers is that it is not compatible with polymer matrix because of hydrophobicity and polymer fibers which,however, may be addressed by chemical treatments modifying the areas of the fibers.

This chapter continues to make use of the polymer composite in which a novel naturalfiber is used from a plant whose scientific name really is Schumannianthus dichotomus Gagnep. Murta is grown in western Bengal and assam India and Bangladesh's northeast regions. In Myanmar, Thailand, Cambodia, Vietnam, the Philippines and Malaysia, murta plants are found on the basis of the Wikipedia. Figure 4.1 shows the image of murta plant life. Many handcraft items such as mat (sometimes called local sitalpati), handbag, cap, handfan, etc., are produced from murta fiber, which means that many typical people in BangLadesh and India survive on it. This means that they are made of murta fiber. Details of the murta plant and of small-scale murta fiber companies are registered. There is just one study on the analysis of the polyster composite reinforced murta mat. The inner (so-called maji) portion of

the murta stem was used in the existing work for reinforcement of the polymer matrix and this interior part of the murta stem was often thrown during the creation of the murta mat.

Fig.4.1 Murta plants

4.1.1 Characteristics of Fiber, Density, SEM images and IR spectra

Table 4.1 records the characteristics and chemical makeup of the murta central element. Table 4.1 also gives comparisons of the characteristics and chemical compositions of a number of realised natural fibers. 29 The fiber's typical diameter and density have been calculated to be 0.14 ± 0.01 mm and 0.94 ± 0.01 g cm-3, respectively. The density of the polymer matrix exploratory value is 1.05 ± 0.01 g-cm and that of the composites is shown in Figure 4.2

Table 4.1 Composition and properties of murta and other fibers

Fiber	Cellulose (%)	Hemicellulose (%)	Lignin (%)	Density (g cm^{-3})	TS (MPa)
Murta core fiber	38	26	22	0.94	242 ± 24
Jute	71	20	13	1.30	393 - 773
Sisal	65	12	10	1.50	511 - 635
Coir	43	0.3	45	1.20	175
bamboo	26 - 43	30	21 - 31	0.80	140 - 230
Flax	71	21	2	1.50	345 - 1035
Kenaf	72	20	9	1.20	930

There has been discovered that the density of composites is unimportant dependent onthe fiber's length, but the fiber's weight percent has grown. Composites have a greater density than polymers and fibers and the most notable density is 1.22 g cm-3, which is 35 percent weight. Density expansion indicates that there is no void and that composites are minimum because to strong connections between the fibers and polymers. The fiber's antiacide treatment should result in a particularly strong link between the fiber and the polymer. Figure 4.3 shows the SEM images of the non- treated and processed fiber and it is very obvious that the external side of the treatment fiber with fillers and splitting is uneven and unpleasant. The hard surface of the processed fibers is used to limit the fiber to the polymer.

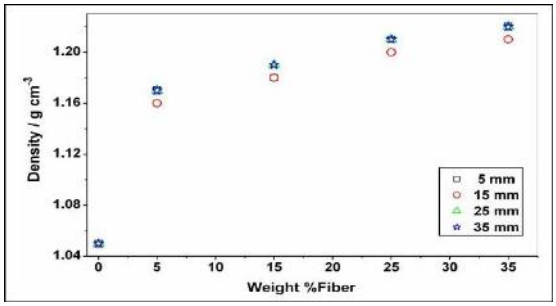

Fig.4.2 Density (± 0.01 g cm^{-3}) of the polymer composite as a function ofweight %of fiber of different lengths

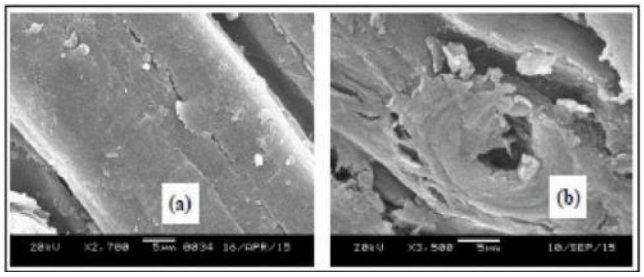

Fig. 4.3 SEM images of (a) untreated fiber and (b) treated fiber.

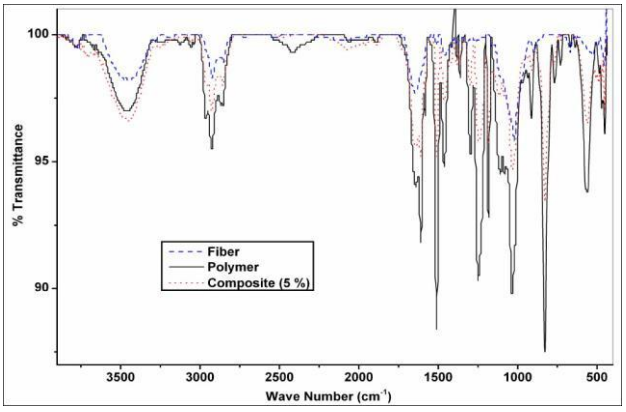

Fig.4.4 FTIR spectra of the fiber, polymer and composite (containing 5weights %fiber). The inset shows expanded view of the band near 3460 cm^{-1}

The strong partnership of the fiber and the polymer from the IR spectrum in Figure 4.4 is also apparent. The IR band in the fiber is 3450 cm-1 with the OH band while the IR band

in the polymer is 3 460 cm-1 with the OH band exactly as the NH band isin the polymer. In addition, the IR belt with 3455 cm-1 compared to the OH and NH extension in the polymer composite. The expanded and expanded belt force in the composite polymer shows that hydrogen retention between fibers and polymers is improved throughout the composite development.

4.1.2 Thermal Behaviour

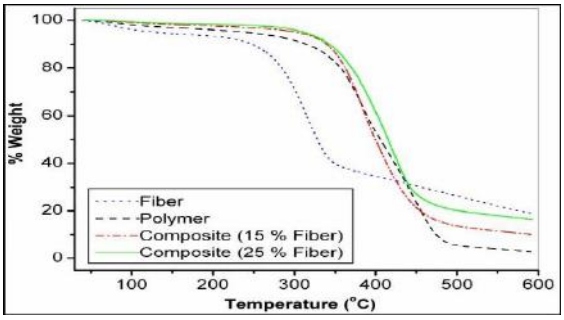

Fig.4.5 Thermograms of the fiber, polymer and composites obtained from theTGA

Figure 4.5 displays the thermograms of the TGA-acquired fiber, polymer and composites. Two stages of thermal fiber corruption occur. The main decay of fiber occurs rapidly and starts from 228 °C to 357 °C. 62% of the fiber weight at this stage is corrupted, due to cellulose, hemicellulose and less lignin thermal degradation. The second phase is a result of the slow thermal degradation of hemicelluloses and lignine,which begins when temperature exceeds 357 °C. At 6000C the fiber corruption is 80 percent in weight. This debasement is a little bit lethargical. Somewhere between 293 and 485°C, the polymer corruption occurs in one rapid step. The amount of polymer corrupted at 485 °C is 93 percent weight. The concept of composite thermograms resembles that of the polymer and the bulk of the corruption occurs quickly. The bribery starts at approximately 305°C and continues to 460°C in both compositional products with 15 and 25 percent fiber. Therefore the composite is slightly more thermal than the polymer. The thermal sounds of the polymer matrix may thus be improved by murta fibers; in the present instance, 293 to 305°C. The heat degradationis almost insignificant in the composites above 460 °C because of the polymer. As the fiber weight percentage increases, in general the composite decrease is because the lignin total increases in a composite with the expanding fiber.

4.1.3 Tensile Strength

The intentional strength of the fiber's tensile strength (TS) is equal to 242 ± 24 MPa and the strength of the polymer and composites in Table 4.2 are shown in Figure 4.6. Figure 4.6 shows that both the fiber length and the measurement of the TS in the composite are susceptible. TS is common in natural fiber-reinforced composites witha fiber total and length. The composite TS is administered by a couple of variables such as matrix fiber selection, the matrix fiber orientation, fiber length measurement, fiber matrix adhesion measurement, and so on. The sum, length, and compatibility of the fiber surface are thus restricted to these amount of variables in order to ensure homogeneous compound and advancement of the fiber-matrix-Interfaces pressuremove instrument. The largest TS is achieved with a fiber load of 25 percent weight and a fiber length of 25 mm on the composite being investigated. The highest extreme of the TS is 57.6 MPa, an expansion of 145% compared to the clean polymer TS. At 25% fiber loads, the growth of TS is about 19% by extending the fiber length from 5to 25 mm, while by increasing the fiber longitudinal from 25 to 35 mm TS has decreased by roughly 14%. The base fiber length is 25 mm along these lines and the main fiber charge for the present composite is 25 percent by weight. At the time of theexpansion of fiber load above 25 percent TS the load started to decrease. This is attributed to fiber aggregation creating interruptions in fiber adhesion and weakening. The SEM photos in Figure 4.7 show that the fibers are more than 25 weights percent agglomerated.

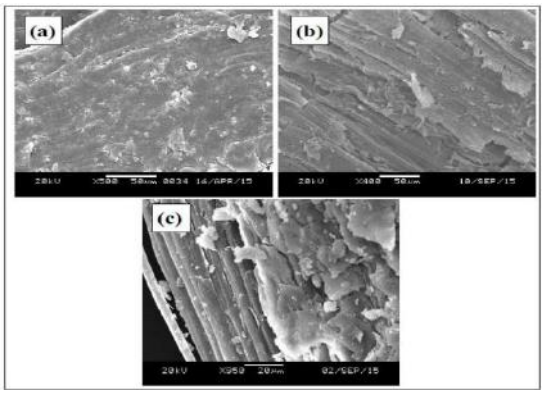

Fig.4.6 SEM images of (a) neat polymer, (b) 5 % fiber composite and (c) 35 % fibercomposite

Table 4.2 Tensile strengths of the composite as functions of fiber load and fiberlength

Weight % Fiber	Fiber length (mm)			
	5	15	25	35
	Tensile Strength (MPa) (TS of Neat Polymer = 23.5 MPa)			
5	35.6	37.6	36.6	34.9
15	39.5	40.0	41.5	41.7
25	48.3	52.6	**57.6**	49.6
35	41.5	45.6	48.6	42.6

4.1.4 Strength

Like TS, when the composite includes 25 percent weight of

25mm fiber it is anything but an important factor to get a flexural strength (FS) of the polymer by constructing the fiber (Table 4.3 and Figure 4.8). As with TS, therefore, the optimal FS for the polymer composite is both the length and the fiber measurement. The highest FS value is 64.8 MPa, which is around 126% more than the FS of clean polymer. FSstarts to decrease by about 25 percent, and by around 6 percent, the fiber load falls at 35 percent of FS of the composite. In Figure 4.9, the FS-Ts ratio (force ratio) was compared to the fiber total. Most FS is greater than TS, such that the bending force is larger than the extending force. The FS comes out to not be precisely the TS if the fiber length exceeds the basic length which shows that the characteristics of the stacked fiber below or below the base length are differentiated. The SEM images in Figure 4.7 show the buildup of 35 mm long fibers effectively revealed.

Table 4.3 Flexural strengths of the composite as functions of fiber load and fiberlength

Weight % Fiber	Fiber length (mm)			
	5	15	25	35
	Flexural Strength (MPa) (FS of Neat Polymer = 28.7 MPa)			
5	42.7	45.5	46.3	30.0
15	45.6	50.6	48.6	36.3
25	49.3	53.6	**64.8**	44.5
35	44.6	52.3	60.6	40.5

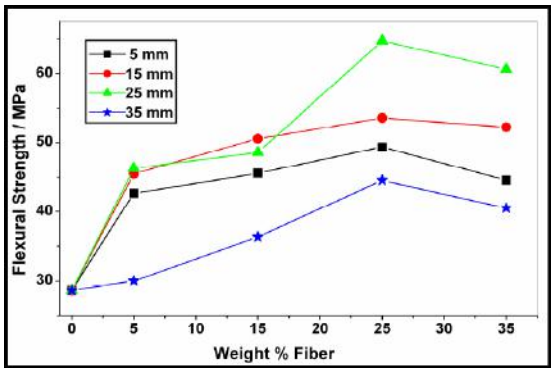

Fig.4.8 Variation of flexural strength of the composite with weight % of fiberat fixed fiber lengths

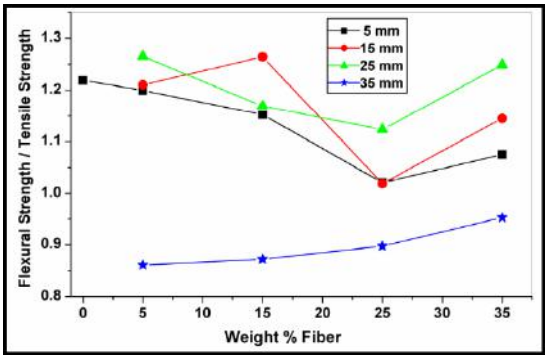

Fig.4.9 The ratio of flexural strength to tensile strength as a function of fiber amount at fixed fiber lengths

V. CONCLUSION

Composite materials have a very adaptable component lay out above normal materials due to their clear strength, strength, and exhaustive characteristics. Composite materials consist of at least two components having truly split phases. However, it is regarded as comparable to a composite material only when composites exhibit significantly distinct real characteristics.

Composites are materials that include material with solid loads (known as supports) (known as matrix). Composite materials, plastics and ceramics were the predominant materials over the past thirty years. Composite material volume and quantity of applications have continuously evolved, entering and overcoming new economic areas. Current composite materials provide a wide rise from common goods to refinedspecialised applications on the designed material market. While composites haveproved their worth as weight saving materials, they are financially knowledgeable. The present test. Several innovative assembly methods have lately been used for the composite industry in the attempts to create financially attractive composites.

REFERENCES

[1] Huang H. M. (2020). Medical Application of Polymer-Based Composites. Polymers, 12(11), 2560. https://doi.org/10.3390/polym12112560

[2] Isiaka Oluwole Oladele, Taiwo Fisayo Omotosho, Adeolu Adesoji Adediran, "Polymer-Based Composites: An Indispensable Material for Present and Future Applications", International Journal of Polymer Science, vol. 2020, Article ID 8834518, 12 pages

[3] Mr. Berhanu Tolessa, (2020), Mechanical Properties of Natural Fiber Reinforced Hybrid Polymer Composites: A Review, International Research Journal of Engineering and Technology (IRJET), Volume: 07 Issue: 05 | May 2020

[4] Somnath Bhattacharya –Mechanical properties of hybrid polymer composites: a review‖ 42, Article number: 431 (2020)

[5] Witold Brostow –MECHANICAL AND TRIBOLOGICAL PROPERTIES OF POLYMERS AND POLYMER-BASED COMPOSITES‖ Vol. 14, No. 4, pp. 514–520 Chem. Chem. Technol., 2020

[6] Y. Laidani, S. Hanini, G. Mortha, and G. Haninia, *Iran. J. Chem. Chem.Engg.,* 31(2012), 119-129.

[7] Yongli Zhang, Yan Li, Hao Ma and Tao Yu (2013), –Tensile and interfacial properties of unidirectional flax/glass fiber reinforced hybrid composites‖. Composites Science and Technology, 88, pp.172–177.

[8] Venkateshwaran N, Elaya Perumal A, Alavudeen A and Thiruchitrambalam M (2011), –Mechanical and water absorption behaviour of banana/sisal reinforced hybrid

composites‖ Materials & Design, 32(7), pp. 4017-4021

[9] Velmurugan R and Manikandan V (2007), ―Mechanical properties of palmyra/glass fiber hybrid composites‖ Composites Part A: applied science and manufacturing, 38, 10, pp. 2216-2226

[10] V Bhanutej J and Nagaraju B (2019) - Polymer Based Composites via Fused Filament Fabrications (FFF) - A Review and Prospective. International Journal of Engineering Research & Technology (IJERT) ISSN: 2278-0181 Published by, www.ijert.org AMDMM - 2019 Conference Proceedings

Journal of Molecular Liquids 344 (2021) 117780

Contents lists available at ScienceDirect

Journal of Molecular Liquids

journal homepage: www.elsevier.com/locate/molliq

Thermophysical properties of amino acids L-serine and L-leucine in aqueous diammonium hydrogen phosphate solutions: Volumetric and acoustic studies

Harsh Kumar [a,*], Vaneet Kumar [b,c,*], Seema Sharma [b,d], Ayman A. Ghfar [e], Arjuna Katal [f], Meenu Singla [a], Khyati Girdhar [g]

[a] Department of Chemistry, Dr B R Ambedkar National Institute of Technology, Jalandhar, Punjab 144011, India
[b] IKG Panjab Technical University, Kapurthala Road, Jalandhar, Punjab, India
[c] Department of Applied Sciences, CT Group of Institutions (CTIEMT), Shahpur, Jalandhar, Punjab, India
[d] MRPD Govt Arts and Science College, Talwara, Punjab 144216, India
[e] Department of Chemistry, College of Science, King Saud University, P.O.Box 2455, Riyadh 11451, Saudi Arabia
[f] YRBN GSSS Darbar Pandori, Gurdaspur, Punjab 143531, India
[g] Department of Biology, Boston College, Chestnut Hill, MA 02467, USA

ARTICLE INFO

Article history:
Received 17 August 2021
Revised 22 September 2021
Accepted 5 October 2021
Available online 8 October 2021

Keywords:
L-serine
L-leucine
Diammonium hydrogen phosphate (DAP)
Solute-solvent interactions

ABSTRACT

Densities and speeds of sound measurements have been done for the amino acids (AAs) L-serine and L-leucine in aqueous diammonium hydrogen phosphate (DAP) solution at different temperatures with a specific interval of temperature. Thermophysical parameters including apparent molar volume (V_ϕ), partial molar volume (V_ϕ^0), apparent molar isentropic compression ($K_{\phi,s}$), partial molar isentropic compression ($K_{\phi,s}^0$) and transfer volumes like partial molar volumes of transfer (ΔV_ϕ^0) and partial molar isentropic compression of transfer ($\Delta K_{\phi,s}^o$) were determined using the measured experimental data. The co-sphere overlap model was used to interpret the sort of interactions dominating in the system. The obtained transfer quantities are positive which indicates the dominance of ion-hydrophilic and hydrophilic–hydrophilic interactions existing among the amino acids and diammonium hydrogen phosphate salt solution in aqueous medium. Pair and triple interaction coefficients calculated for the system of amino acids and phosphate salt in aqueous medium. Overall results have been elaborated in terms of the solute-solvent or solute-solute interactions prevailing in the system.

1. Introduction

Due to numerous specific interactions, it becomes onerous to recognize the interaction behavior of large biomolecules such as hormones, enzymes, and especially proteins. The stabilization or destabilization of the proteins is communicated by the addition of specific or external molecules to protein solutions [1,2]. Amino acids are well known versatile constituents and these are the fundamental substances for building proteins [3]. Conformational appearances of proteins depend upon the properties and the interaction with the surrounding environment [4]. The interactions are mostly taking place among the protein molecules and the ions of solvent. Therefore, one useful approach is to investigate interactions of the model compounds of proteins i.e. amino acids, in aqueous and mixed aqueous solutions. Hydrophobic group or charged atomic groups and ions are components of almost every biologically important system [5]. It is generally recognized that the hydration of such atomic groups plays an important role in the conformational stability of biopolymers [6]. Consequently, characterization of the hydration properties of both hydrophobic and charged groups should provide insights into the role of solute-solvent interactions associated with fundamental protein phenomena such as folding/unfolding transitions, solubility, and denaturation [7,8]. Because proteins are large complex molecules, the direct study of protein– electrolyte interactions is difficult. It is therefore, useful to investigate the interaction of model compounds such as amino acids, peptides, and their derivatives that constitute part of the protein structures [5,9]. Thermodynamic variables like temperature and pressure affect the proteins in aqueous medium and play a key role in

* Corresponding authors.
E-mail addresses: manchandah@nitj.ac.in (H. Kumar), vaneet2106@gmail.com (V. Kumar).

https://doi.org/10.1016/j.molliq.2021.117780
0167-7322/

establishing a complete interpretation of the physical immutability. Thus their thermodynamic properties in a variety of media can provide valuable information about the stability and denaturation of proteins [10–13]. Amino acids, the biologically important compounds are of immense importance as their behavior in aqueous and mixed aqueous solutions is different. There are intensive work reported in the literature for the amino acids in various solutions like ionic liquids [9,14–22] salts [23–26] drugs [29–31], carbohydrates [10,11,31]. Along with this the amino acids are also utilized in different field [22,32–38]. In this paper we are using the amino acids in combination with the diammonium hydrogen phosphate salt solutions in aqueous media. The densities and speeds of sound measurement have been done are further values utilized to acquire the thermodynamic properties. Experimental data of the densities and speeds of sound of amino acids L-serine and L-leucine in aqueous solution of salt diammonium hydrogen phosphate at different molal concentrations and different temperatures have been recorded. The obtained data of densities and speeds of sound have been utilized to know about the thermodynamic properties and reviewed in terms of solute-solute and solute-solvent interactions in the current system of amino acids and salt. These properties are further helpful in explaining the structure making/breaking nature of solutes and the dominance of the sort of interactions prevailing in the system.

2. Materials and methods

2.1. Chemicals

The chemicals taken for the study are amino acids L-Serine, L-leucine and salt diammonium hydrogen phosphate were procured from different sources. The amino acid L-Serine was procured from Merck, Germany and the amino acid L-leucine and salt diammonium hydrogen phosphate were purchased from HiMedia Chemicals. Pvt. Ltd., India. All the chemicals were vacuum dried and stored in desiccators over P_2O_5 for at least 48 h before their use. Specification of the chemicals has been mentioned in the Table 1.

2.2. Apparatus and procedure

All the samples were prepared by weighting mass on a Sartorius CPA225D balance having precision of ± 0.00001 g. The densities and speeds of sound of the mixtures were measured at different temperatures with a Anton Paar DSA 5000 M densimeter with proportional temperature control that kept the samples at working temperature within ± 1 × 10^{-3} K by a built-in Peltier device. The Anton Paar DSA 5000 M densimeter was calibrated before each measurement. The details of calibration of the densimeter and procedure for measurements are already reported in our earlier study [14]. The relative uncertainty in molality for the compounds with purity 99% is $u_r(m)$ = 0.01. The speeds of sound measurements were carried out at a frequency of 3 MHz's. As per the instrument sensitivity, densities and speeds of sound can be measured to ± 1 × 10^{-3} kg m^{-3} and 1 × 10^{-2} m s^{-1}, respectively. The density and speed of sound measurements have a standard uncertainty of ± 0.15 kg m^{-3} and 0.8 m s^{-1}, respectively.

3. Results and discussion

3.1. Density measurements

The experimental values of densities, ρ for both the AAs L-leucine, L-serine in (0.5, 1.0, 1.5, 2.0) mol kg^{-1} aqueous solutions of diammonium hydrogen phosphate DAP at temperatures range from 288.15 K to 318.15 K measured at the interval of 10 K. The experimental values of densities for amino acids in aqueous solutions of DAP has been mentioned in Table 2. It is observed that the obtained values are positive for each measurement of density and increases with the rise in the concentration of the amino acids. The obtained values of densities for the AAs and for the salt have been compared with the literature [39–45]. It is obtained that the values of amino acids measured experimentally are in good agreement with the literature as mentioned in Table 2 and graphically shown in the Figs. 1–4. The densities values for aqueous solutions of salt DAP at different concentration and different temperatures are also reported in the Table 2. The obtained densities values are compared with the literature [46–48] and found in good agreement. Also the graphical representation for the same have been done and mentioned in the Fig. 5. In Fig. 5 the plots 5(a)–5(d) are representing the temperature wise comparison of the densities data with literature.

3.1.1. Apparent molar volume

The apparent molar volumes (V_ϕ) are calculated from the experimental values of density (ρ) using the equation (1) given as follow

$$V_f = [(M/r) - \{(r - r_0) / (m_A r r_0)\}] \quad (1)$$

where M is the molar mass of the solute (kg·mol^{-1}), m_A is the molality (mol·kg^{-1}) of the amino acids, i.e., the amount of solute (amino acids) per kilogram of solvent (mixture of water and DAP), and ρ_0 and ρ are the densities (kg·m^{-3}) of the solvent and solution, respectively. Apparent molar volumes signify the sort of interactions favored in the system. The positive values of apparent molar volumes (V_ϕ) values signify solute-solvent interactions between amino acids and ions of salt which undergo dissociation in aqueous medium. The experimental values of densities along with apparent molar volume values obtained by equation (1) are reported in Table 2. It is determined from Table 2 the obtained values are positive for the apparent molar volumes. The apparent molar volumes values signify the sort of interactions prevailing in the system [4,14]. Obtained values are positive which demonstrate that the solute-solvent interactions existing in the ternary system of amino acids, DAP and aqueous. The values are rising with the increase in temperature shows that solute-solvent interactions are more dominating with the temperature. The graphical representations of the values of V_ϕ for both the amino acids have been done and represented in the supplementary file as Figure S1 to S3. Figure S1 and S2 showing the values of V_ϕ for L-serine and Figure S3 representing the same for L-leucine. These figures demonstrate that the all the values are positive and rises with the temperature which causes a greater affinity for solvent and therefore intensifies the pronounced solute-solvent interactions occurring among the zwitterions of amino

Table 1
Specification of studied chemicals.

Chemical	CAS number	Source	Purification method	[a]Mass fraction purity
L-serine	56–45-1	Merck, Germany	Drying over P_2O_5	≥ 0.99
L-leucine	61–90-5	Hi Media Chem. Pvt. Ltd., India	Drying over P_2O_5	≥ 0.99
Diammonium hydrogen phosphate	7783–28-0	Hi Media Chem. Pvt. Ltd., India	Drying over P_2O_5	≥ 0.99

[a] As declared by supplier

Table 2
Densities, ρ and apparent molar volumes,$V_\phi$of amino acids in aqueous solutions of DAP at different temperatures and experimental pressure, p = 0.1 MPa.

[a]m_A/ (mol·kg^{-1})	$\rho \times 10^{-3}$ / (kg·m^{-3})				$V_\phi \times 10^6$ / (m^3·mol^{-1})			
	T = 288.15 K	T = 298.15 K	T = 308.15 K	T = 318.15 K	T = 288.15 K	T = 298.15 K	T = 308.15 K	T = 318.15 K
L-serine + aqueous 0.5 mol·kg^{-1} DAP								
0.00000	1.032460	1.030238	1.026598	1.022501				
	1.032480[b]	1.030218[b]	1.026633[b]	1.022480[b]				
	1.032884[c]	1.030119[c]	1.026582[c]					
	1.032626[d]	1.030712[d]	1.026097[d]	1.022846[d]				
0.10030	1.03681	1.03455	1.03088	1.02675	60.82	61.24	61.60	61.96
0.20033	1.04115	1.03885	1.03515	1.03099	60.57	60.99	61.34	61.71
0.29859	1.04542	1.04308	1.03935	1.03516	60.32	60.74	61.10	61.46
0.39885	1.04977	1.04739	1.04363	1.03941	60.07	60.49	60.84	61.21
0.47751	1.05318	1.05077	1.04699	1.04275	59.87	60.29	60.65	61.02
0.59662	1.05835	1.05589	1.05207	1.04780	59.58	60.00	60.36	60.72
0.69108	1.06245	1.05995	1.05611	1.05180	59.35	59.77	60.13	60.49
L-serine + aqueous1.0 mol·kg^{-1}DAP								
0.00000	1.066201	1.063979	1.060019	1.055685				
	1.066233[b]	1.063997[b]	1.060051[b]	1.055717[b]				
	1.066397[c]	1.064032[c]	1.060217[c]	1.055590[c]				
0.09037	1.066201	1.063979	1.060019	1.055685	61.05	61.45	61.81	62.27
0.198196	1.070033	1.067775	1.063787	1.059417	60.79	61.19	61.55	62.01
0.29959	1.074605	1.072303	1.068284	1.063870	60.55	60.95	61.31	61.77
0.39727	1.078904	1.076562	1.072512	1.068058	60.32	60.72	61.08	61.54
0.49680	1.083045	1.080664	1.076585	1.072092	60.08	60.49	60.84	61.30
0.59755	1.087265	1.084845	1.080736	1.076203	59.85	60.25	60.61	61.06
0.69784	1.091537	1.089076	1.084937	1.080364	59.62	60.02	60.37	60.83
L-serine + aqueous 1.5 mol·kg^{-1}DAP								
0.00000	1.097287	1.095067	1.09078	1.086289				
	1.097301[b]	1.095097[b]	1.09076[b]	1.086332[b]				
	1.097529[c]	1.095182[c]	1.090108[c]	1.086187[c]				
0.10001	1.101397	1.099147	1.094820	1.090289	61.41	61.72	62.16	62.63
0.19962	1.105491	1.103211	1.098845	1.094274	61.18	61.49	61.93	62.39
0.29714	1.109499	1.107190	1.102784	1.098175	60.96	61.27	61.71	62.17
0.39659	1.113587	1.111248	1.106802	1.102153	60.74	61.04	61.49	61.95
0.49608	1.117676	1.115307	1.110822	1.106132	60.52	60.82	61.27	61.72
0.59518	1.121749	1.119350	1.114825	1.110096	60.30	60.60	61.05	61.50
0.70098	1.126097	1.123667	1.119100	1.114328	60.06	60.37	60.81	61.27
L-serine + aqueous2.0 mol·kg^{-1}DAP								
0.00000	1.125765	1.123499	1.119175	1.114703				
	1.125824[b]	1.123553[b]	1.119143[b]	1.114667[b]				
0.10000	1.129725	1.127399	1.123035	1.118543	61.89	62.43	62.87	63.16
0.20028	1.133696	1.131310	1.126906	1.122394	61.67	62.21	62.65	62.94
0.29871	1.137594	1.135149	1.130705	1.126173	61.46	62.00	62.44	62.73
0.40167	1.141671	1.139164	1.134679	1.130127	61.24	61.78	62.22	62.51
0.49460	1.145351	1.142788	1.138267	1.133696	61.04	61.59	62.03	62.31
0.59858	1.149469	1.146844	1.142280	1.137688	60.83	61.37	61.81	62.09
0.69012	1.153094	1.150414	1.145814	1.141204	60.63	61.18	61.62	61.90
L-leucine + aqueous 0.5 mol·kg^{-1}DAP								
0.00000	1.032460	1.030238	1.026598	1.022501				
	1.032480[b]	1.030218[b]	1.026633[b]	1.022480[b]				
	1.032884[c]	1.030119[c]	1.026582[c]					
	1.032626[d]	1.030712[d]	1.026097[d]	1.022846[d]				
0.01084	1.032645	1.030421	1.026781	1.022685	110.98	111.38	111.72	112.00
0.02061	1.032812	1.030586	1.026946	1.022851	110.97	111.36	111.70	111.99
0.03833	1.033115	1.030886	1.027246	1.023153	110.93	111.33	111.67	111.95
0.05913	1.033471	1.031237	1.027597	1.023506	110.90	111.29	111.63	111.91
0.08001	1.033828	1.031590	1.027950	1.023861	110.86	111.25	111.59	111.87
0.09961	1.034163	1.031921	1.028281	1.024194	110.82	111.22	111.55	111.84
0.12119	1.034532	1.032286	1.028646	1.024561	110.78	111.18	111.51	111.80
L-leucine + aqueous 1.0 mol·kg^{-1}DAP								
0.00000	1.066201	1.063979	1.060019	1.055685				
	1.066233[b]	1.063997[b]	1.060051[b]	1.055717[b]				
	1.066397[c]	1.064032[c]	1.060217[c]	1.055590[c]				
0.00999	1.066331	1.064109	1.060149	1.055815	111.58	111.79	112.16	112.57
0.01962	1.066456	1.064234	1.060274	1.055940	111.56	111.77	112.15	112.56
0.03947	1.066714	1.064492	1.060532	1.056198	111.54	111.75	112.12	112.53
0.05947	1.066974	1.064752	1.060792	1.056458	111.51	111.72	112.09	112.50
0.07910	1.067229	1.065007	1.061047	1.056713	111.48	111.69	112.06	112.48
0.09875	1.067485	1.065263	1.061303	1.056969	111.46	111.66	112.04	112.45
0.11938	1.067753	1.065531	1.061571	1.057237	111.43	111.64	112.01	112.42
L-leucine + aqueous 1.5 mol·kg^{-1}DAP								
0.00000	1.097287	1.095067	1.09078	1.086289				
	1.097301[b]	1.095097[b]	1.09076[b]	1.086332[b]				
	1.097529[c]	1.095182[c]	1.090108[c]	1.086187[c]				

(*continued on next page*)

Table 2 (*continued*)

[a]m_A/ (mol·kg^{-1})	$\rho \times 10^{-3}$ / (kg·m^{-3})				$V_\phi \times 10^6$ / (m^3·mol^{-1})			
	T = 288.15 K	T = 298.15 K	T = 308.15 K	T = 318.15 K	T = 288.15 K	T = 298.15 K	T = 308.15 K	T = 318.15 K
0.01002	1.097380	1.095160	1.090873	1.086382	111.81	112.02	112.43	112.94
0.01968	1.097470	1.095250	1.090963	1.086472	111.80	112.01	112.42	112.89
0.03994	1.097658	1.095438	1.091151	1.086660	111.78	111.99	112.40	112.85
0.05979	1.097843	1.095623	1.091336	1.086845	111.76	111.97	112.38	112.83
0.07963	1.098028	1.095808	1.091521	1.087030	111.74	111.95	112.36	112.80
0.09977	1.098215	1.095995	1.091708	1.087217	111.72	111.93	112.34	112.78
0.11934	1.098397	1.096177	1.091890	1.087399	111.70	111.91	112.32	112.76
L-leucine + aqueous 2.0 mol·kg^{-1}DAP								
0.00000	1.125765	1.123499	1.119175	1.114703				
	1.125824[b]	1.123553[b]	1.119143[b]	1.114667[b]				
0.00997	1.125820	1.123553	1.119229	1.114757	112.17	112.47	112.89	113.32
0.01969	1.125873	1.123605	1.119281	1.114809	112.17	112.46	112.88	113.32
0.03998	1.125985	1.123715	1.119391	1.114919	112.15	112.45	112.87	113.30
0.05996	1.126095	1.123823	1.119499	1.115027	112.14	112.44	112.86	113.29
0.07977	1.126204	1.123930	1.119606	1.115134	112.13	112.43	112.85	113.28
0.10010	1.126316	1.124040	1.119716	1.115244	112.12	112.42	112.84	113.27
0.11948	1.126422	1.124144	1.119820	1.115348	112.11	112.41	112.83	113.26

[a] m_A is the molality of amino acids in aqueous DAP solutions. [b, c, d] values of densities from reference [46–48] respectively. Standard relative uncertainties in molality are u_r (m) = 0.5 %, Standard uncertainties u (T) = 0.001 K, u (ρ) = 0.15 kg·m^{-3}, and u (p) = 0.01 MPa (0.68 level of confidence).

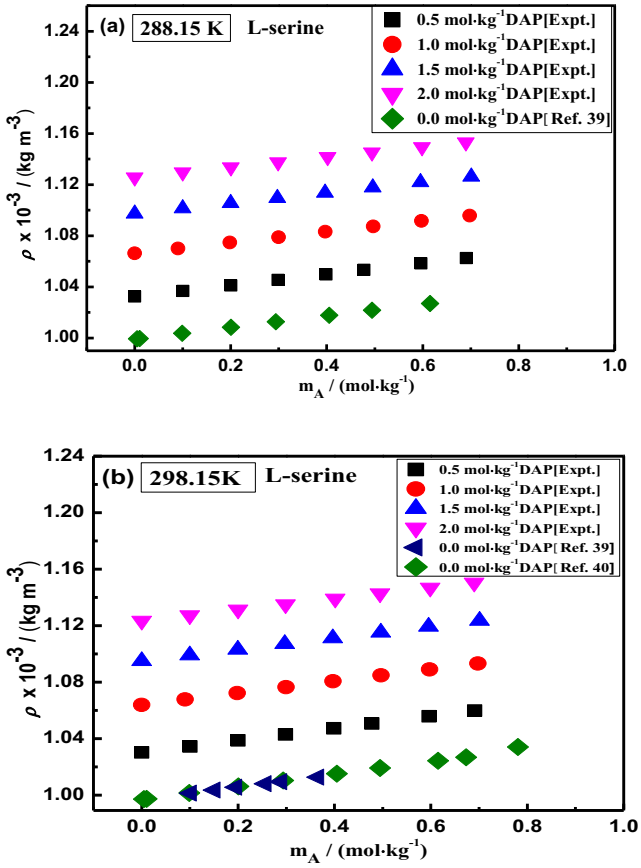

Fig. 1. Plots of comparison of densities values of L-serine in aqueous [39–40] and experimental density values for L-serine in aqueous solution of DAP (Diammonium hydrogen phosphate) at different concentrations (a) 288.15 K (b) 298.15 K.

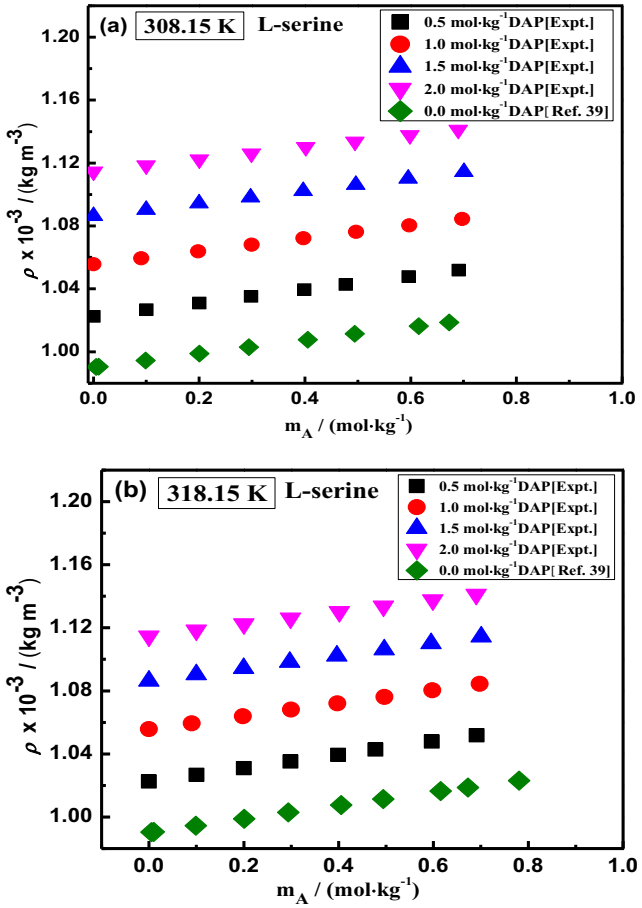

Fig. 2. Plots of comparison of densities values of L-serine in aqueous [39] and experimental density values for L-serine in aqueous solution of DAP at different concentrations (a) 308.15 K (b) 318.15 K.

acids and ions of the salt [3,14]. It is also observed that the values of apparent molar volumes are more for the L-leucine compared to L-serine, which signifies the predominance of solute-solvent interactions in L-leucine with the DAP solution in aqueous medium.

3.1.2. Partial molar volume at infinite dilution

Partial molar volume at infinite dilution $V_\phi^o$is free from the solute-solute interactions and depends upon the solute-solvent interactions. Partial molar volume at infinite dilution V_ϕ^0gives

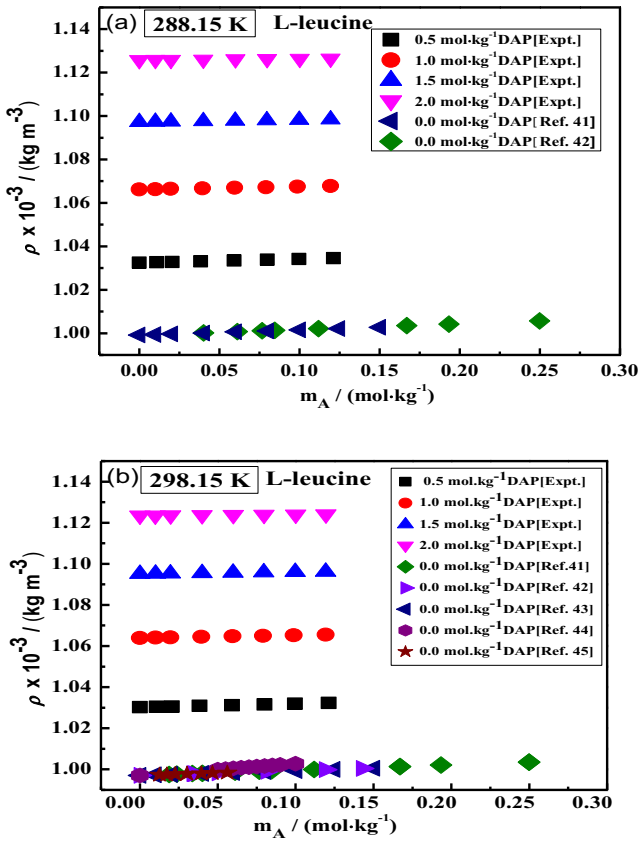

Fig. 3. Plots of comparison of densities values of L-leucine in aqueous [41–45] and experimental density values for L-leucine in aqueous solution of DAP at different concentrations (a) 288.15 K (b) 298.15 K.

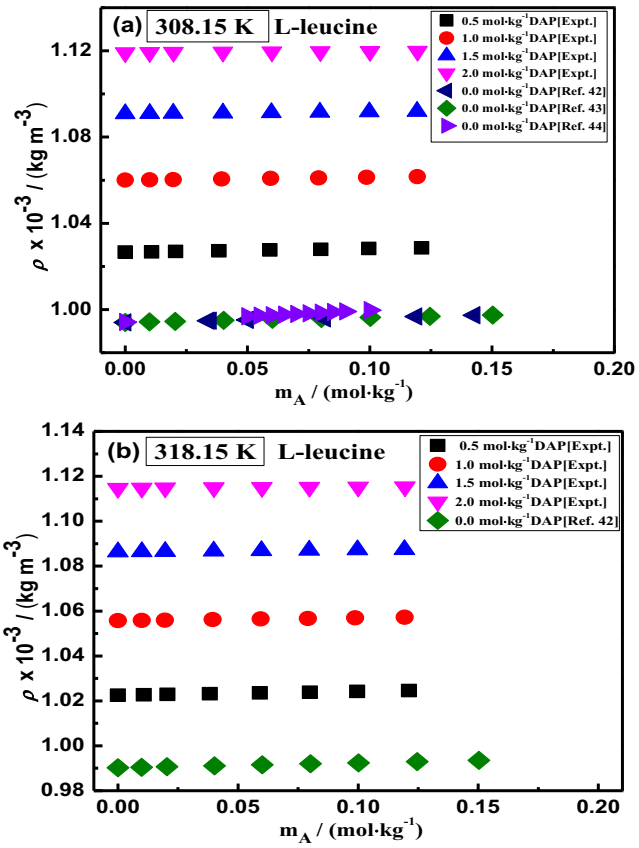

Fig. 4. Plots of comparison of densities values of L-leucine in aqueous [42–44] and experimental density values for L-leucine in aqueous solution of DAP at different concentrations (a) 308.15 K (b) 318.15 K.

information about the structural volume of solute in solvent and also volume change of solvent in the process of the shell formation around the ion [23,24]. Partial molar volume at infinite dilution V_ϕ^0 is free from solute-solute interactions and depends on solute-solvent interactions. Because it is assumed that at infinite dilution solute particles are surrounded by the solvent molecules, so the property partial molar volume gives the information of solute-solvent interactions. Partial molar volume at infinite dilution$V_\phi^0$is calculated by employing the least-squares fit of V_ϕ values using equation (2)

$$V_\phi = V_\phi^0 + S_V^* mA \tag{2}$$

where S_V^* the experimental slope is the volumetric pairwise interaction coefficient or semi empirical solute-solute interaction [49–50] parameter and m_A is the molality of amino acids in aqueous DAP solution. The obtained values of V_ϕ^0 and S_V^* calculated by least-squares fitting of V_ϕ values by equation (2) are revealed in Table 3 along with standard error deviations. It is observed that obtained values of partial molar volume at infinite dilutionV_ϕ^0 are positive for both amino acids. It is analyzed that values are larger for L-leucine than for L-serine. The large values of partial molar volume at infinite dilution$V_\phi^0$for L-leucine are due to the more hydration of the ions which undergoes greater interaction [3,23,43]. The values increase with the rise in temperature as well as with the rise in the concentrations, whereas in the case of L-leucine, the values increase with temperature but following an uneven trend with the rise in the concentration of the DAP. The change of partial molar volume at infinite dilution with temperature is due to different parameters such as thermal expansion, weakening of H-bond network, and release of molecules from solvation layers [15,49]. Along with the values of partial molar volume at infinite dilution the values of experimental slope S_V^* are also given in Table 3. It is noticed from Table 3 the obtained values of the experimental slope are negative. The values of experimental slope provide useful information about the solute-solute interactions [50,51]. The positive sign of the slope indicates that the solute-solute interactions existing in the system, while the negative sign leads to the solute-solvent interaction [52]. The obtained negative values of S_V^* indicates that the solute-solute interactions are less dominating as compare to solute-solvent interactions. So, from above discussion it is analyzed that the solute-solvent interactions are more dominating as compare to solute-solute interactions.

3.1.3. Partial molar volume of transfer

Partial molar volume of transfer at infinite dilution is the change in volume observed at infinite dilution and have been determined using the following equation (3)

$$\Delta V_\phi^0 = V_\phi^0(in\ aqueous\ DAP\ solutions) - V_\phi^0\ (in\ water) \tag{3}$$

The values of V_ϕ^0 for amino acids in water have been taken from already published work [39,53]. The positive values of Partial molar volume of transfer at infinite dilution demonstrate the strong ion–ion interactions existing in the system. It also favors the structure maker of promoter nature of the which is due to the solvophobic solvation as well as the structural interaction for two co-spheres as given by co-sphere overlap model [38,54–56]. These values of ΔV_ϕ^0 have been reported in Table 4. The obtained values of partial molar volume of transfer at infinite dilution are

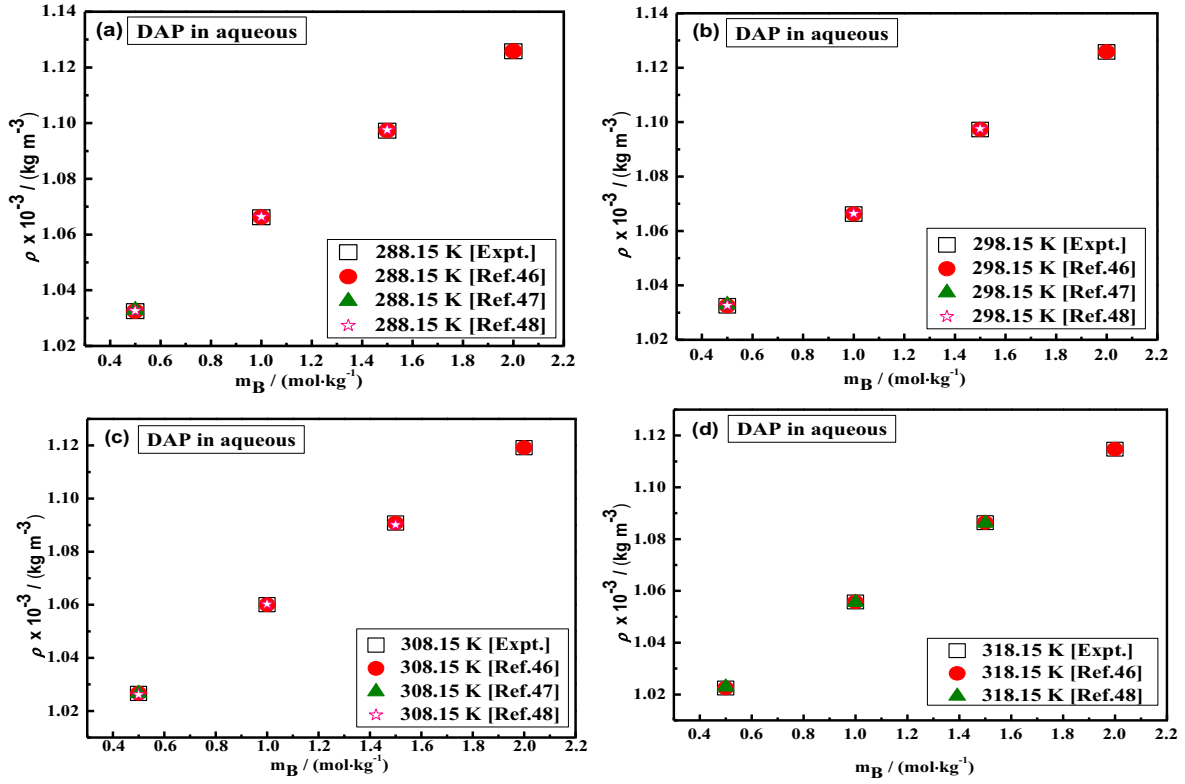

Fig. 5. Plots of comparison of densities values of DAP in aqueous experimental and literature [46–48] (a) 288.15 K (b) 298.15 K (c) 308.15 K (d) 318.15 K.

Table 3
Partial molar volumes, V_ϕ^o and experimental slopes, S_V^* of amino acids in aqueous solutions of DAP at different temperatures.

$^a m_B$/(mol kg^{-1})	$V_\phi^o \times 10^6$ / (m^3 mol^{-1})				$S_V^* \times 10^6$ / (m^3 kg mol^{-2})			
	T = 288.15 K	T = 298.15 K	T = 308.15 K	T = 318.15 K	T = 288.15 K	T = 298.15 K	T = 308.15 K	T = 318.15 K
L-serine								
0.5	61.06 (±0.004)	61.48 (±0.003)	61.84 (±0.003)	62.21 (±0.002)	−2.48 (±0.008)	−2.48 (±0.008)	−2.49 (±0.008)	−2.49 (±0.005)
1.0	61.26 (±0.004)	61.66 (±0.003)	62.02 (±0.003)	62.48 (±0.003)	−2.36 (±0.007)	−2.36 (±0.007)	−2.37 (±0.007)	−2.37 (±0.007)
1.5	61.63 (±0.003)	61.94 (±0.003)	62.38 (±0.003)	62.84 (±0.003)	−2.24 (±0.006)	−2.24 ±0.006)	−2.24 (±0.006)	−2.26(±0.009)
2.0	62.10 (±0.002)	62.64 (±0.002)	63.08 (±0.002)	63.37 (±0.002)	−2.13 (±0.006)	−2.12 (±0.006)	−2.12 (±0.005)	−2.13 (±0.005)
L-leucine								
0.5	111.00 (±0.003)	111.40 (±0.003)	111.74 (±0.003)	112.02 (±0.003)	−1.83 (±0.004)	−1.82 (±0.004)	−1.84 (±0.004)	−1.86 (±0.004)
1.0	111.59 (±0.002)	111.80 (±0.002)	112.17 (±0.002)	112.59 (±0.002)	−1.36 (±0.002)	−1.36 (±0.002)	−1.37 (±0.002)	−1.38 (±0.002)
1.5	111.82 (±0.001)	112.03 (±0.001)	112.44 (±0.001)	112.93 (±0.012)	−0.95 (±0.001)	−0.95 (±0.001)	−0.96 (±0.001)	−1.53 (±0.017)
2.0	112.18 (±0.003)	112.47 (±0.003)	112.89 (±0.003)	113.33 (±0.003)	−0.55 (±0.003)	−0.54 (±0.003)	−0.54 (±0.003)	−0.55 (±0.003)

Table 4
Partial molar volume of transfer, ΔV_ϕ^0 of both the amino acids in aqueous solutions of DAP at different temperatures.

$^a m_B$/ (mol·kg^{-1})	$\Delta V_\phi^0 \times 10^6$ (m^3·mol^{-1})			
	T = 288.15 K	T = 298.15 K	T = 308.15 K	T = 318.15 K
L-serine				
0.5	3.04	2.66	2.97	1.34
1.0	3.24	2.84	3.15	1.61
1.5	3.61	3.12	3.51	1.97
2.0	4.08	3.82	4.21	2.50
L-leucine				
0.5	4.28	3.81	3.14	2.64
1.0	4.87	4.21	3.57	3.21
1.5	5.10	4.44	3.84	3.55
2.0	5.46	4.88	4.29	3.95

all positive. It has been observed that the values of transfer volume do not follow any regular trend in the case of L-serine, and in the case of L-leucine, the values increase with increase in the concentration of DAP. The co-sphere overlap model [38,54–56] plays a vital role in determining the sort of interactions occurring in the system. According to this model, various kind of interactions arise in the system of AAs in aqueous DAP solutions are ion-hydrophilic interactions, hydrophilic-hydrophilic interactions, ion-

hydrophobic interactions and hydrophobic-hydrophobic interactions. A negative contribution of transfer volume is carried by ion-hydrophobic interactions and hydrophobic-hydrophobic interactions, whereas ion-hydrophilic and hydrophilic-hydrophilic interactions show opposite contributions toward ΔV_{ϕ}^{0}values. In present work the obtained values of transfer volumes are positive which indicates that the ion-hydrophilic or hydrophilic-hydrophilic interactions are dominating in the ternary mixtures.

3.1.4. Temperature dependent partial molar volume at infinite dilution

The use of general polynomial equation (4) leads to the study of variation of V_{ϕ}^{0} with temperature.

$$V_{\phi}^{0} = A + B(T - -T_{ref}) + C(T - -T_{ref})^{2} \quad (4)$$

where T is the temperature in Kelvin, and A, B, and C are empirical constants. The values of empirical constants for amino acids in aqueous DAP solutions are given in Table 5. The value of empirical constants for both the amino acids in aqueous solutions of DAP was determined using weighted regressions and are listed in Table 5.

The ARD (σ) deviations are calculated using equation (5) given as follows

$$\sigma = (1/n)\Sigma[abs((Y_{exptl.} - Y_{calc.})/Y_{exptl.})] \quad (5)$$

where $Y = V_{\phi}^{0}$(apparent molar volume at infinite dilution). From Table 5, it is observed that small values of deviations have been obtained, which indicates that the polynomial equation fits well in the current study of AAs and DAP in aqueous solution. The temperature dependence of partial molar volume at infinite dilution is expressed in terms of the absolute temperature (T).

The limiting apparent molar expansibilities are calculated using the following equation (6)

$$\phi_{E}^{0} = \left(\partial V_{\phi}^{0}/\partial T\right)_{p} = B + 2C(T - -T_{ref}) \quad (6)$$

Limiting apparent molar expansibilities at infinite dilution, $E_{\phi}^{o} = (\partial V_{\phi}^{0}/\partial T)_{p}$, is convenient to recognize that solute-solvent interactions predominate in the solution. Hepler [57] derived the thermodynamic equation (7) to determine the structure-making or structure-breaking nature of the solute, as given

$$\left(\partial\phi_{E}^{0}/\partial T\right)_{p} = \left(\partial^{2}V_{\phi}^{o}/\partial T^{2}\right)_{p} = 2C \quad (7)$$

The calculated values of E_{ϕ}^{o} for amino acids at different temperature are given in Table 6. The obtained values of E_{ϕ}^{o} and $(\partial\phi_{E}^{0} / \partial T)_{p}$ are positive. The positive E_{ϕ}^{o}values signify the existence of solute-solvent interactions between amino acid zwitterions and solvated ions of DAP in aqueous medium. The sign of $(\partial\phi_{E}^{0} / \partial T)_{p}$ determines the tendency of a dissolved solute as a structure maker or structure breaker in a solvent. It recommends that positive and small negative $(\partial\phi_{E}^{0} / \partial T)_{p}$ values are obtained for solutes having structure making capacity, whereas negative $(\partial\phi_{E}^{0} / \partial T)_{p}$ values for structure breaking solutes [57,58]. The positive values of $(\partial\phi_{E}^{0} / \partial T)_{p}$ depict the structure making ability of amino acids in aqueous DAP solutions. Hence from above explanation it is revealed that the solute-solvent interactions are occurring in the system and also the values of limiting apparent molar expansibilities further helpful to determining the structure-making nature of the solute.

3.2. Speeds of sound measurements

The experimental measurement of speeds of sound, u of L-serine and L- leucine in (0.5, 1.0, 1.5, 2.0) mol kg^{-1} aqueous solutions of DAP at temperatures T = (288.15, 298.15, 308.15, 318.15) K have been done. The experimental values of speeds of sound for amino acids in aqueous solutions of DAP has been mentioned in Table 7. It is observed that the obtained values are positive for each measurement of speeds of sound and increases with the rise

Table 5
Values of empirical parameters of Eq.(4) for amino acids in aqueous DAP solutions.

[a]m_B / (mol·kg−1)	$a \times 10^6$ / (m^3 mol^{-1})	b x10^6 / (m^3 mol^{-1} K^{-1})	$c \times 10^6$/ (m^3 mol^{-1} K^{-2})	R^2	$ARD(\sigma)$
L-serine					
0.5	61.47	0.0393	−0.0001	0.9999	0.00011
1.0	61.64	0.0388	0.0001	0.9999	0.00024
1.5	61.95	0.0370	0.0004	0.9999	0.00020
2.0	62.64	0.0487	−0.0006	0.9999	0.00009
L-leucine					
0.5	111.40	0.0366	−0.0003	0.9999	0.00004
1.0	111.82	0.0285	0.0005	0.9999	0.00011
1.5	112.04	0.0305	0.0007	0.9999	0.00010
2.0	112.49	0.0352	0.0003	0.9999	0.00009

[a] m_B is the molality of aqueous solutions of DAP

Table 6
Limiting apparent molar expansibilities $E_{\phi}^{o}$for amino acids in aqueous DAP solutions at different temperatures.

[a]m_B / (mol·kg^{-1})	$E_{\phi}^{o} \times 10^6$ / (m^3 mol^{-1} K^{-1})				$(\partial E_{\phi}^{o}/\partial T)_{p}$/ (m^3 mol^{-1} K^{-2})
	T = 288.15 K	T = 298.15 K	T = 308.15 K	T = 318.15 K	
L-serine					
0.5	0.0421	0.0393	0.0364	0.0336	0.0003
1.0	0.0360	0.0388	0.0417	0.0445	0.0003
1.5	0.0291	0.0370	0.0448	0.0527	0.0008
2.0	0.0611	0.0487	0.0363	0.0239	0.0012
L-leucine					
0.5	0.0419	0.0366	0.0313	0.0260	0.0005
1.0	0.0184	0.0285	0.0387	0.0489	0.0010
1.5	0.0163	0.0305	0.0446	0.0588	0.0014
2.0	0.0283	0.0352	0.0422	0.0491	0.0007

[a] m_B is the molality of aqueous solutions of DAP

Table 7
Values of speeds of sound, u and apparent molar isentropic compression, $K_{\phi,s}$of amino acids in aqueous solutions of DAP at different temperatures and experimental pressure, p = 0.1 MPa.

[a]m_A / (mol·kg^{-1})	u / (ms^{-1})				$K_{\phi,s} \times 10^6$ / (m^3·mol^{-1}·GPa^{-1})			
	T = 288.15 K	T = 298.15 K	T = 308.15 K	T = 318.15 K	T = 288.15 K	T = 298.15 K	T = 308.15 K	T = 318.15 K
L-serine + aqueous 0.5 mol·kg^{-1} DAP								
0.00000	1518.07	1545.27	1563.85	1582.08				
	1517.47[b]	1544.86[b]	1564.56[b]	1581.15[b]				
	1517.08[c]	1544.36[c]	1564.22[c]	1517.08[c]				
	1517.70[d]	1544.30[d]	1564.83[d]	1581.30[d]				
0.10030	1524.52	1552.04	1570.42	1588.37	−43.20	−41.68	−40.67	−39.77
0.20033	1531.41	1558.95	1576.83	1595.24	−43.59	−42.05	−41.04	−40.13
0.29859	1538.18	1565.74	1583.14	1602.00	−43.83	−42.28	−41.27	−40.36
0.39885	1545.09	1572.67	1589.57	1608.88	−44.05	−42.49	−41.47	−40.55
0.47751	1550.51	1578.11	1594.62	1614.29	−44.21	−42.65	−41.62	−40.70
0.59662	1558.72	1586.34	1602.26	1620.47	−44.45	−42.87	−41.84	−40.91
0.69108	1565.23	1592.86	1608.32	1626.96	−44.63	−43.04	−42.01	−41.08
L-serine + aqueous1.0 mol·kg^{-1} DAP								
0.00000	1573.06	1598.13	1615.41	1628.39				
	1572.99[b]	1597.11[b]	1614.09[b]	1628.34[b]				
	1572.00[d]	1597.90[d]	1614.10[d]	1628.30[d]				
0.09904	1579.29	1603.36	1620.44	1634.42	−40.20	−38.98	−38.16	−37.51
0.19820	1585.52	1609.30	1626.48	1640.56	−40.56	−39.33	−38.50	−37.84
0.29959	1591.90	1615.37	1632.65	1646.83	−40.78	−39.54	−38.71	−38.05
0.39727	1598.04	1621.22	1638.60	1652.88	−40.97	−39.72	−38.89	−38.22
0.49680	1604.30	1627.18	1644.66	1659.03	−41.14	−39.89	−39.05	−38.38
0.59755	1610.64	1633.21	1650.79	1665.27	−41.32	−40.06	−39.22	−38.54
0.69784	1616.94	1639.22	1656.90	1671.48	−41.49	−40.22	−39.38	−38.70
L-serine + aqueous 1.5 mol·kg^{-1} DAP								
0.00000	1629.88	1650.87	1665.43	1677.69				
	1629.80[b]	1650.73[b]	1664.95[b]	1676.87[b]				
	1629.60[d]	1650.40[d]	1664.40[d]	1676.60[d]				
0.10001	1637.80	1657.79	1672.15	1684.11	−37.48	−36.53	−35.90	−35.38
0.19962	1645.68	1664.68	1679.04	1691.00	−37.77	−36.82	−36.18	−35.66
0.29714	1653.40	1671.42	1685.78	1697.74	−37.96	−37.00	−36.36	−35.84
0.39659	1661.27	1678.30	1692.66	1704.62	−38.13	−37.16	−36.52	−36.00
0.49608	1669.15	1685.18	1699.54	1711.50	−38.28	−37.31	−36.67	−36.14
0.59518	1676.99	1692.04	1706.40	1718.36	−38.44	−37.46	−36.81	−36.28
0.70098	1685.37	1699.36	1713.72	1725.68	−38.59	−37.61	−36.96	−36.43
L-serine + aqueous 2.0 mol·kg^{-1} DAP								
0.00000	1689.58	1708.27	1718.45	1728.5				
	1689.62[b]	1707.04[b]	1718.38[b]	1727.84[b]				
0.10000	1696.14	1713.83	1724.71	1734.11	−34.88	−34.16	−33.71	−33.34
0.20028	1702.71	1720.40	1730.98	1740.18	−35.14	−34.41	−33.97	−33.59
0.29871	1709.16	1726.85	1737.14	1746.14	−35.31	−34.58	−34.13	−33.75
0.40167	1715.91	1733.60	1743.58	1752.37	−35.46	−34.72	−34.27	−33.89
0.49460	1722.00	1739.69	1749.39	1758.00	−35.59	−34.85	−34.39	−34.01
0.59858	1728.82	1746.51	1755.90	1764.30	−35.73	−34.98	−34.52	−34.14
0.69012	1734.82	1752.51	1761.62	1769.84	−35.84	−35.09	−34.63	−34.25
L-leucine + aqueous 0.5 mol·kg^{-1} DAP								
0.00000	1507.4	1535.1	1556.0	1571.1				
	1507.20[b]	1534.68[b]	1555.74[b]	1570.81[b]				
	1507.3[d]	1534.9[d]	1555.9[d]	1570.9[d]				
0.01084	1519.70	1547.01	1565.88	1583.33	−39.68	−38.26	−37.32	−36.47
0.02061	1521.58	1548.71	1567.58	1585.00	−41.47	−40.00	−39.02	−38.15
0.03833	1525.00	1551.81	1570.68	1588.03	−42.40	−40.89	−39.91	−39.02
0.05913	1529.01	1555.45	1574.32	1591.58	−42.78	−41.27	−40.28	−39.38
0.08001	1533.04	1559.10	1577.97	1595.15	−42.98	−41.46	−40.46	−39.57
0.09961	1536.82	1562.53	1581.40	1598.50	−43.09	−41.57	−40.57	−39.67
0.12119	1540.98	1566.30	1585.17	1602.18	−43.18	−41.65	−40.65	−39.76
L-leucine + aqueous 1.0 mol·kg^{-1} DAP								
0.00000	1544.5	1569.6	1588.8	1602.4				
	1544.35[b]	1569.47[b]	1588.63[b]	1602.26[b]				
	1544.3[d]	1569.7[d]	1588.9[d]	1602.6[d]				
0.00999	1574.87	1599.26	1616.04	1629.87	−36.87	−35.74	−34.96	−34.34
0.01962	1576.62	1601.03	1617.62	1631.40	−38.62	−37.44	−36.64	−36.00
0.03947	1580.23	1604.67	1620.86	1634.55	−39.54	−38.34	−37.53	−36.88
0.05947	1583.86	1608.35	1624.14	1637.72	−39.85	−38.64	−37.83	−37.18
0.07910	1587.42	1611.95	1627.35	1640.83	−40.01	−38.80	−37.98	−37.33
0.09875	1590.99	1615.55	1630.56	1643.95	−40.11	−38.89	−38.08	−37.42
0.11938	1594.73	1619.34	1633.93	1647.22	−40.18	−38.96	−38.15	−37.49
L-leucine + aqueous 1.5 mol·kg^{-1} DAP								
0.00000	1579.6	1602.7	1619.7	1632.0				
	1579.46[b]	1602.24[b]	1619.54[b]	1631.66[b]				
	1579.0[d]	1602.4[d]	1619.9[d]	1631.1[d]				

Table 7 (*continued*)

[a]m_A / (mol·kg^{-1})	u / (ms^{-1})				$K_{\phi,S} \times 10^6$ / (m^3·mol^{-1}·GPa^{-1})			
	T = 288.15 K	T = 298.15 K	T = 308.15 K	T = 318.15 K	T = 288.15 K	T = 298.15 K	T = 308.15 K	T = 318.15 K
0.01002	1632.00	1652.69	1667.05	1679.01	−36.68	−35.60	−34.84	−34.29
0.01968	1634.05	1654.44	1668.80	1680.76	−38.38	−37.27	−36.48	−35.92
0.03994	1638.34	1658.12	1672.48	1684.44	−39.26	−38.13	−37.33	−36.76
0.05979	1642.55	1661.72	1676.08	1688.04	−39.57	−38.43	−37.63	−37.06
0.07963	1646.76	1665.32	1679.68	1691.64	−39.73	−38.59	−37.78	−37.21
0.09977	1651.02	1668.97	1683.33	1695.29	−39.84	−38.69	−37.88	−37.31
0.11934	1655.17	1672.52	1686.88	1698.84	−39.91	−38.76	−37.95	−37.38
L-leucine + aqueous 2.0 mol·kg^{-1} DAP								
0.00000	1613.5	1634.1	1649.6	1660.5				
	1613.60[b]	1634.12[b]	1649.64[b]	1660.38[b]				
0.00997	1690.80	1708.33	1719.43	1729.03	−34.54	−33.65	−33.05	−32.55
0.01969	1692.00	1709.36	1720.38	1729.98	−36.07	−35.15	−34.54	−34.03
0.03998	1694.49	1711.51	1722.37	1731.97	−36.88	−35.95	−35.32	−34.81
0.05996	1696.95	1713.62	1724.32	1733.92	−37.15	−36.21	−35.58	−35.07
0.07977	1699.38	1715.72	1726.26	1735.86	−37.28	−36.34	−35.71	−35.20
0.10010	1701.88	1717.88	1728.25	1737.85	−37.37	−36.42	−35.80	−35.28
0.11948	1704.26	1719.93	1730.15	1739.75	−37.43	−36.48	−35.85	−35.34

[a] m_A is the molality of amino acids in aqueous DAP solutions; [b, d] Values of ultrasonic speed taken from reference [46–48]. Standard relative uncertainties in molality are u_r (m) = 0.5%, Standard uncertainties u (T) = 0.001 K, u (u) = 0.8 m·s^{-1} and u (p) = 0.01 MPa (0.68 level of confidence).

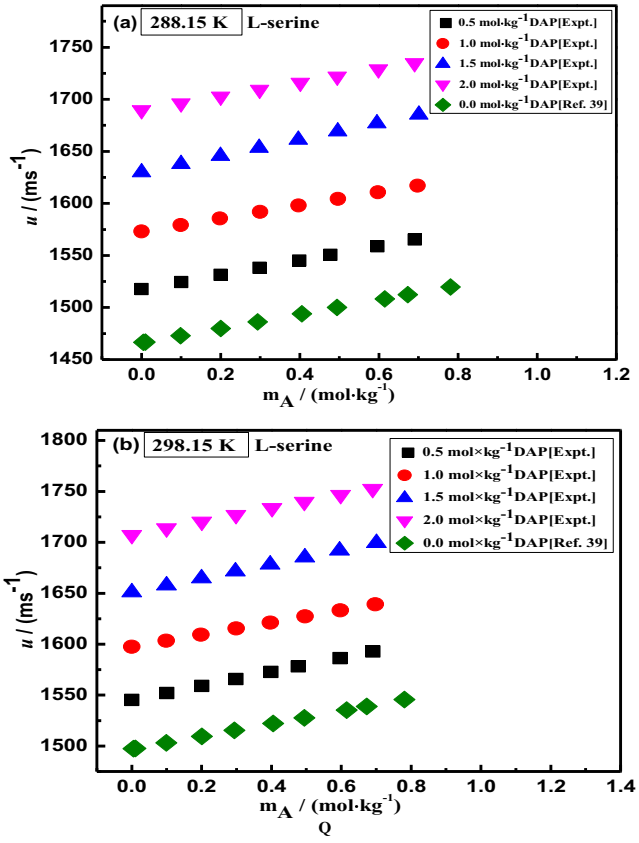

Fig. 6. Plots of comparison of speeds of sound values of L-serine in aqueous [39] and experimental speed of sound values for L-serine in aqueous solution of DAP at different concentrations (a) 288.15 K (b) 298.15 K.

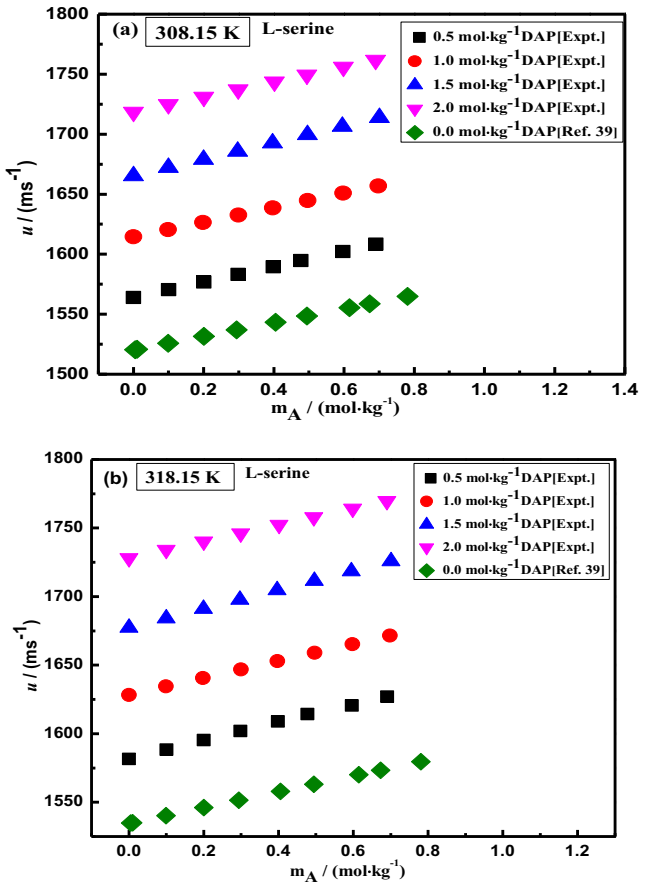

Fig. 7. Plots of comparison of speeds of sound values of L-serine in aqueous [39] and experimental speed of sound values for L-serine in aqueous solution of DAP at different concentrations (a) 308.15 K (b) 318.15 K.

in the concentration of the amino acids. The obtained values of speeds of sound for the AAs and for the salt have been compared with the literature [39,42,44]. It is obtained that the values of amino acids measured experimentally are in good agreement with the literature as mentioned in Table 7 and graphically shown in the Figs. 6-9. The speeds of sound values for aqueous solutions of salt DAP at different concentration and different temperatures are also reported in the Table 7. The obtained speeds of sound values are compared with the literature [46–48]and found in good agreement. Also the graphical representation for the same have been done and mentioned in the Fig. 10. In Fig. 10 the plots 10(a)–10 (d) are representing the temperature wise comparison of the speeds of sound data with literature.

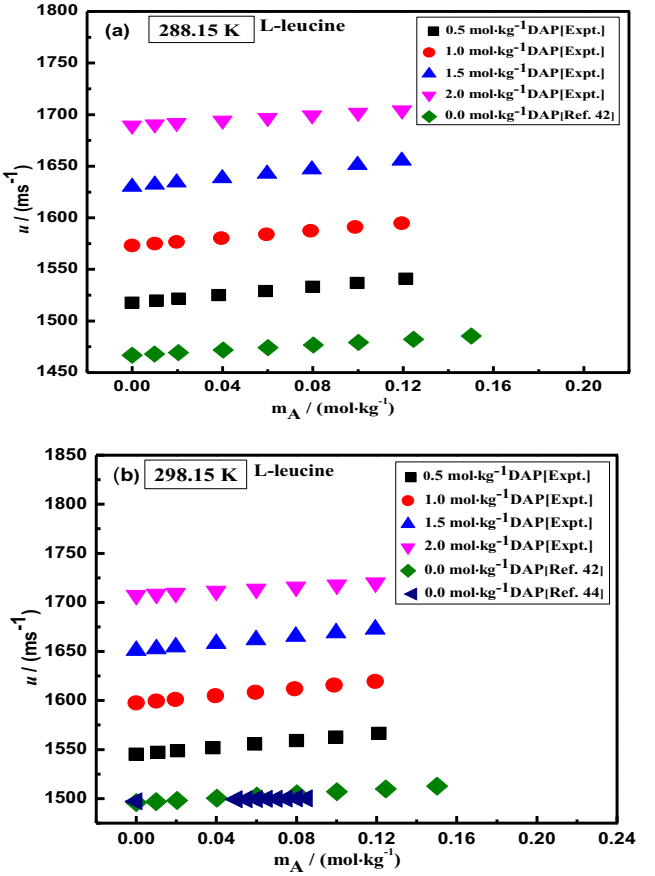

Fig. 8. Plots of comparison of speeds of sound values of L-leucine in aqueous [42,44] and experimental speed of sound values for L-leucine in aqueous solution of DAP at different concentrations (a) 288.15 K (b) 298.15 K.

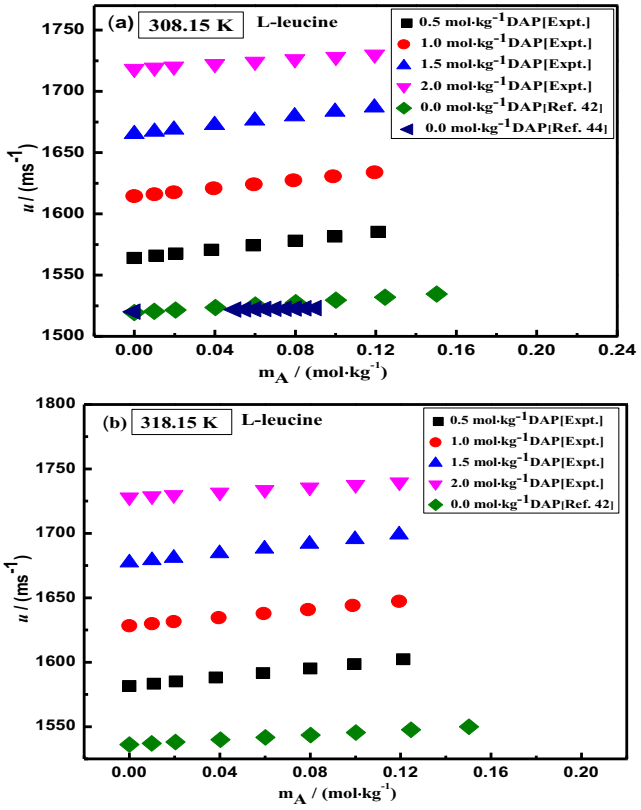

Fig. 9. Plots of comparison of speeds of sound values of L-leucine in aqueous [42,44] and experimental speed of sound values for L-leucine in aqueous solution of DAP at different concentrations (a) 308.15 K (b) 318.15 K.

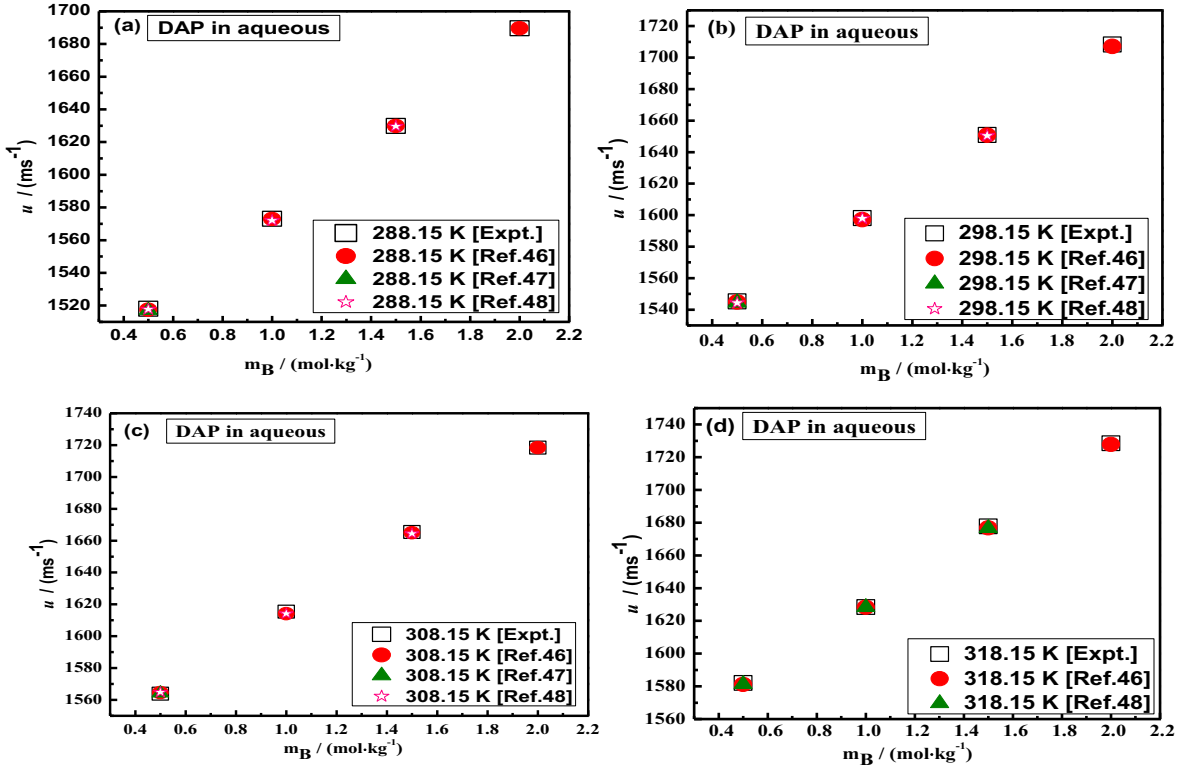

Fig. 10. Plots of comparison of speeds of sound values of DAP in aqueous experimental and literature [46–48] (a) 288.15 K (b) 298.15 K (c) 308.15 K (d) 318.15 K.

3.2.1. Apparent molar isentropic compression

Apparent molar isentropic compression for amino acids in aqueous solutions of DAP is obtained by utilizing equation (8)

$$K_{f,s} = [(M\kappa_S/r) - \{(\kappa_S r_0 - \kappa_{S,0} r)/ (m_A r r_0)\}] \quad (8)$$

where M is the molar mass of the solute (kg·mol^{-1}), m_A is the molality (mol·kg^{-1}) of the amino acids, i.e., the amount of solute (amino acids) per kilogram of solvent (mixture of water and DAP), ρ_0 and ρ are the densities (kg·m^{-3}) of the solvent and solution, respectively, and $\kappa_{S,0}$ and κ_S are the isentropic compressibility's of pure solvent and solution, respectively. Using the following equation (9), the isentropic compressibility is calculated as

$$\kappa_S = 1 / (u^2 r) \quad (9)$$

where u is speed of sound and ρ is density of solution. Apparent molar isentropic compression demonstrates the ordering of water molecules around the solute. The calculated values of $K_{\phi,s}$ as well as speeds of sound values for molal concentrations (m_A) of amino acids in (0.5, 0.1, 1.5, 0.2) mol kg^{-1}) DAP solution at different temperatures are outlined in Table 7. From Table 7, it is observed that all of the values $K_{\phi,s}$ are negative at all temperatures. The negative values of $K_{\phi,s}$ predict that the molecules in the bulk solution are more compressible than water molecules surrounding the ionic charged groups of amino acids. This additionally indicates the strong solute-solvent interactions between zwitterions of amino acid and salt molecules attributing the ordering of water molecules around solute [4,59,60]. So the negative values of the apparent molar isentropic compression demonstrate the solute-solvent interactions and favor the volumetric data.

3.3. Partial molar isentropic compression

The partial molar isentropic compression at infinite dilution $K_{\phi,s}$ can be calculate by using equation (10) given as follows

$$K_{\phi,s} = K^0_{\phi,s} + S^*_K mA \quad (10)$$

where $K^0_{\phi,s}$ the partial molar isentropic compression at infinite dilution, S^*_K is the experimental slope, and m_A is the molality of amino acids in aqueous DAP solutions. The values of experimental slope, S^*_K indicates the solute-solvent interactions and values of partial molar isentropic compression at infinite dilution, $K^0_{\phi,s}$ reveal the type of interactions existing in the mixtures. Negative values of partial molar isentropic compression at infinite dilution for amino acids are attributed to the strong attractive interactions between amino acids and salt solution [61,62]. The obtained values of $K^0_{\phi,s}$ and S^*_K from equation (10) along with the standard error are reported in Table 8. From the Table 8 it is observed that the values are more negative for partial molar isentropic compression and less negative for the experimental slope, which elucidate that the solute-solvent interactions are stronger and solute-solute interactions are weak [3,63]. The negative values of $K^0_{\phi,s}$ decrease with an increase in temperature and concentration of DAP in aqueous medium.

3.4. Partial molar compressibility of transfer at infinite dilution

Using the equation. (11), we have calculated the partial molar isentropic compressions of transfer ($\Delta K^o_{\phi,s}$) of amino acid from water to aqueous DAP solutions at infinite dilution.

$$\Delta K^o_{\phi,s} = K^o_{\phi,s}(in\ aqueous\ DAP\ solutions) - K^o_{\phi,s}\ (in\ water) \quad (11)$$

The values of partial molar isentropic compressions of transfer $\Delta K^o_{\phi,s}$ at different concentrations of DAP in aqueous medium, are reported in Table 9. It is observed from the Table 9 the obtained values are positive for both the amino acids except some values for L-serine at DAP concentration 0.5 mol·kg^{-1} in aqueous. The positive values of $\Delta K^o_{\phi,s}$ indicate the prevalence of interactions between the zwitterionic center of amino acid and DAP solution, indicating the structure-making tendency of the ions. The positive values of $\Delta K^o_{\phi,s}$ indicate the release of water molecules from the secondary solvation layer of AAs into the bulk. The release of water molecules indicates the prevalence of hydrophilic – hydrophilic interactions in AAs.

3.5. Pair and triplet interaction coefficients

According to McMillan–Mayer theory [64] of solutions, the pair and triplet interaction coefficients have been calculated which permits the separation of effects due to interaction between the pairs of solute molecules and those due to its interaction between more than two solute molecules. Further discussed by Friedmann and Krishnan [65] the solute-solvent interactions can be included in the solvation spheres.

Partial molar volume of transfer and partial molar isentropic compression of transfer can be expressed by

$$\Delta V^0_f(water\ to\ aqueous\ DAP\ solution) = 2\ V_{AB} m_B + 3\ V_{ABB} m_B^2 \quad (12)$$

$$\Delta K^0_{\phi,S}(Water\ to\ aqueous\ DAP\ solution) = 2\ K_{AB} m_B + 3\ K_{ABB} m_B^2 \quad (13)$$

where A denotes amino acid, B denotes DAP and m_B is the molality of aqueous DAP solutions. The pair and triplet interaction coefficients are described by the corresponding parameters V_{AB}, V_{ABB} for partial molar volume and K_{AB}, K_{ABB} for isentropic compression.

Table 8
Partial molar isentropic compression, $K^o_{\phi,s}$ and experimental slopes, S^*_K for amino acids in aqueous solutions of DAP at different temperatures.

[a]m_B / (mol·kg^{-1})	$K^o_{\phi,s} \times 10^6$ / (m^3·mol^{-1}·GPa^{-1})				$S^*_K \times 10^6$ / (kg·m^3·mol^{-2}·GPa^{-1})			
	T = 288.15 K	T = 298.15 K	T = 308.15 K	T = 318.15 K	T = 288.15 K	T = 298.15 K	T = 308.15 K	T = 318.15 K
L-serine								
0.5	−43.08(±0.059)	−41.56(±0.057)	−40.56(±0.056)	−39.66(±0.055)	−2.32(±0.133)	−2.23(±0.129)	−2.17(±0.127)	−2.12(±0.125)
1.0	−40.10(±0.056)	−38.89(±0.054)	−38.07(±0.053)	−37.42(±0.053)	−2.06(±0.125)	−1.98(±0.122)	−1.94(±0.120)	−1.90(±0.119)
1.5	−37.38(±0.045)	−36.44(±0.044)	−35.81(±0.044)	−35.30(±0.043)	−1.79(±0.101)	−1.73(±0.099)	−1.70(±0.098)	−1.67(±0.098)
2.0	−34.80(±0.040)	−34.08(±0.039)	−33.64(±0.039)	−33.26(±0.039)	−1.57(±0.090)	−1.52(±0.088)	−1.50(±0.088)	−1.48(±0.087)
L-leucine								
0.5	−40.66(±0.558)	−39.21(±0.541)	−38.25(±0.531)	−37.39(±0.524)	−25.51(±7.724)	−24.71(±7.483)	−24.28(±7.356)	−23.94(±7.252)
1.0	−37.84(±0.540)	−36.68(±0.526)	−35.89(±0.519)	−35.26(±0.514)	−24.26(±7.545)	−23.62(±7.347)	−23.30(±7.247)	−23.09(±7.183)
1.5	−35.38(±0.473)	−34.48(±0.463)	−33.87(±0.459)	−33.37(±0.456)	−21.13(±6.582)	−20.68(±6.441)	−20.49(±6.381)	−20.36(±6.342)
2.0	−33.02(±0.421)	−32.33(±0.414)	−31.90(±0.412)	−31.53(±0.411)	−18.61(±5.847)	−18.29(±5.750)	−18.20(±5.719)	−18.14(±5.701)

[a] m_B is the molality of aqueous solutions of DAP.

Table 9
Partial molar isentropic compression of transfer $\Delta K^{o}_{\phi,s}$of amino acids in aqueous solutions of DAP at different temperatures.

[a]m_B / (mol·kg^{-1})	$\Delta K^{o}_{\phi,S} \times 10^6$ (m^3·mol^{-1} GPa^{-1})			
	T = 288.15 K	T = 298.15 K	T = 308.15 K	T = 318.15 K
L-serine				
0.5	−0.64	−0.84	−1.10	−0.97
1.0	2.34	1.83	1.39	1.27
1.5	5.06	4.28	3.65	3.39
2.0	7.64	6.64	5.82	5.43
L-leucine				
0.5	2.79	2.55	2.21	2.17
1.0	5.61	5.08	4.57	4.30
1.5	8.07	7.28	6.59	6.19
2.0	10.43	9.43	8.56	8.03

[a] m_B is the molality of aqueous solutions of DAP

Table 10
Pair and triplet interaction coefficients of amino acids in aqueous solutions of DAP at different temperatures.

T / (K)	$V_{AB} \times 10^6$ / (m^3 mol^{-2} kg)	$V_{ABB} \times 10^6$ / (m^3 mol^{-3} kg^2)	$K_{AB} \times 10^6$ / (m^3 mol^{-2} kg GPa^{-1})	$K_{ABB} \times 10^6$ / (m^3 mol^{-3} kg^2 GPa^{-1})
L-serine				
288.15	2.59	−0.55	−0.05	0.68
298.15	2.19	−0.43	−0.28	0.68
308.15	2.45	−0.49	−0.54	0.69
318.15	1.12	−0.18	−0.49	0.64
L-leucine				
288.15	3.89	−0.87	2.95	−0.11
298.15	3.36	−0.74	2.67	−0.11
308.15	2.79	−0.60	2.35	−0.07
318.15	2.43	−0.50	2.26	−0.08

The obtained values of transfer parameters ΔV^{0}_{ϕ} and $\Delta K^{0}_{\phi,S}$ were fitted to above equations (12) and (13). The values of pair and triple interaction coefficients determined from these equations are reported in Table 10. The positive values have been observed for pair interaction coefficients V_{AB}, K_{AB} whereas triplet interaction coefficients V_{ABB} and K_{ABB} are negative at all temperatures. The positive value of *VAB, KAB* predicts that the pair wise interaction between AAs and DAP and occurs due to the overlap of hydration spheres of solute-cosolute molecules [24,35]. The positive values of pair interaction coefficient for volumetric and compressibility measurements signify that pair wise interactions are dominating in the (amino acid + DAP + water) mixtures.

4. Conclusion

The densities and speeds of sound measurements of L-serine and L-leucine in aqueous diammonium hydrogen phosphate solutions have been carried out in the present study. Thermodynamic properties like apparent molar properties and partial molar properties computed from densities and speeds of sound data indicates that strong solute-solvent interactions dominating in the mixture of amino acids and DAP in aqueous media. The interactions between amino acids and DAP molecules are evident from the interpretation of the data. The apparent molar volume, partial molar volume at infinite dilution are calculated, which were found to be positive and increase with the temperature of the DAP solution. This indicates greater solvation and interaction between the amino acid and aqueous DAP solutions. The transfer properties indicate that the ion–hydrophilic and hydrophilic–hydrophilic interactions are dominion over hydrophobic– hydrophobic and ion–hydrophobic interactions. Negative values of partial molar isentropic compression conclude that hydrophilic interactions are prevailing in the mixtures. Also the structure making property of amino acids in DAP solution is shown by the second derivative of temperature$(\partial^2 V^{o}_{\phi}/\partial T^2)_p$. The positive values of pair interaction coefficient for volumetric and compressibility measurements suggest that pair wise interactions are dominating in the (amino acid + DAP + water) mixtures due to the overlap of hydration spheres of amino acids and ions of phosphate salt. The considered mixture provides significant fundamental experimental data and theoretical supports for further exploring interactions of various amino acids with different additives.

CRediT authorship contribution statement

Harsh Kumar: Conceptualization, Resources, Supervision, Writing – review & editing. **Vaneet Kumar:** Supervision, Resources. **Seema Sharma:** Investigation, Writing – original draft. **Ayman A. Ghfar:** Resources, Writing – review & editing. **Arjuna Katal:** Writing – review & editing. **Meenu Singla:** . **Khyati Girdhar:** Writing – review & editing.

Declaration of Competing Interest

The authors declare that they have no known competing financial interests or personal relationships that could have appeared to influence the work reported in this paper.

Acknowledgement

The authors are grateful to the Researchers Supporting Project Number (RSP-2021/407), King Saud University, Riyadh, Saudi Arabia for the financial support.

References

[1] M. Singla, R. Jindal, H. Kumar, Thermochim. Acta 591 (2014) 140–151.
[2] H. Kumar, K. Kaur, J. Chem. Thermodyn. 53 (2012) 86–92.
[3] A. Pal, S. Kumar, J. Mol. Liq. 109 (2004) 23–31.
[4] I. Behal, H. Kumar, J. Mol. Liq. 244 (2017) 27–38.
[5] H. Kumar, I. Behal, M. Singla, J. Chem. Thermodyn. 95 (2016) 1–14.
[6] M. Kikuchi, M. Sakurai, K. Nitta, J. Chem. Eng. Data 40 (1996) 935–942.

[7] A. Kumar, M. Bisht, P. Venkatesu, Int. J. Biol. Macromol. 96 (2017) 611–651.
[8] A. Kumar, P. Venkatesu, Int. J. Biol. Macromol. 63 (2014) 244–253.
[9] H.R. Rafiee, F. Frouzesh, J. Mol. Liq. 230 (2017) 6–14.
[10] S. Kumar, G. Singh, R. Kataria, H. Kumar, Thermochim. Acta 589 (2014) 123–130.
[11] S. Kumar, G. Singh, H. Kumar, R. Kataria, Thermochim. Acta 607 (2015) 1–8.
[12] P.K. Chang, C.A. Prestidge, T.J. Barnes, K.E. Bremmell, RSC Adv. 6 (2016) 78970–78978.
[13] I. Jha, P. Attri, P. Venkatesu, Phys. Chem. Chem. Phys. 16 (2014) 5514–5526.
[14] H. Kumar, A. Katal, P.K. Sharma, J. Chem. Eng. Data 65 (2020) 1473–1487.
[15] Z. Yan, X. Chen, L. Liu, X. Cao, J. Chem. Thermodyn. 138 (2019) 1–13.
[16] M. Bisht, I. Jha, P. Venkatesu, Chem. Sel. 1 (2016) 3510–3519.
[17] R. Gaba, A. Pal, H. Kumar, D. Sharma, Navjot, J. Mol. Liq. 242 (2017) 739–746
[18] H. Shekaari, F. Jebali, Fluid Phase Equilib. 295 (2010) 68–75.
[19] V. Singh, P.K. Chhotaray, P.K. Banipal, T.S. Banipal, R.L. Gardas, Fluid Phase Equilib. 385 (2015) 258–274.
[20] H. Kumar, R. Sharma, J. Mol. Liq. 304 (2020) 112666–112679.
[21] H.Y. Chen, S. Fang, L. Wang, J. Mol. Liq. 225 (2017) 706–712.
[22] P. Patyar, T. Kaur, O. Sethi, J. Chem. Thermodyn. 125 (2018) 278–295.
[23] R. Jindal, M. Singla, H. Kumar, J. Mol. Liq. 206 (2015) 343–349.
[24] H. Kumar, M. Singla, H. Mittal, J. Chem. Thermodyn. 94 (2016) 204–220.
[25] H. Kumar, M. Singla, R. Jindal, J. Chem. Thermodyn. 67 (2013) 170–180.
[26] M.T. Zafarani-Moattar, J. Gasemi, Fluid Phase Equilib. 198 (2002) 281–291.
[29] K. Kaur, H. Kumar, J. Mol. Liq. 177 (2013) 49–53.
[30] H. Kumar, K. Kaur, J. Mol. Liq. 173 (2012) 130–136.
[31] R. Bhat, N. Kishore, J.C. Ahluwalia, J. Chem. Soc. Faraday Trans. 84 (1988) 2651–2665.
[32] G. Tao, L. He, W. Liu, L. Xu, W. Xiong, T. Wang, Y. Kou, Green Chem. 8 (2006) 639–646.
[33] A. Pinazo, R. Pons, M. Bustelo, M.Á. Manresa, C. Morán, M. Raluy, L. Pérez, J. Mol. Liq. 289 (2019) 111156–111170.
[34] K. Das, B. Sarkar, P. Roy, C. Basak, R. Chakraborty, R.L. Gardas, J. Mol. Liq. 291 (2019) 111255–111266.
[35] V. Singh, P.K. Chhotaray, R.L. Gardas, Thermochim. Acta. 610 (2015) 69–77.
[36] S. Bose, D.W. Armstrong, J.W. Petrich, J. Phys. Chem. B. 114 (2010) 8221–8227.
[37] Z. Yan, L. Ma, S. Shen, J. Li, J. Mol. Liq. 255 (2018) 530–540.
[38] S.K. Sharma, G. Singh, H. Kumar, R. Kataria, J. Chem. Thermodyn. 115 (2017) 318–331.
[39] H. Kumar, M. Singla, R. Jindal, J. Mol. Liq. 208 (2015) 170–182.
[40] T.S. Banipal, D. Kaur, P.K. Banipal, G. Singh, J. Chem. Thermodyn. 39 (2007) 371–384.
[41] M.M. Duke, A.W. Hakin, R.M. Mckay, K.E. Preus, Can. J. Chem. 72 (1993) 1489–1494.
[42] H. Kumar, I. Behal, J. Chem. Eng. Data 61 (2016) 3740–3751.
[43] A. Pal, N. Chauhan, J. Chem. Thermodyn. 43 (2011) 140–146.
[44] S. Chauhan, K. Kumar, J. Chem. Eng. Data 59 (2014) 1375–1384.
[45] T.S. Banipal, D. Kaur, P.K. Banipal, J. Chem. Eng. Data 49 (2004) 1236–1246.
[46] H. Kumar, I. Behal, J. Mol. Liq. 241 (2017) 751–763.
[47] R. Sadeghi, H.B. Kahaki, Fluid Phase Equilib. 306 (2011) 219–228.
[48] H. Kumar, I. Behal, S. Siraswar, J. Chem. Eng. Data 64 (2019) 3772–3780.
[49] S. Sharma, M. Singh, S. Sharma, J. Singh, A.K. Sharma, M. Sharma, J. Mol. Liq. 303 (2020) 112596–112611.
[50] B. Sinha, A. Sarkar, P.K. Roy, D. Brahman, Int. J. Thermophys. 32 (2011) 2062–2078.
[51] S.S. Dhondge, S.P. Zodape, D.V. Parwate, J. Chem. Thermodyn. 48 (2012) 207–212.
[52] Ł. Marcinkowski, M. Śmiechowski, E. Szepiński, A. Kloskowski, D. Warmińska, J. Mol. Liq. 286 (2019) 110875–110886.
[53] M. Singla, H. Kumar, R. Jindal, J. Chem. Thermodyn. 76 (2014) 100–115.
[54] W.H. Streng, W.Y. Wen, J. Solution Chem. 3 (1974) 865–880.
[55] S. Ryshetti, B.K. Chennuri, R. Noothi, S.J. Tangeda, R.L. Gardas, Thermochim. Acta 597 (2014) 71–77.
[56] A. Pal, S. Kumar, J. Chem. Thermodyn. 37 (2005) 1085–1092.
[57] L.G. Hepler, Can. J. Chem. 47 (1969) 4613–4617.
[58] A. Pal, H. Kumar, R. Maan, H. Kumar, S. Sharma, J. Chem. Thermodyn. 91 (2015) 146–155.
[59] H. Kumar, I. Behal, J. Mol. Liq. 219 (2016) 756–764.
[60] H. Kumar, V. Kumar, M. Sharma, I. Behal, J. Chem. Thermodyn. 119 (2018) 1–12.
[61] H. Kumar, M. Singla, R. Jindal, J. Mol. Liq. 199 (2014) 385–392.
[62] H. Kumar, K. Kaur, S.P. Kaur, M. Singla, J. Chem. Thermodyn. 59 (2013) 173–181.
[63] C. Chadha, M. Singla, H. Kumar, J. Mol. Liq. 218 (2016) 68–82.
[64] W.G. Mcmillan, J.E. Mayer, J. Chem. Phys. 13 (1945) 276–305.
[65] H.L. Friedman, C.V. Krishnan, J. Sol. Chem. 2 (1973) 119–140.

Further reading

[27] K.S. Egorova, V.P. Ananikov, J. Mol. Liq. 272 (2018) 271–300.
[28] S. Kumar, G. Singh, H. Kumar, R. Kataria, J. Chem. Thermodyn. 98 (2016) 214–230.

J. Chem. Thermodynamics 155 (2021) 106350

Contents lists available at ScienceDirect

J. Chem. Thermodynamics

journal homepage: www.elsevier.com/locate/jct

Volumetric and acoustic properties of amino acids L-Leucine and L-Serine in aqueous solution of ammonium dihydrogen phosphate (ADP) at different temperatures and concentrations

Harsh Kumar [a,*], Vaneet Kumar [b,c], Seema Sharma [b,d], Arjuna Katal [a], Asma A. Alothman [e]

[a] Department of Chemistry, Dr B R Ambedkar National Institute of Technology, Jalandhar 144011, Punjab, India
[b] IKG Panjab Technical University, Kapurthala Road, Jalandhar, Punjab, India
[c] Department of Applied Sciences, CTIEMT, CT Group of Institutions, Shahpur, Jalandhar, Punjab, India
[d] MRPD Govt Arts and Science College, Talwara 144216, Punjab, India
[e] Department of Chemistry, College of Science, King Saud University, Riyadh-11451, Saudi Arabia

ARTICLE INFO

Article history:
Received 30 April 2020
Received in revised form 18 November 2020
Accepted 19 November 2020
Available online 23 November 2020

Keywords:
Density
Speed of sound
Apparent molar volume
Solute–solvent interaction
Ammonium dihydrogen phosphate
Amino acids

ABSTRACT

The physicochemical properties of amino acids like L-Leucine and L-Serine in aqueous solution of ammonium dihydrogen Phosphate (ADP) at different temperature analysed by volumetric and acoustic methods. By using density data, apparent molar volume V_ϕ, partial molar volume V_ϕ^0 and standard partial molar volume of transfer ΔV_ϕ^0 have been evaluated. From speed of sound data, apparent molar isentropic compression $K_{\phi,s}$ apparent partial molar isentropic compression $K_{\phi,s}^0$ and partial molar isentropic compression of transfer $\Delta K_{\phi,s}^o$ have been calculated. The pair and triplet interaction coefficient have also been calculated. The results have been interpreted in terms of solute–solute and solvent–solvent interactions.

1. Introduction

Amino acids and proteins are the building blocks of life which have great impact that elevated the conformation of proteins and solvation [1,2]. Because proteins are large complex molecules, the direct study of protein–electrolyte interactions is difficult. It is therefore, useful to investigate the interaction of model compounds such as amino acids, peptides, and their derivatives that constitute part of the protein structures [3]. Amino acids are bioactive organic compounds containing amine and carboxylic acid group with side chains in all organism on earth. Amino acids differ from each other in size, charge, hydrogen-bonding capacity, hydrophobicity and chemical reactivity. Because of their biological significance amino acids are important in nutrition and are commonly used in nutritional supplements, fertilizers and food technology. Therefore, protein model compounds such as amino acids and peptides, which are basic components of proteins, have been investigated in detail with respect to their thermodynamic properties in aqueous and mixed aqueous solutions [4–10].Thermodynamic properties of amino acids, as fundamental structural units of proteins in aqueous electrolyte solutions provide important information about solute – solvent and solute – solute interactions that can be of great help in understanding several processes, such as protein hydration, denaturation, and protein aggregation [11,12]. Amino acids, the biologically important compounds is of immense importance as their behaviour in aqueous and mixed aqueous solutions in different temperature range determines how the proteins tends to behave in living cells and this leads to open field of curious research [13–15]. The solution structure of amino acids/peptides is because of the intermolecular interactions and the understanding of these intermolecular interactions have a decisive role for determining the outcome in biological systems and even these are in close contact with the thermodynamic properties of liquids, solids and gases. Research has been carried out on thermodynamic properties of amino acids in aqueous electrolyte solutions, carbohydrates, surfactants, *etc.* but the phosphates salts are still found in limited study. The phosphates are biologically and industrially important salts which are employed in food, cosmetics, and pharmaceutical industries and also in numerous biochemical studies. The present work is just a continuation of our earlier lab-

* Corresponding Author.
E-mail addresses: h.786.man@gmail.com, manchandah@nitj.ac.in (H. Kumar).

https://doi.org/10.1016/j.jct.2020.106350
0021-9614/

oratory work on the volumetric and ultrasonic properties of amino acids and peptides with phosphate salts of biological importance.

Amino acids are charged molecules which show a very high solubility in aqueous medium. Because of solvent effects of their direct binding the protein conformation is sometimes influenced by these added co-solutes [16–20]. The interactions of water with various functional groups of amino acids play a crucial role. Ammonium dihydrogen phosphate (ADP), $NH_4H_2PO_4$ commonly called mono ammonium phosphate (MAP) is a chemical compound. It is a white crystalline solid. It is a water-soluble salt which is used as fertilizer, dry chemical fire extinguisher and in building materials. On studying thermodynamic properties of biological molecules in aqueous solution are important as many biochemical processes occur in aqueous solution. Valuable information on solute – solute and solute – solvent interactions is furnished by physicochemical and thermodynamics properties of amino acids in aqueous solutions [21–26]. Our study is mainly focused on the measurement of densities and ultrasonic properties of amino acids in aqueous ADP as a function of different molal concentration at different temperatures (288.15, 298.15, 308.15 and 318.15) K and atmospheric pressure. The density and speed of sound data has been used to determine different physical parameters such as apparent molar volume V_ϕ, partial molar volume V_ϕ^0, partial molar volume of transfer ΔV_ϕ^0 ,apparent molar isentropic compression $K_{\phi,s}$, partial molar isentropic compression $K_{\phi,s}^0$and partial molar isentropic compression of transfer $\Delta K_{\phi,s}^o$that will be inspected in terms of solute – solvent and solute – solute interactions which are operative in ternary mixture.

2. Material and methods

2.1. Chemicals

The chemicals used in our study L-Leucine, L-Serine and ammonium dihydrogen phosphate (ADP) were of high pureness (>0.99 mass fraction). They were used without further purification. However before use, the amino acids were stored over P_2O_5 in a desiccator for at least 48 h. The detailed description of chemicals is specified in Table 1.

2.2. Apparatus and procedure

For measuring the density and speed of sound, the samples were prepared using Sartorius CPA225D balance having precision of ± 0.00001 g. Freshly prepared triple distilled and degassed water (specific conductance < 10^{-6} S·cm^{-1}) was used for the preparation of solutions. Anton Paar DSA 5000 M densimeter was used for the measurements of densities and speeds of sound of the mixtures. The details of calibration and other procedures have been specified in our earlier paper [27]. Standard relative uncertainty in molality for samples as per stated purities of the compounds is $u_r(m) = 2\%$. The speed of sound measurements was carried out at a frequency of 3 MHz Both the density and speed of sound are extremely sensitive to temperature, so it was controlled to ±1 × 10^{-3} K by built in Peltier Device. The sensitivity of instrument of instrument corresponds to a precision in density and speeds of sound measurements of 1×10^{-3} kg·m^{-3} and 1×10^{-2} m·s^{-1}.The standard uncertainty of density and speed of sound at a confidence level of 0.68 are 1 kg·m^{-3} and 1.6 m·s^{-1} respectively.

3. Results and discussion

3.1. Density measurements

The experimental value of solution densities, ρ of L-Leucine, L-Serine in (0.5, 1.0, 1.5, 2.0) mol·kg^{-1} aqueous solutions of ADP were measured at temperatures T (288.15, 298.15, 308.15 and 318.15) K. The experimental values of density for amino acids in aqueous solutions of ADP have been compared graphically with literature density values of aqueous solutions of amino acids [28–34] at different temperatures as shown in Figs. 1–4 and values are found to follow the regular trend with respect to each other. The values of density for all the solutions at different temperatures are listed in Table 2. It is observed that density of solution increases with rise in concentration of amino acids and decreases slightly with increase in temperature of solution. The experimental values of density for aqueous solutions of ADP at different temperatures have been compared with the literature [35–40] values. Out of these, Refs. [35 and 37] are our previous publications. The graphical comparison has been represented in Figs. 5 and 6 at different temperatures. The values reported in references [38–40] are not the same as the studied compositions and temperatures in presented study. To avoid confusion, the graphical comparison comprising of these references are presented in Figs. S1 of supporting information. Figs. 5 and 6 represent the graphical comparison of aqueous solutions of ADP on the molality scale at different temperatures. The collective comparison of density values of the aqueous ADP solutions in terms of molality units at different temperatures is represented in Fig.. S1(a), whereas the literature comparison of the density values of aqueous ADP solutions in mass fraction units is given in Fig. S1(b) of supporting information. It is observed from Fig. S1(a) that the density values are in good agreement with literature values [35–37]. On the other hand, He et al., Xie et al. and Yang et al. have made studies on the solid–liquid phase equilibria comprising of the ADP as one of the component and reported the density values for the aqueous ADP in mass fraction units [38–40]. So, for graphical comparison of density values we have converted the molality units to mass fraction units and plotted the density values at different temperatures as presented in Fig. S1 (b). From Fig. S1(b) it is observed that deviations between the experimental values and literature values have been noticed.

3.1.1. Apparent molar volume

The volumetric behaviour of solutions provides useful information about the solute – solvent and solute – solute interactions. Property like apparent molar volume has proved to be very useful in the study of molecular and ionic interactions occurring in solutions [31]. The important relevance is regarding the nature of the interactions of water with solute molecules, especially with that effect the structural properties of water. So, the volumetric parameters like the apparent molar volume, partial molar volumes and

Table 1
Specification of studied chemicals.

Chemical	CAS number	Source	Purification method	[a]Mass fraction purity
L-Serine	56-45-1	Merck, Germany	Drying over P_2O_5	≥0.99
L-Leucine	61-90-5	HI Media Chem. Pvt. Ltd., India	Drying over P_2O_5	≥0.99
Ammonium dihydrogen phosphate	7722-76-1	HI Media Chem. Pvt. Ltd., India	Drying over P_2O_5	≥0.99

[a] As declared by supplier.

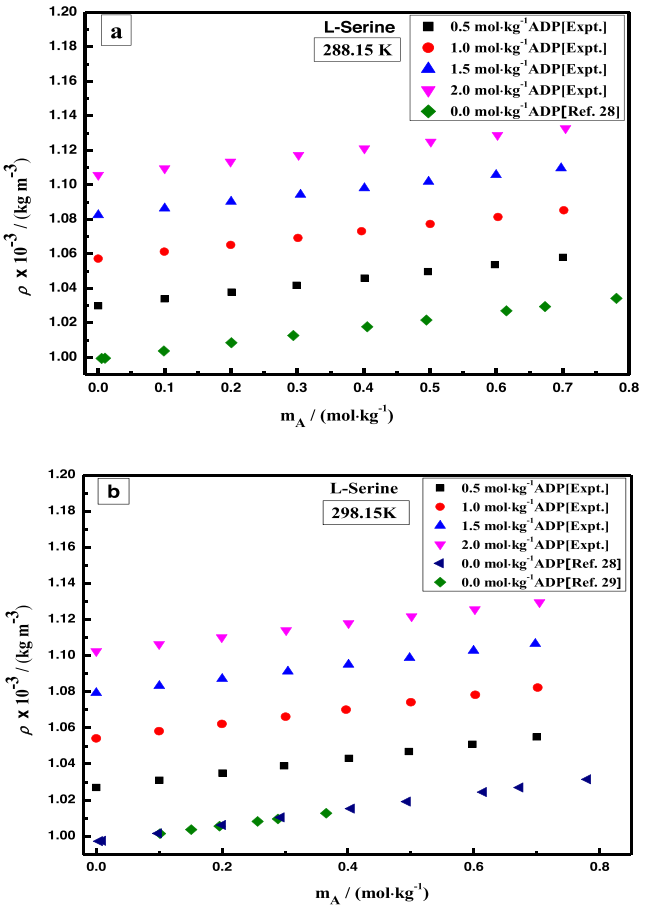

Fig. 1. Plots of comparison of density values of L-serine in aqueous [28,29] and experimental density values for L-serine in aqueous solution of ADP (Ammonium dihydrogen phosphate) at different concentrations (a) 288.15 K (b) 298.15 K.

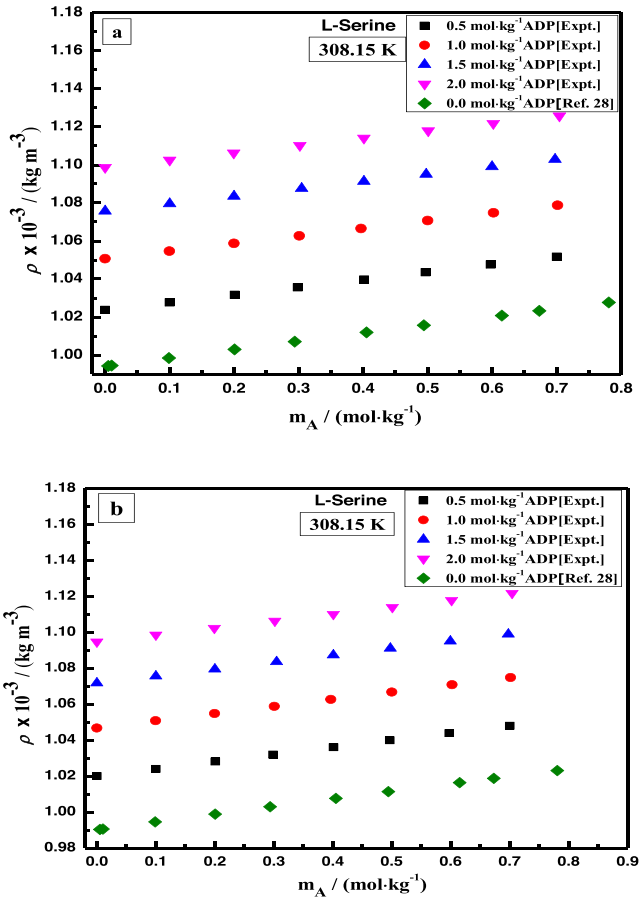

Fig. 2. Plots of comparison of density values of L-serine in aqueous [28] and experimental density values for L-serine in aqueous solution of ADP at different concentrations (a) 308.15 K (b) 318.15 K.

partial molar expansibilities of solute are found to be very useful in predicting and elucidating the structural interactions occurring in solutions [41].

The values of apparent molar volume (V_ϕ) are calculated from experimental values of density (ρ) by using following equation.

$$V_\phi = [(M/\rho) - \{(\rho - \rho_0)/(m_A \rho \rho_0)\}] \quad (1)$$

where M is molar mass of solute (kg·mol^{-1}), m_A is molality (mol·kg^{-1}) of amino acids *i.e.* amount of solute (amino acids) per one kilogram of solvent (mixture of water + ADP) and ρ and ρ_0 are densities (kg·m^{-3}) of solution and solvent respectively. The values of apparent molar volume are reported in Table 2. The magnitude of the apparent molar volumes predicts about the nature of interactions prevailing the mixtures. The positive values of apparent molar volumes V_ϕ indicate strong solute – solvent interactions. The calculated values of apparent molar volume are graphically presented in Figs. S2 and S3 of Supplementary information. From graphical representation it is observed that apparent molar volumes for L-Leucine and L-Serine are positive and the values are rises with the rise in the temperature. The increase in the values of apparent molar volume with the rise in temperature causes greater affinity for the solvent hence the solute – solvent interactions enhance. The positive values of V_ϕ are indicative of greater solute – solvent interactions present in the system. It is also noticed that the values of apparent molar volumes are more for corresponding L-Leucine as compared to L-Serine, which signifies the predominance of solute – solvent interactions in case of L-leucine as compared to L-serine. The rise in the volume occurs due to the increase in surface of solute to interact with solvent [27].

3.1.2. Partial molar volume

Partial molar volume or the apparent molar volume at infinite dilution calculated by using equation (2), partial molar volume V_ϕ^0 is calculated by means of least squares fit of V_ϕ values. The values of the apparent molar volume at infinite dilution are an important property because each ion is surrounded only by the solvents molecules and the ions are infinitely distant from each other. So the values of partial molar volume signify the presence of ion–solvent or solute – solvent interaction and it is unaffected by solute – solute or ion-ion interactions [42,43]. The infinite dilution thermodynamic quantities reflect the solute – solvent interactions and the concentration dependence of these properties provide information about solute – solute interactions. The V_ϕ^0 is very sensitive to solute salvation as it reflects structural volume change of solvent in the process of shell formation around the ion [44,45]. The utilized equation for the determination of the values of partial molar volume V_ϕ^0 s given as following.

$$V_\phi = V_\phi^0 + S_V^* m_A \quad (2)$$

The S_V^* the experimental slope is the volumetric pairwise interaction coefficient or semi empirical solute – solute interaction [35,36] parameter and m_A is the molality of amino acids in aqueous ADP. The values obtained for V_ϕ^0 and S_V^* also helps in predicting the

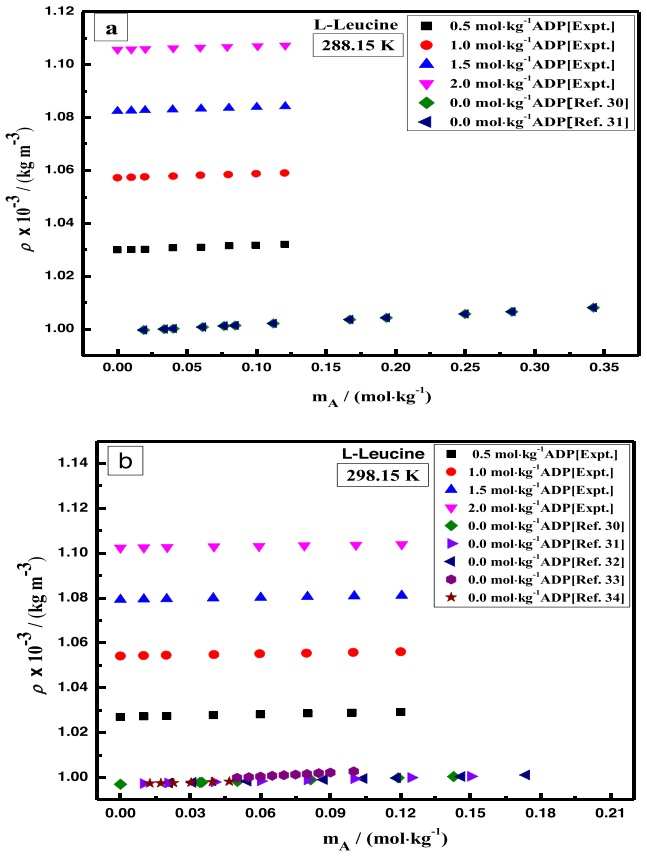

Fig. 3. Plots of comparison of density values of L-leucine in aqueous [30–34] and experimental density values for L-leucine in aqueous solution of ADP at different concentrations (a) 288.15 K (b) 298.15 K.

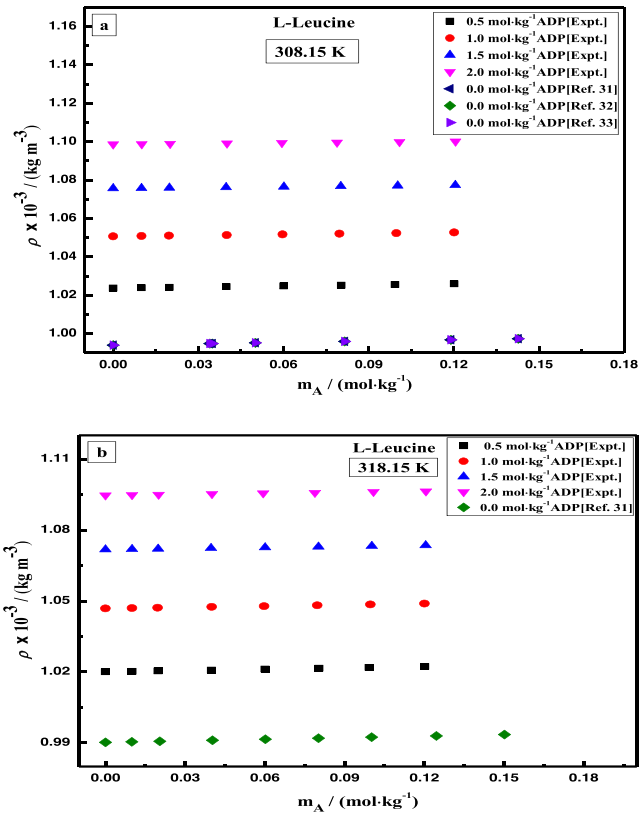

Fig. 4. Plots of comparison of density values of L-leucine in aqueous [31–33] and experimental density values for L-leucine in aqueous solution of ADP at different concentrations (a) 308.15 K (b) 318.15 K.

solute – solvent interactions, solute – co-solute interactions and solute–solute interactions. Partial molar volume at infinite dilution V_ϕ^0 depends on solute – solvent interactions not on solute – solute interactions. Because at infinite dilution, solvent molecules surround each ion goes infinitely apart so, the value of V_ϕ^0 by definition are free from solute – solute interaction and therefore provides information regarding solute – solvent interactions as explained earlier. The Values of V_ϕ^0 and S_V^*together with standard errors derived by least squares fitting of V_ϕ values to equation (2) are defined in Table 3 along with standard error deviations. The obtained values of the partial molar volumes are positive for both the amino acids. It is also noticed that the values of V_ϕ^0 are more at the lower concentrations of the salt as mentioned in the Table 3. For the lower concentration of ADP, the large values of the partial molar volume are attributed to the attractive interactions which may be due to the hydration of the ions. As the concentration of the ADP increases, the small volumes have been recognized which are responsible for the strong attractive interactions. According to co-sphere overlap model if the overlap occurring among the ionic species the positive rise in the volume take place and negative volume obtained during the overlap of hydrophobic-hydrophobic species. Obtained values of the partial molar volume employ the solute – solvent or ion-hydrophilic interactions dominating in the ternary mixtures of amino acids, salt and water. The increase in V_ϕ^0 values with an increase in temperature for all amino acids may be explained as release of some solvation molecules from the loose solvation layers of the solutes in solution. The change in V_ϕ^0 with temperature may involve many reasons such as thermal expansion, weakening of H-bond network and molecules being loosened from the solvation layers [46,47]. In simple terms, an increase in temperature reduces the electrostriction and which leads to the increase in the V_ϕ^0values. The positive sign of the slope indicates that the two hydrophilic groups interact in solution, while the negative sign leads to the hydrophobic cospheres [48]. The positive values of experimental slopeS_V^* employ the presence of solute – solute interactions in the system and the obtained experimental values for the same have been mentioned in the Table 3. It is observed that the negative values have been obtained for the experimental slope which indicates that the solute – solvent interactions are more dominating than the solute – solute interactions.

3.1.3. Partial molar volume of transfer

The partial molar volume of transfer for both the amino acids has been calculated by using the values of partial molar volume of the amino acids in aqueous solution of the ADP and partial molar volume of amino acids in water. The following equation has been utilized to determine the values of partial molar volume of transfer at infinite dilution.

$$\Delta V_\phi^0 = V_\phi^0 \text{ (in aqueous ADP solution)} - V_\phi^0\text{(in water)} \qquad (3)$$

The calculated values of partial molar volumes of transfer are reported in Table 4. The values of V_ϕ^0 for amino acids in water have been taken from already published work [28,49]. From the Table 4 it is observed that the values of ΔV_ϕ^0 are positive as well as negative. The values of partial molar volume of transfer at infinite dilution are positive for the L-serine and negative for the L-leucine. To know the sort of interactions occurring in the solutions, co-sphere

Table 2
Densities, ρ and apparent molar volumes, V_ϕ of amino acids in aqueous solutions of ADP at different temperatures and experimental pressure, p = 0.1 MPa.

[a]m_A/(mol·kg^{-1})	$\rho \times 10^{-3}$/(kg·m^{-3})				$V_\phi \times 10^6$/(m^3·mol^{-1})			
	T = 288.15 K	T = 298.15 K	T = 308.15 K	T = 318.15 K	T = 288.15 K	T = 298.15 K	T = 308.15 K	T = 318.15 K
L-Serine + aqueous 0.5 mol·kg^{-1}ADP								
0.00000	1.02986	1.02700	1.02369	1.02002				
	1.029895[b]	1.026926[b]	1.023680[b]	1.019889[b]				
	1.029605[c]	1.026684[c]	1.023344[c]	1.019518[c]				
	1.029999[d]	1.026452[d]	1.023325[d]	1.019736[d]				
0.10024	1.03362	1.03076	1.02744	1.02378	66.45	66.53	66.63	66.74
0.20083	1.03739	1.03454	1.03122	1.02755	66.21	66.29	66.39	66.50
0.29877	1.04106	1.03821	1.03489	1.03122	65.97	66.06	66.15	66.26
0.40147	1.04491	1.04206	1.03874	1.03507	65.73	65.81	65.91	66.01
0.49696	1.04850	1.04564	1.04232	1.03865	65.50	65.59	65.68	65.79
0.59791	1.05228	1.04943	1.04611	1.04244	65.27	65.35	65.44	65.55
0.70029	1.05612	1.05327	1.04995	1.04628	65.03	65.11	65.20	65.31
L-Serine + aqueous1.0 mol·kg^{-1} ADP								
0.00000	1.05723	1.05419	1.05069	1.04679				
	1.057212[b]	1.054111[b]	1.050638[b]	1.046759[b]				
	1.056922[c]	1.053869[c]	1.050302[c]	1.046388[c]				
	1.057615[d]	1.054224[d]	1.050982[d]	1.046479[d]				
0.09981	1.06053	1.05749	1.05399	1.05008	69.66	69.78	69.91	70.06
0.19972	1.06382	1.06078	1.05728	1.05338	69.45	69.56	69.69	69.84
0.30100	1.06717	1.06413	1.06063	1.05672	69.23	69.34	69.47	69.62
0.39698	1.07033	1.06729	1.06379	1.05989	69.02	69.14	69.27	69.41
0.50020	1.07374	1.07070	1.06720	1.06330	68.81	68.92	69.05	69.19
0.60235	1.07711	1.07407	1.07057	1.06667	68.59	68.70	68.83	68.97
0.70168	1.08039	1.07735	1.07385	1.06994	68.38	68.49	68.62	68.76
L-Serine + aqueous 1.5 mol·kg^{-1} ADP								
0.00000	1.08244	1.07936	1.07568	1.07170				
	1.082488[b]	1.079387[b]	1.075632[b]	1.071692[b]				
	1.082198[c]	1.079145[c]	1.075296[c]	1.071321[c]				
	1.082555[d]	1.079601[d]	1.075845[d]	1.071755[d]				
0.10012	1.08635	1.08327	1.07958	1.07561	63.57	63.66	63.76	63.87
0.19998	1.09024	1.08716	1.08348	1.07950	63.35	63.43	63.53	63.64
0.30470	1.09433	1.09125	1.08756	1.08358	63.11	63.19	63.29	63.40
0.40108	1.09808	1.09500	1.09132	1.08734	62.89	62.98	63.08	63.18
0.49786	1.10186	1.09878	1.09510	1.09112	62.68	62.76	62.86	62.97
0.59962	1.10583	1.10275	1.09906	1.09509	62.45	62.54	62.63	62.74
0.69758	1.10965	1.10657	1.10288	1.09891	62.24	62.32	62.42	62.52
L-Serine + aqueous2.0 mol·kg^{-1} ADP								
0.00000	1.10570	1.10243	1.09867	1.09468				
	1.105650[b]	1.102498[b]	1.098679[b]	1.094705[b]				
	1.105360[c]	1.102256[c]	1.098343[c]	1.094334[c]				
0.10001	1.10955	1.10628	1.10252	1.09853	63.34	63.43	63.54	63.65
0.19933	1.11338	1.11010	1.10634	1.10236	63.12	63.21	63.32	63.43
0.30181	1.11732	1.11405	1.11029	1.10630	62.89	62.99	63.09	63.20
0.40105	1.12114	1.11787	1.11411	1.11012	62.68	62.77	62.88	62.99
0.50100	1.12499	1.12172	1.11796	1.11397	62.47	62.56	62.66	62.77
0.60163	1.12887	1.12559	1.12183	1.11785	62.25	62.34	62.44	62.55
0.70424	1.13282	1.12954	1.12578	1.12180	62.03	62.12	62.22	62.33
L-Leucine + aqueous 0.5 mol·kg^{-1} ADP								
0.00000	1.02986	1.02700	1.02369	1.02002				
	1.029895[b]	1.026926[b]	1.023680[b]	1.019889[b]				
	1.029605[c]	1.026684[c]	1.023344[c]	1.019518[c]				
	1.029999[d]	1.026452[d]	1.023325[d]	1.019736[d]				
0.01001	1.03010	1.02724	1.02393	1.02026	104.62	104.85	105.11	105.41
0.01980	1.03034	1.02748	1.02417	1.02050	104.60	104.82	105.09	105.38
0.03988	1.03082	1.02796	1.02465	1.02098	104.55	104.77	105.04	105.33
0.06007	1.03131	1.02845	1.02514	1.02147	104.50	104.72	104.99	105.28
0.08034	1.03180	1.02894	1.02563	1.02196	104.45	104.67	104.94	105.23
0.09930	1.03225	1.02939	1.02608	1.02241	104.40	104.63	104.89	105.19
0.12018	1.03276	1.02990	1.02659	1.02292	104.35	104.58	104.84	105.13
L-Leucine + aqueous 1.0 mol·kg^{-1} ADP								
0.00000	1.05723	1.05419	1.05069	1.04679				
	1.057212[b]	1.054111[b]	1.050638[b]	1.046759[b]				
	1.056922[c]	1.053869[c]	1.050302[c]	1.046388[c]				
	1.057615[d]	1.054224[d]	1.050982[d]	1.046479[d]				
0.00996	1.05747	1.05443	1.05093	1.04703	102.48	102.72	102.99	103.29
0.01961	1.05770	1.05466	1.05116	1.04726	102.46	102.70	102.96	103.27
0.04004	1.05820	1.05516	1.05166	1.04776	102.41	102.65	102.92	103.22
0.05971	1.05867	1.05563	1.05213	1.04823	102.37	102.60	102.87	103.17
0.07973	1.05915	1.05611	1.05261	1.04871	102.32	102.55	102.82	103.12
0.09977	1.05963	1.05659	1.05309	1.04919	102.28	102.51	102.78	103.08

(*continued on next page*)

Table 2 (*continued*)

[a]m_A/(mol·kg^{-1})	$\rho \times 10^{-3}$/(kg·m^{-3})				$V_\phi \times 10^6$/(m^3·mol^{-1})			
	T = 288.15 K	T = 298.15 K	T = 308.15 K	T = 318.15 K	T = 288.15 K	T = 298.15 K	T = 308.15 K	T = 318.15 K
0.12012	1.06013	1.05709	1.05359	1.04969	102.23	102.46	102.73	103.03
			L-Leucine + aqueous 1.5 mol·kg^{-1} ADP					
0.00000	1.08244	1.07936	1.07568	1.07170				
	1.082488[b]	1.079387[b]	1.075632[b]	1.071692[b]				
	1.082198[c]	1.079145[c]	1.075296[c]	1.071321[c]				
	1.082555[d]	1.079601[d]	1.075845[d]	1.071755[d]				
0.01000	1.08268	1.07960	1.07592	1.07194	100.59	100.82	101.09	101.39
0.01980	1.08292	1.07984	1.07616	1.07218	100.57	100.79	101.07	101.37
0.03977	1.08340	1.08032	1.07664	1.07266	100.52	100.75	101.02	101.32
0.06012	1.08389	1.08081	1.07713	1.07315	100.48	100.70	100.98	101.27
0.08019	1.08437	1.08129	1.07761	1.07363	100.43	100.66	100.93	101.23
0.10023	1.08486	1.08178	1.07810	1.07412	100.39	100.61	100.89	101.18
0.12057	1.08535	1.08227	1.07859	1.07461	100.34	100.57	100.84	101.14
			L-Leucine + aqueous 2.0 mol·kg^{-1} ADP					
0.00000	1.10570	1.10243	1.09867	1.09468				
	1.105650[b]	1.102498[b]	1.098679[b]	1.094705[b]				
	1.105360[c]	1.102256[c]	1.098343[c]	1.094334[c]				
0.01003	1.10594	1.10267	1.09891	1.09492	98.90	99.13	99.40	99.69
0.01485	1.10606	1.10279	1.09903	1.09504	98.89	99.12	99.39	99.68
0.01889	1.10616	1.10289	1.09913	1.09514	98.88	99.11	99.38	99.67
0.02501	1.10630	1.10303	1.09927	1.09528	98.86	99.10	99.37	99.66
0.02852	1.10639	1.10312	1.09936	1.09537	98.86	99.09	99.36	99.65
0.04012	1.10667	1.10340	1.09964	1.09565	98.83	99.07	99.34	99.63
0.05941	1.10713	1.10386	1.10010	1.09611	98.79	99.02	99.29	99.58

[a] m_A is the molality of amino acids in aqueous ADP solutions. [b, c, d] values of densities from reference [35–37]. Standard relative uncertainties in molality are u_r (m) = 2%, Standard uncertainties u (T) = 0.001 K, u (ρ) = 1 kg·m^{-3}, $u(V_\phi)$ = ±(0.03–0.05) × 10^6/(m^3·mol^{-1}) and u (p) = 0.01 MPa (0.68 level of confidence).

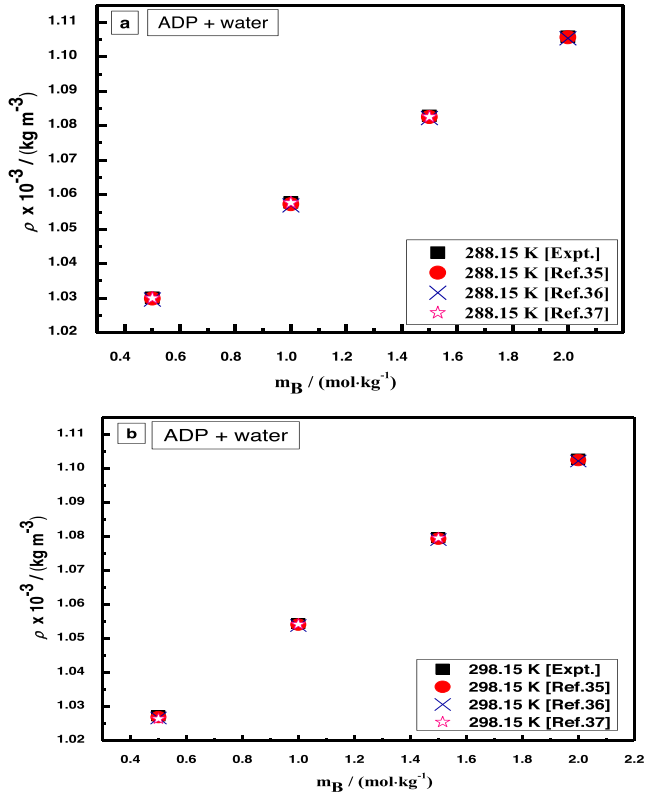

Fig. 5. Plots of comparison of density values of ADP experimental and literature [35–37] (a) 288.15 K (b) 298.15 K. Reference 35 and 37 are our previous publications.

overlap model play a significant role to explain these interactions. Depending upon the co-sphere overlap model regarding the values of ΔV_ϕ^0, there is negligible contribution from solute – solute interactions and hence they provide information regarding solute – solvent interactions. The various interactions that occur between amino acids and ADP molecules can be categorized as: (i) ion-hydrophilic interactions (between zwitterionic centres of amino acids and polar groups of ADP) (ii) hydrophilic-hydrophilic interactions (between polar groups of amino acids and polar groups of ADP) (iii) ion-hydrophobic interactions (between zwitterionic centres of amino acids and non-polar groups of ADP) and (iv) hydrophobic-hydrophobic interactions (between non-polar groups of amino acids and non-polar groups of ADP). According to co-sphere overlap model, ion-hydrophobic interactions and hydrophobic-hydrophobic interactions contribute negatively whereas ion-hydrophilic and hydrophilic-hydrophilic interactions contribute positively to the ΔV_ϕ^0values. Therefore, in our present study of (amino acid + water + ADP), it is deduced that ion–hydrophilic and hydrophilic– hydrophilic interactions are dominating over the last two interactions. Positive values of the transfer parameters indicate that ion–hydrophilic and hydrophilic – hydrophilic interactions are dominating in case of L-serine. In case of L-leucine negative values of the transfer volume employ that the domination of the hydrophobic-hydrophilic and hydrophobic-hydrophobic interactions. Because the addition of co-solute to the aqueous solution of ADP destroys the cage structure of the solvent and solute. Hence the positive data for the partial molar volume of transfer reflect that ion-ion or solute – solute interactions are dominating in the (L-serine + ADP + water) system and have the structure-making nature. Whereas the negative contribution of the transfer volume for the (L-leucine + ADP + water) system indicates the hydrophobic-hydrophilic and hydrophobic-hydrophobic interactions and structure breaker nature.

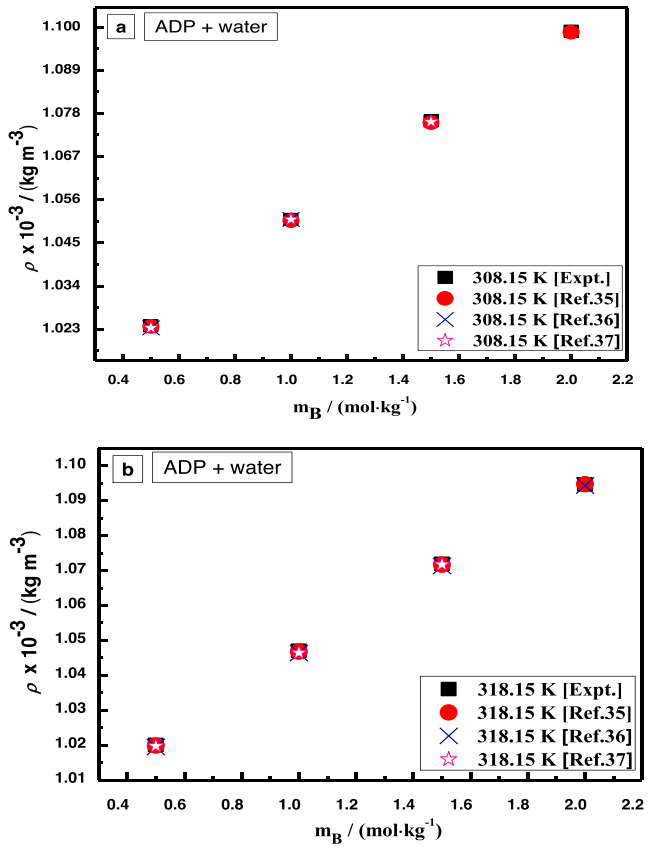

Fig. 6. Plots of comparison of density values of ADP experimental and literature [35–37] (a) 308.15 K (b) 318.15 K. Reference 35 and 37 are our previous publications.

3.1.4. Temperature dependent partial molar volume at infinite dilution

Temperature dependent partial molar volume at infinite dilution was evaluated for the present system of (amino acids + ADP + water). Study of the variation of the V_ϕ^0 with temperature made use of equation (4) as noted below

$$V_\phi^0 = a + b(T - -T_{ref}) + c(T - -T_{ref})^2 \quad (4)$$

where T is temperature in Kelvin, T_{ref} = 298.15 K, and a, b and c are empirical constants. Temperature dependence of partial molar property provides information on (solute + solvent) interactions *i.e.* (ion + solvent) or (zwitterions + solvent) interactions present in solutions, as, (solute + solute) interactions like (ion + ion) or (zwitterion + zwitterion) interactions at infinite dilution are negligible. The obtained values of the empirical constants have been reported in Table S1 of supporting information. The obtained values of the empirical constants are positive except two values of parameter c for L-leucine. The empirical constants are utilized to calculate the theoretical V_ϕ^0 values, and the obtained deviations from experimental V_ϕ^0 and theoretical V_ϕ^0 values have been reported in Table S1 of supporting information along with the empirical constants. Deviations were obtained by utilizing the values of experimental V_ϕ^0 and theoretical V_ϕ^0 by using the Eq. (5) given as follows:

$$\sigma = (1/n)\Sigma[abs((Y_{exptl.} - Y_{calc.})/Y_{exptl.})] \quad (5)$$

where $Y = V_\phi^0$ apparent molar volume at infinite dilution or partial molar volume. From Table 5 it is noticed that small values have been obtained for the deviations which indicate that the equation fits well in the present system of amino acids in aqueous ADP solution.

The temperature dependence of partial molar volume at infinite dilution (V_ϕ^0) is expressed in terms of the absolute temperature (T). Also, the partial molar expansibilities at infinite dilution have been evaluated. The partial molar expansibilities at infinite dilution E_ϕ^o have been calculated by differentiating equation (4)

$$\phi_E^0 = (\partial/\partial T)_p = B + 2C(T - -T_{ref}) \quad (6)$$

$$(\partial\phi_E^0/\partial T)_p = (\partial^2 V_\phi^o/\partial T^2)_p = 2C \quad (7)$$

The calculated values of E_ϕ^o for both the amino acids in aqueous ADP solutions at different temperature are given in Table S2 of supporting information. The values of E_ϕ^o are positive at all temperatures and concentration of ADP. From positive values of E_ϕ^o signify the presence of interactions between amino acid zwitterions and solvated ions of phosphate salt in these mixtures. The E_ϕ^o values rise with the rise in the temperature. With the rise in the concentration of ADP, values are not following any regular trend. The values of the partial molar isobaric expansivity E_ϕ^o are an important indicator of solute – solvent interactions. These values are also employed in interpreting of the structure making or breaking properties of various solutes. Positive expansivity (*i.e.* increasing volume with increasing temperature) is a characteristic property of non-aqueous solutions of hydrophobic solvation [50]. The packing effect [51,52] point towards the positive E_ϕ^o values indicating the interactions between amino acids and ADP molecules.

Table 3
Partial molar volumes, V_ϕ^o and experimental slopes, S_V^* of amino acids in aqueous solutions of ADP at different temperatures.

[a]m_B/(mol·kg^{-1})	$V_\phi^o \times 10^6$/(m^3·mol^{-1})				$S_V^* \times 10^6$/(m^3·kg·mol^{-2})			
	T = 288.15 K	T = 298.15 K	T = 308.15 K	T = 318.15 K	T = 288.15 K	T = 298.15 K	T = 308.15 K	T = 318.15 K
				L-Serine				
0.5	66.68(±0.03)	66.77(±0.03)	66.87(±0.03)	66.98(±0.03)	−2.36(±0.007)	−2.37(±0.007)	−2.38(±0.007)	−2.39(±0.007)
1.0	69.87(±0.02)	69.99(±0.02)	70.12(±0.02)	70.27(±0.02)	−2.13(±0.005)	−2.14(±0.005)	−2.15(±0.005)	−2.16(±0.005)
1.5	63.79(±0.03)	63.88(±0.03)	63.98(±0.03)	64.10(±0.03)	−2.23(±0.006)	−2.24(±0.006)	−2.25(±0.006)	−2.27(±0.006)
2.0	63.55(±0.03)	63.64(±0.03)	63.75(±0.03)	63.87(±0.03)	−2.15(±0.006)	−2.16(±0.006)	−2.17(±0.006)	−2.18(±0.006)
				L-Leucine				
0.5	104.64(±0.0006)	104.87(±0.0006)	105.14(±0.0006)	105.43(±0.0006)	−2.44(±0.0008)	−2.45(±0.0008)	−2.47(±0.0008)	−2.48(±0.0008)
1.0	102.51(±0.0005)	102.74(±0.0005)	103.01(±0.0005)	103.31(±0.0005)	−2.33(±0.0007)	−2.34(±0.0007)	−2.36(±0.0007)	−2.37(±0.0007)
1.5	100.61(±0.0005)	100.84(±0.0005)	101.11(±0.0005)	101.41(±0.0005)	−2.23(±0.0007)	−2.25(±0.0007)	−2.26(±0.0007)	−2.27(±0.0007)
2.0	98.92(±0.0001)	99.15(±0.0001)	99.42(±0.0001)	99.71(±0.0001)	−2.15(±0.0003)	−2.16(±0.0003)	−2.18(±0.0003)	−2.19(±0.0003)

[a] m_B is the molality of aqueous ADP solutions. Standard relative uncertainties in molality are $u_r(m)$ = 2%, Standard uncertainties $u(T)$ = 0.001 K. $u(V_\phi)$ = ±(0.03–0.05) × 10^6/(m^3·mol^{-1}) (0.68 level of confidence).

Table 4
Partial molar volume of transfer, ΔV_{ϕ}^{0} of amino acids in aqueous solutions of ADP at different temperatures.

[a]m_B/(mol·kg^{-1})	$\Delta V_{\phi}^{0} \times 10^{6}$ (m^3·mol^{-1})			
	T = 288.15 K	T = 298.15 K	T = 308.15 K	T = 318.15 K
		L-Serine		
0.5	8.68	7.95	7.01	6.11
1.0	11.87	11.17	10.26	9.40
1.5	5.79	5.06	4.12	3.23
2.0	5.55	4.82	3.89	3.00
		L-Leucine		
0.5	−2.08	−2.69	−3.46	−4.70
1.0	−4.21	−4.82	−5.59	−6.82
1.5	−6.11	−6.72	−7.49	−8.72
2.0	−7.80	−8.41	−9.18	−10.42

[a] m_B is the molality of aqueous solutions of ADP. Standard relative uncertainties in molality are $u_r(m)$ = 2%, Standard uncertainties $u(T)$ = 0.001 K, $u(V_{\phi})$ = ±(0.03–0.05) × 10^6/(m^3·mol^{-1}) (0.68 level of confidence).

3.2. Speed of sound

The experimentally measured speed of sound, u of L-Serine and L-Leucine in (0.5, 1.0, 1.5, 2.0) mol·kg^{-1}aqueous solutions of ADP at temperatures (288.15, 298.15, 308.15, 318.15) K are listed in Table 5. It is observed that speeds of sound of amino acids in aqueous solutions of ADP increases with increase in temperature and concentration of ADP and with increase in concentration of amino acids. The experimental values of speed of sound for amino acids in aqueous solutions of ADP solution are compared graphically with speed of sound values of aqueous amino acids solutions [28,31,33] as shown in Figs. 7–10. From these figures it is observed that speeds of sound values follow the regular trend and are in good agreement with literature values [28,31,33]. The experimental values of speeds of sound for aqueous solutions of ADP at different temperatures have also been compared with literature values [35,37,53] and are graphically represented in Figs. 11 and 12. It is hereby noted that references [35,37] are our previous publications. From the comparison it is observed that values are in good agreement with literature values except for values reported in reference [53] where the values shows some deviations from the experimental values.

3.2.1. Apparent molar isentropic compression

The apparent molar isentropic compression for amino acids in aqueous and mixed aqueous solutions of ADP at different temperatures was determined by using equation (8):

$$K_{\phi,s} = [(M\kappa_S/\rho) - \{(\kappa_S\rho_0 - \kappa_{S,0}\rho)/(m_A\rho\rho_0)\}] \quad (8)$$

where M is molar mass of solute (kg•mol^{-1}), m_A is molality (mol•kg^{-1}) of amino acids *i.e.* amount of solute (amino acids) per one kilogram of solvent (mixture of water + ADP) and ρ and ρ_0 are densities (kg•m^{-3}) of solution and solvent respectively, $\kappa_{S,0}$ and κ_S are isentropic compressibility of pure solvent and solution respectively. The isentropic compressibility is calculated by utilizing equation (9):

$$\kappa_S = 1/(u^2\rho) \quad (9)$$

Here u is speed of sound and ρ is density of solution.

The calculated values of $K_{\phi,s}$as well as speeds of sound values for molar concentrations (m_A) of amino acids (0.5, 1.0, 1.5, 2.0) mol·kg^{-1} ADP at different temperatures have been outlined in Table 5 The $K_{\phi,s}$ values are negative at all temperatures and concentrations of ADP as marked from Table 6. The negative $K_{\phi,s}$values show that water molecules around the solute are less compressible than water molecules in the bulk because it is assumed that amino acids and ions are not pressure dependent and electrostricted water molecules are already compressed to its maximum extent by the charge on the ions and the amino acids. Therefore, the compressibility of a solution is mainly due to pressure on the bulk water molecules. The $K_{\phi,s}$values become less negative with increase in temperature. The water molecules in the bulk solution are more compressible than water molecules surrounding the ionic charged groups of amino acids as predicted by negative $K_{\phi,s}$values. This indicates the strong solute solvent interactions between ions of amino acids and salt molecules. The negative $K_{\phi,s}$values indicate greater loss of structural compressibility of water involving a greater ordering effect by solute on solvent [54,55]. More negative values of $K_{\phi,S}$ at lower temperatures imply that the water molecule around amino acid molecules are less compressible than the water molecules in the bulk solution [56,57] due to the hydrophobic interactions of a non-polar group resulting in the tightening of the water molecules around it. This further supports the conclusion that there are strong solute – solvent interactions and weak solute – solute interactions in these mixtures. The hydrophilic-hydrophilic group interactions between the groups of amino acids and ADP dominate in these mixtures.

3.2.2. Partial molar isentropic compression

The variation of apparent molar isentropic compression $K_{\phi,s}$with molar concentration of amino acids can be represented by using Eq. (10).

$$K_{\phi,s} = K_{\phi,s}^{0} + S_K^{*}m_A \quad (10)$$

where $K_{\phi,s}^{0}$ is the partial molar isentropic compression and S^{*}_K is the experimental slope indicates solute - solute interactions, m_A is molality of amino acids in aqueous ADP solutions. The values of $K_{\phi,s}^{0}$and S^{*}_K values are described along with standard errors determined using by least squares fit in Table 6. The small S^{*}_K values predict that solute – solute interactions are negligible in comparison to solute solvent interactions [50].

The values of $K_{\phi,s}^{0}$ are found to become less negative with increase in temperature as well as increase in concentration of ADP. The values of $K_{\phi,s}^{0}$ for amino acids in aqueous ADP solutions are less negative than their corresponding values in pure water. The negative values of $K_{\phi,s}^{0}$ suggest that water molecules around amino acids are less compressible than that the water molecules in the bulk solution [56,58] and less negative values of $K_{\phi,s}^{0}$ at higher temperatures indicates the lesser electrostriction of water molecules around amino acids. The $K_{\phi,s}^{0}$ values can be expressed as the extent to which hydration around the solute molecule can be compressed. The negative values of $K_{\phi,s}^{0}$ (loss of compressibility

Table 5
Values of ultrasonic speed, u, and apparent molar isentropic compression, $K_{\phi,s}$ of amino acids in aqueous solutions of ADP at different temperatures and experimental pressure, p = 0.1 MPa.

[a]m_A/(mol·kg^{-1})	u/(m·s^{-1})				$K_{\phi,s} \times 10^6$/(m^3·mol^{-1}·GPa^{-1})			
	T = 288.15 K	T = 298.15 K	T = 308.15 K	T = 318.15 K	T = 288.15 K	T = 298.15 K	T = 308.15 K	T = 318.15 K
				L-Serine + aqueous 0.5 mol·kg^{-1}ADP				
0.00000	1507.4	1535.1	1556.0	1571.1				
	1507.20[b]	1534.68[b]	1555.74[b]	1570.81[b]				
	1507.3[d]	1534.9 [d]	1555.9 [d]	1570.9 [d]				
0.10024	1513.3	1540.7	1561.2	1576.0	−43.76	−42.20	−41.07	−40.28
0.20083	1519.2	1546.3	1566.4	1580.9	−44.13	−42.55	−41.41	−40.62
0.29877	1524.9	1551.8	1571.5	1585.7	−44.36	−42.77	−41.63	−40.83
0.40147	1531.0	1557.5	1576.8	1590.7	−44.56	−42.96	−41.82	−41.02
0.49696	1536.6	1562.8	1581.8	1595.3	−44.73	−43.13	−41.98	−41.18
0.59791	1542.5	1568.5	1587.0	1600.3	−44.91	−43.30	−42.15	−41.34
0.70029	1548.5	1574.2	1592.3	1605.3	−45.08	−43.47	−42.31	−41.51
				L-Serine + aqueous1.0 mol·kg^{-1}ADP				
0.00000	1544.5	1569.6	1588.8	1602.4				
	1544.35[b]	1569.47[b]	1588.63[b]	1602.26[b]				
	1544.3[d]	1569.7 [d]	1588.9 [d]	1602.6 [d]				
0.09981	1549.7	1574.8	1594.0	1607.0	−41.68	−40.35	−39.38	−38.72
0.19972	1554.9	1580.0	1599.2	1611.6	−42.00	−40.66	−39.69	−39.02
0.30100	1560.5	1585.2	1604.3	1615.5	−42.19	−40.85	−39.87	−39.20
0.39698	1565.2	1590.3	1609.4	1620.6	−42.35	−41.01	−40.02	−39.35
0.50020	1570.5	1595.6	1614.8	1625.4	−42.50	−41.16	−40.17	−39.49
0.60235	1575.8	1600.9	1620.1	1630.1	−42.65	−41.30	−40.31	−39.63
0.70168	1581.0	1606.1	1625.3	1634.6	−42.79	−41.43	−40.44	−39.76
				L-Serine + aqueous 1.5 mol·kg^{-1}ADP				
0.00000	1579.6	1602.7	1619.7	1632.0				
	1579.46[b]	1602.24[b]	1619.54[b]	1631.66[b]				
	1579.0[d]	1602.4 [d]	1619.9 [d]	1631.1 [d]				
0.10012	1585.6	1608.3	1624.8	1636.9	−39.89	−38.74	−37.93	−37.36
0.19998	1591.7	1613.8	1629.8	1641.7	−40.20	−39.05	−38.23	−37.66
0.30470	1598.0	1619.7	1635.1	1646.8	−40.41	−39.25	−38.44	−37.86
0.40108	1603.8	1625.0	1640.0	1651.5	−40.58	−39.41	−38.59	−38.02
0.49786	1609.7	1630.4	1644.9	1656.2	−40.74	−39.57	−38.74	−38.16
0.59962	1615.8	1636.0	1650.0	1661.1	−40.89	−39.72	−38.90	−38.31
0.69758	1621.8	1641.5	1654.9	1665.9	−41.04	−39.87	−39.04	−38.45
				L-Serine + aqueous 2.0 mol·kg^{-1}ADP				
0.00000	1613.5	1634.1	1649.6	1660.5				
	1613.60[b]	1634.12[b]	1649.64[b]	1660.38[b]				
0.10001	1618.6	1639.0	1654.2	1664.9	−38.24	−37.28	−36.58	−36.10
0.19933	1623.6	1644.1	1658.7	1669.2	−38.53	−37.57	−36.86	−36.37
0.30181	1628.8	1649.3	1663.4	1673.7	−38.72	−37.75	−37.04	−36.56
0.40105	1633.8	1654.3	1667.9	1678.0	−38.87	−37.91	−37.19	−36.71
0.50100	1638.9	1659.4	1672.5	1682.4	−39.02	−38.05	−37.34	−36.85
0.60163	1644.0	1664.5	1677.1	1686.8	−39.17	−38.20	−37.48	−36.99
0.70424	1649.2	1669.7	1681.8	1691.3	−39.31	−38.34	−37.62	−37.13
				L-Leucine + aqueous 0.5 mol·kg^{-1}ADP				
0.00000	1507.4	1535.1	1556.0	1571.1				
	1507.20[b]	1534.68[b]	1555.74[b]	1570.81[b]				
	1507.3[d]	1534.9 [d]	1555.9 [d]	1570.9 [d]				
0.01001	1508.5	1536.2	1557.0	1572.0	−39.88	−38.43	−37.38	−36.64
0.01980	1509.7	1537.2	1557.9	1572.8	−41.94	−40.43	−39.34	−38.57
0.03988	1512.0	1539.3	1559.8	1574.5	−43.02	−41.47	−40.36	−39.58
0.06007	1514.3	1541.5	1561.8	1576.3	−43.39	−41.83	−40.71	−39.93
0.08034	1516.7	1543.6	1563.7	1578.0	−43.59	−42.02	−40.90	−40.11
0.09930	1518.9	1545.6	1565.5	1579.6	−43.70	−42.14	−41.01	−40.22
0.12018	1521.3	1547.8	1567.5	1581.4	−43.80	−42.23	−41.10	−40.31
				L-Leucine + aqueous 1.0 mol·kg^{-1}ADP				
0.00000	1544.5	1569.6	1588.8	1602.4				
	1544.35[b]	1569.47[b]	1588.63[b]	1602.26[b]				
	1544.3[d]	1569.7 [d]	1588.9 [d]	1602.6 [d]				
0.00996	1545.8	1570.8	1589.9	1603.3	−38.18	−36.94	−36.03	−35.40
0.01961	1547.0	1571.9	1590.9	1604.2	−40.04	−38.76	−37.82	−37.17
0.04004	1549.5	1574.3	1593.0	1606.2	−41.05	−39.74	−38.78	−38.12
0.05971	1552.0	1576.5	1595.1	1608.1	−41.39	−40.07	−39.10	−38.45
0.07973	1554.4	1578.8	1597.2	1610.0	−41.57	−40.25	−39.28	−38.62
0.09977	1556.9	1581.1	1599.3	1611.9	−41.70	−40.37	−39.40	−38.74
0.12012	1559.5	1583.5	1601.4	1613.8	−41.79	−40.46	−39.49	−38.83
				L-Leucine + aqueous 1.5 mol·kg^{-1}ADP				
0.00000	1579.6	1602.7	1619.7	1632.0				
	1579.46[b]	1602.24[b]	1619.54[b]	1631.66[b]				

(*continued on next page*)

Table 5 (*continued*)

[a]m_A/(mol·kg^{-1})	u/(m·s^{-1})				$K_{\phi,s} \times 10^6$/(m^3·mol^{-1}·GPa^{-1})			
	T = 288.15 K	T = 298.15 K	T = 308.15 K	T = 318.15 K	T = 288.15 K	T = 298.15 K	T = 308.15 K	T = 318.15 K
	1579.0[d]	1602.4 [d]	1619.9 [d]	1631.1 [d]				
0.01000	1581.1	1604.0	1621.0	1633.1	−36.68	−35.60	−34.84	−34.29
0.01980	1582.5	1605.2	1622.2	1634.1	−38.38	−37.27	−36.48	−35.92
0.03977	1585.5	1607.7	1624.7	1636.2	−39.26	−38.13	−37.33	−36.76
0.06012	1588.6	1610.3	1627.3	1638.4	−39.57	−38.43	−37.63	−37.06
0.08019	1591.6	1612.8	1629.8	1640.5	−39.73	−38.59	−37.78	−37.21
0.10023	1594.7	1615.3	1632.3	1642.6	−39.84	−38.69	−37.88	−37.31
0.12057	1597.7	1617.9	1634.9	1644.8	−39.91	−38.76	−37.95	−37.38
			L-Leucine + aqueous 2.0 mol·kg^{-1}ADP					
0.00000	1613.5	1634.1	1649.6	1660.5				
	1613.60[b]	1634.12[b]	1649.64[b]	1660.38[b]				
0.01003	1614.5	1635.0	1650.6	1661.6	−35.29	−34.40	−33.73	−33.26
0.01485	1615.1	1635.5	1651.2	1662.1	−36.31	−35.40	−34.72	−34.25
0.01889	1615.5	1636.0	1651.6	1662.5	−36.77	−35.84	−35.16	−34.69
0.02501	1616.1	1636.6	1652.2	1663.1	−37.18	−36.25	−35.56	−35.08
0.02852	1616.5	1637.0	1652.6	1663.5	−37.34	−36.40	−35.71	−35.23
0.04012	1617.7	1638.2	1653.8	1664.7	−37.67	−36.73	−36.03	−35.55
0.05941	1619.8	1640.2	1655.9	1666.8	−37.94	−36.99	−36.29	−35.81

[a] m_A is the molality of amino acids in aqueous ADP solutions; [b, d] Values of ultrasonic speed taken from reference [35,37]. Standard relative uncertainties in molality are u_r (m) = 2%, Standard uncertainties u (T) = 0.001 K, u (u) = 1.6 m·s^{-1}, $u(K\phi,s)$ = ±0.60 × 10^6/(m^3·mol^{-1}·GPa^{-1}) and u (p) = 0.01 MPa (0.68 level of confidence).

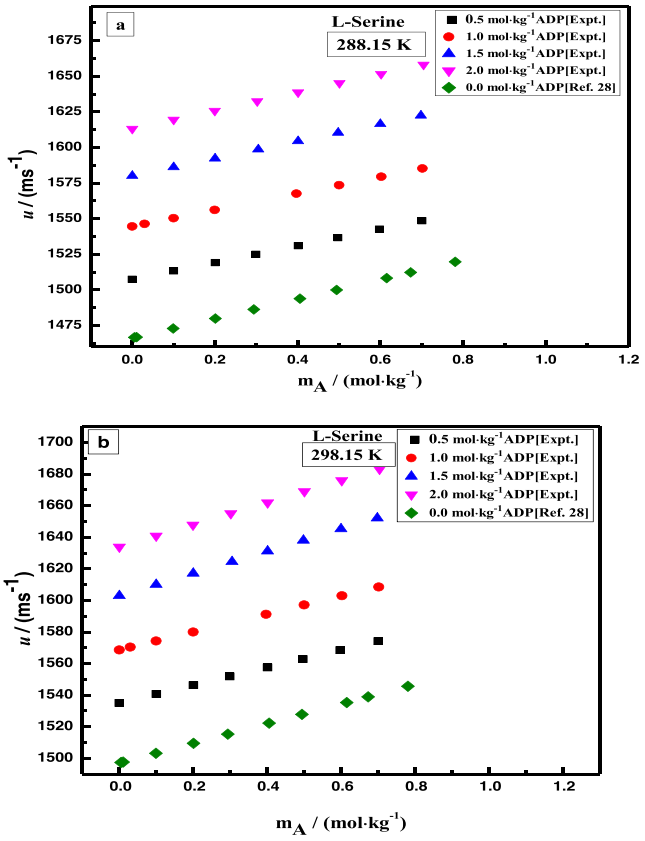

Fig. 7. Plots of comparison of speed of sound values of L-serine in aqueous [28] and experimental speed of sound values for L-serine in aqueous solution of ADP at different concentrations (a) 288.15 K (b) 298.15 K.

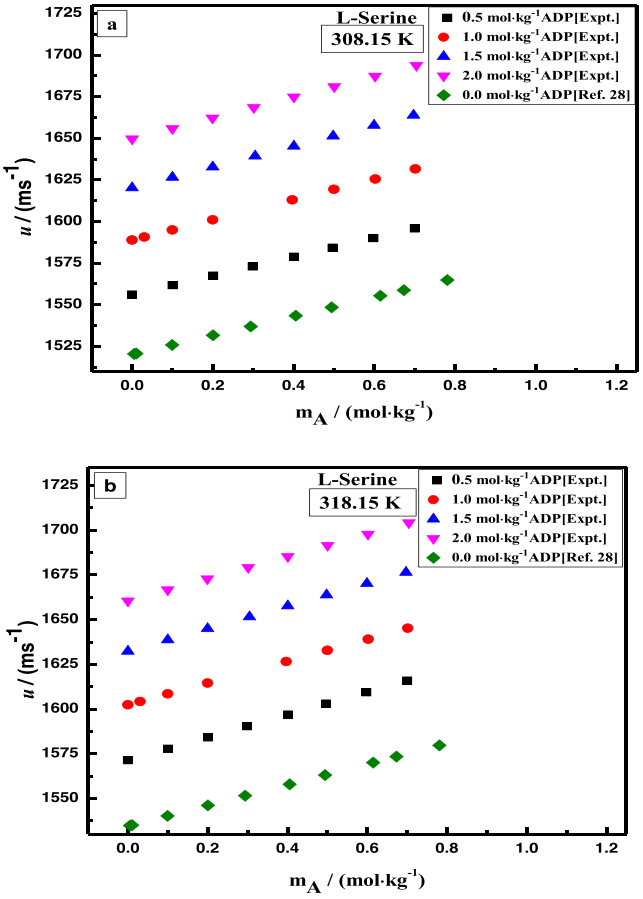

Fig. 8. Plots of comparison of speed of sound values of L-serine in aqueous [28] and experimental speed of sound values for L-serine in aqueous solution of ADP at different concentrations (a) 308.15 K (b) 318.15 K.

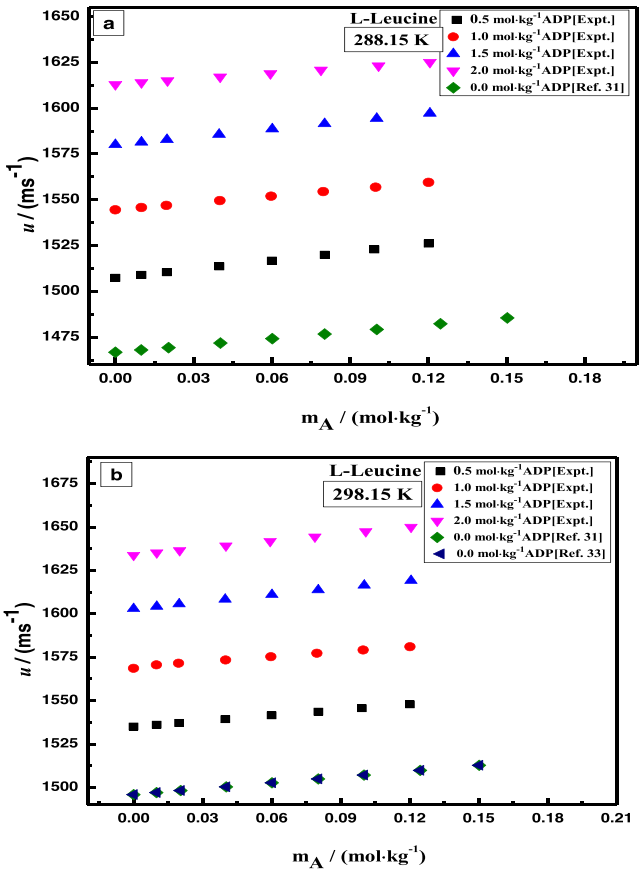

Fig. 9. Plots of comparison of speed of sound values of L-leucine in aqueous [31,33] and experimental speed of sound values for L-leucine in aqueous solution of ADP at different concentrations (a) 288.15 K (b) 298.15 K.

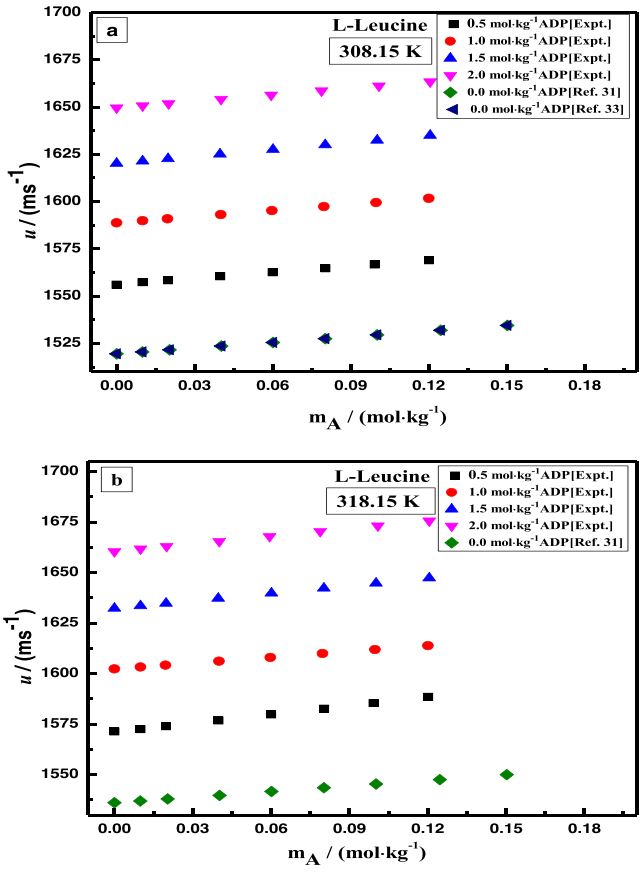

Fig. 10. Plots of comparison of speed of sound values of L-leucine in aqueous [31,33] and experimental speed of sound values for L-leucine in aqueous solution of ADP at different concentrations (a) 308.15 K (b) 318.15 K.

of medium) indicate that the water molecules surrounding the amino acid molecules present greater resistance to compression than water molecules present in the bulk. The negative $K^0_{\phi,S}$ values of amino acids in aqueous ADP solution re-indicate the dominance of hydrophilic-hydrophilic interactions in the solutions. These interactions lead to the formation of compact primary solvation shell of amino acids. The increase of $K^0_{\phi,S}$ values with increase in temperature indicates the release of more water molecules from the secondary solvation layer of amino acids into the bulk, which in turn make the solutions more compressible [59,60]. In the presence of ADP, stronger attraction of ions of ADP and water molecules induce dehydration of saccharide molecules. Therefore, at higher concentration of ADP, water molecules around saccharides are much more compressible than at lower concentration which may be responsible for lesser negative and even positive values of $K^0_{\phi,S}$ at higher concentration and temperature. Moreover, the experimental slope S^*_K which indicates solute – solute interactions is influenced by number of effects [61]. This behaviour shows the existence of solute – solute interactions in these systems.

3.2.3. Partial molar isentropic compression of transfer

Partial molar compressions of transfer at infinite dilution have been evaluated for the present system of amino acids and salt in aqueous media by using the given Eq. (11).

$$\Delta K^o_{\phi,S} = K^0_{\phi,S}(\text{in aqueous ADP solution}) - K^0_{\phi,S}\ (\text{in water}) \qquad (11)$$

Using the above relation we have evaluated the partial molar isentropic compressions of transfer $\Delta K^o_{\phi,S}$ of amino acid from water to aqueous ADP solutions at infinite dilution. We have taken the values of $K^0_{\phi,S}$ for amino acids in water from earlier work [28,49]. The values of $\Delta K^o_{\phi,S}$ at all concentrations of ADP as reported in Table 7 and all the values are positive for each amino acid except one value of L-serine. The $\Delta K^o_{\phi,S}$ values increase with increase in concentration of ADP as well as with the rise in the temperature. The positive values obtained for the partial molar compressions of transfer at infinite dilution reveal predominance of interactions between the zwitterionic centre of amino acid and ADP which are responsible for the structure-making tendency of the ions [27,62]. From the obtained values it is concluded that with increase in concentration of ADP and temperature the structure making tendency of ions increases leading to interaction between zwitterionic centre of amino acids and ADP.

3.3. Pair and triplet interaction coefficients

The pair and triplet interaction coefficients permit the separation of effects due to interaction between the pairs of solute molecules and due to its interaction between more than two solute molecules on the basis of the McMillan – Mayer theory [63]. The solute – co-solute interactions can be included in solvation spheres as discussed by Friedmann and Krishnan [64].

Partial molar volume of transfer and partial molar isentropic compression of transfer can be expressed by

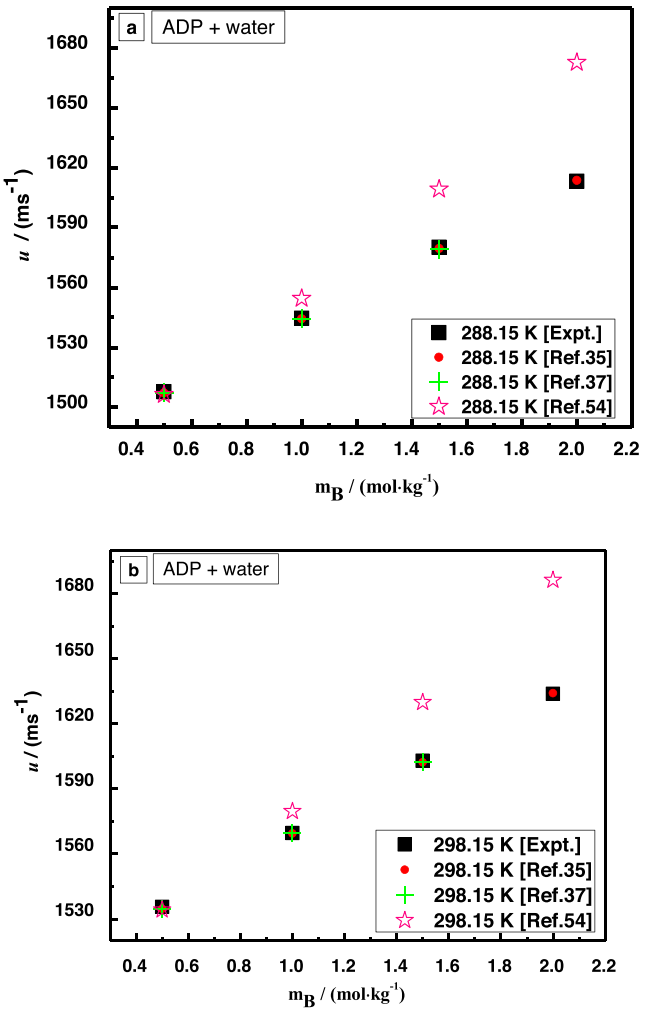

Fig. 11. Plots of comparison of speed of sound values of ADP experimental and literature [35,37,53] (a) 288.15 K (b) 298.15 K.

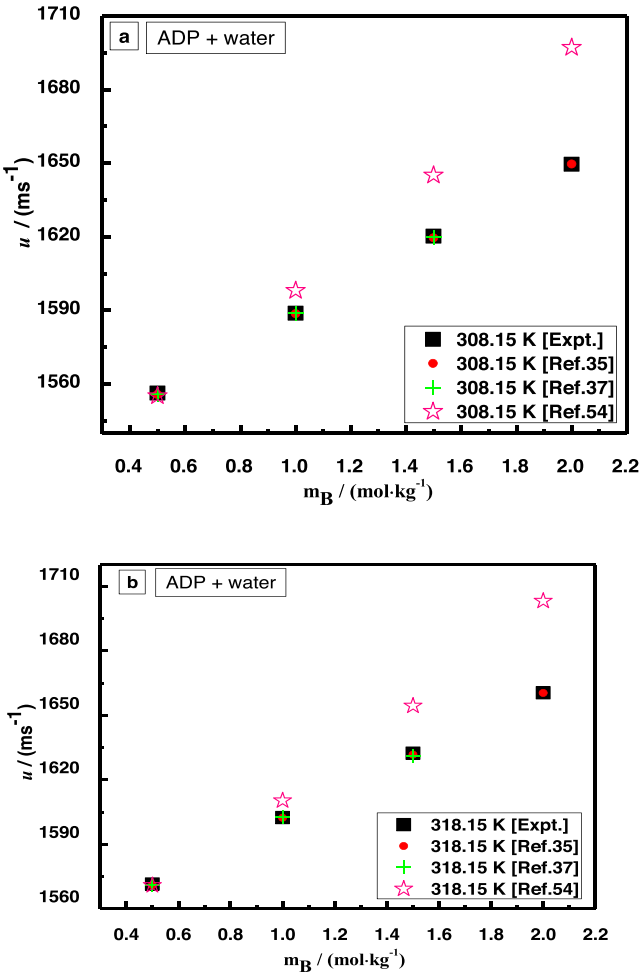

Fig. 12. Plots of comparison of speed of sound values of ADP experimental and literature [35,37,53] (a) 308.15 K (b) 318.15 K.

$$\Delta V_{\phi}^{0}(\text{water to aqueous ADP solution}) = 2\,V_{AB}m_B + 3\,V_{ABB}m_B^2 \quad (12)$$

$$\ldots\Delta K_{\phi,s}^{o}\ldots(\text{Water to aqueous ADP solution}) = 2\,K_{AB}m_B + 3K_{ABB}m_B^2 \quad (13)$$

where A denotes amino acid, B denotes ADP and m_B is the molality of aqueous ADP solutions. The corresponding parameters V_{AB}, V_{ABB} and K_{AB}, K_{ABB} for isentropic compression denote pair and triplet interaction coefficients. These constants were calculated by using the ΔV_{ϕ}^{0} and $\Delta K_{\phi,s}^{o}$ values to the above equations and are reported in Table S3 of supporting information. The positive values have been observed for pair interaction coefficients V_{AB}, K_{AB} whereas triplet interaction coefficients V_{ABB} and K_{ABB} are negative at all temperatures. The higher positive values of pair interaction coefficients V_{AB} as compared to negative values of V_{ABB} for amino acids conclude the overlap of hydration spheres of solute – co-solute molecules which may lead to interactions. The positive values of V_{AB} and K_{AB} suggest that interactions occur due to the overlap of hydration spheres of amino acids and ions of phosphate salt, which again supports the molecular interpretation drawn from the co-sphere overlap model. According to this model, when non-bonding favourable interactions occur, water molecules are released to the bulk from the hydration co-sphere because of their overlap. Because of the different structural organization of water in these two domains, the volume change would be negative when water is released from a co-sphere to the bulk that is more structured than bulk and positive when the bulk is more structured. When groups of amino acids interact in pair wise manner, the overlap of hydration co-sphere results in a positive volume change, as some electrostricted water molecules return to the bulk solvent that is more structured.

Table 6
Partial molar isentropic compression, $K^{o}_{\phi,s}$ and experimental slopes, S^{*}_{K} for amino acids in aqueous solutions of ADP at different temperatures.

[a]m_B/(mol·kg^{-1})	$K^{o}_{\phi,s} \times 10^6$/(m^3·mol^{-1}·GPa^{-1})				$S^{*}_{K} \times 10^6$/(kg· m^3·mol^{-2}·GPa^{-1})			
	T = 288.15 K	T = 298.15 K	T = 308.15 K	T = 318.15 K	T = 288.15 K	T = 298.15 K	T = 308.15 K	T = 318.15 K
				L-Serine				
0.5	−43.66 (±0.059)	−42.10 (±0.058)	−40.97 (±0.057)	−40.19 (±0.056)	−2.10(±0.133)	−2.03(±0.130)	−1.99(±0.127)	−1.96(±0.125)
1.0	−41.60 (±0.054)	−40.28 (±0.053)	−39.31 (±0.052)	−38.65 (±0.051)	−1.76(±0.120)	−1.71(±0.117)	−1.68(±0.115)	−1.65(±0.114)
1.5	−39.79 (±0.049)	−38.65 (±0.048)	−37.84 (±0.047)	−37.27 (±0.047)	−1.86(±0.110)	−1.81(±0.108)	−1.78(±0.106)	−1.76(±0.105)
2.0	−38.15 (±0.045)	−37.20 (±0.044)	−36.49 (±0.044)	−36.01 (±0.043)	−1.71(±0.101)	−1.68(±0.099)	−1.65(±0.098)	−1.64(±0.097)
				L-Leucine				
0.5	−41.01(±0.63)	−39.53(±0.61)	−38.45(±0.60)	−37.70(±0.59)	−28.31(±8.730)	−27.44(±8.464)	−26.88(±8.292)	−26.55(±8.192)
1.0	−39.20(±0.57)	−37.94(±0.56)	−37.01(±0.55)	−36.37(±0.54)	−26.42(±7.943)	−25.73(±7.735)	−25.28(±7.600)	−25.10(±7.528)
1.5	−37.61(±0.52)	−36.52(±0.51)	−35.74(±0.50)	−35.19(±0.49)	−24.94(±7.184)	−24.35(±7.017)	−24.00(±6.918)	−23.81(±6.865)
2.0	−35.63(±0.39)	−34.74(±0.38)	−34.06(±0.38)	−33.60(±0.37)	−45.91 (±12.036)	−45.04 (±11.806)	−44.49 (±11.663)	−44.22 (±11.594)

[a] m_B is the molality of aqueous solutions of ADP. Standard relative uncertainties in molality are u_r (m) = 2%, Standard uncertainties u (T) = 0.001 K, $u(V_\phi)$ = ±(0.03–0.05) × 10^6/(m^3·mol^{-1}) and $u(K\phi,s)$ = ±0.60 × 10^6/(m^3·mol^{-1}·GPa^{-1}) $u(K^{o}_{\phi,s})$ = ±0.75 × 10^6/(m^3·mol^{-1}·GPa^{-1}) u(S^{*}_{K}) = ±0.85 × 10^6/(m3·mol^{-2}·GPa^{-1}). (0.68 level of confidence).

Table 7
Partial molar isentropic compression of transfer $\Delta K^{o}_{\phi,s}$ of amino acids in aqueous solutions of ADP at different temperatures.

[a]m_B/(mol·kg^{-1})	$\Delta K^{o}_{\phi,s} \times 10^6$ (m^3·mol^{-1}.GPa^{-1})			
	T = 288.15 K	T = 298.15 K	T = 308.15 K	T = 318.15 K
		L-Serine		
0.5	−1.22	0.34	1.47	2.25
1.0	0.84	2.16	3.13	3.79
1.5	2.65	3.79	4.60	5.17
2.0	4.29	5.24	5.95	6.43
		L-Leucine		
0.5	2.44	3.92	5.00	5.75
1.0	4.25	5.51	6.44	7.08
1.5	5.84	6.93	7.71	8.26
2.0	7.82	8.71	9.39	9.85

[a] m_B is the molality of aqueous solutions of ADP. Standard relative uncertainties in molality are u_r (m) = 2%, Standard uncertainties u (T) = 0.001 K, $u(V_\phi)$ = ±(0.03–0.05) × 10^6/(m^3·mol^{-1}) and $u(K\phi,s)$ = ±0.60 × 10^6/(m^3·mol^{-1}·GPa^{-1}) $u(K^{o}_{\phi,s})$ = ±0.75 × 10^6/(m^3·mol^{-1}·GPa^{-1}) (0.68 level of confidence.

4. Conclusion

The density and speed of sound measurements provide information regarding the interactions that may occur in mixtures. The apparent molar volume, partial molar volume at infinite dilution and transfer volumes show positive values. The apparent molar properties and partial molar properties anticipate that there exists strong solute – solvent interactions between amino acids and ADP molecules. The magnitude of solute – solvent interaction increases with increase in concentration of ADP solution and with increase in the molar mass of amino acids. The partial molar expansibilities at infinite dilution give information regarding the size of solute and its hydrophobicity. The values of partial molar properties V^{0}_{ϕ} increase with increase in concentration of ADP. $K^{0}_{\phi,S}$Values become less negative with increase in temperature. Negative $K^{0}_{\phi,S}$values conclude that hydrophilic interactions are dominant in the mixtures.

CRediT authorship contribution statement

Harsh Kumar: Conceptualization, Resources, Supervision, Writing - review & editing. **Vaneet Kumar:** Supervision, Resources. **Seema Sharma:** Investigation, Writing - original draft. **Arjuna Katal:** Writing - review & editing. **Asma A. Alothman:** Resources, Writing - review & editing.

Declaration of Competing Interest

The authors declare that they have no known competing financial interests or personal relationships that could have appeared to influence the work reported in this paper.

Acknowledgements

Authors are thankful to The Director and Head, Department of Chemistry, Dr B R Ambedkar National Institute of Technology, Jalandhar for providing necessary facilities. Authors are also thankful to IKG Punjab Technical University, Kapurthala Road, Jalandhar, Punjab. Asma A Alothman also acknowledges the financial support from the Researchers Supporting Project Number (RSP-2020/243) King Saud University, Riyadh, Saudi Arabia.

Appendix A. Supplementary data

Supplementary data to this article can be found online at https://doi.org/10.1016/j.jct.2020.106350.

References

[1] I.J. Castellanos, R. Crespo, K. Griebenow, J. Control. Release 88 (2003) 135–145.
[2] P.H. Von Hippel, T. Schleich, in: S.N. Timasheff, G.D. Fasman (Eds.), Marcel Dekker, New York, 1969, pp. 417–574..
[3] J.A. Siddique, S. Naqvi, J. Chem. Eng. Data 55 (2010) 2930–2934.
[4] T. Owaga, K. Mizutani, M. Yasuda, Bull. Chem. Soc. Jpn. 57 (1984) 2064–2068.
[5] R.K. Wadi, R.K. Goyal, J. Sol. Chem. 21 (1992) 163–170.
[6] R.K. Wadi, R.K. Goyal, J. Chem. Eng. Data 37 (1992) 377–386.
[7] R.K. Wadi, P. Ramasami, J. Chem. Soc., Faraday Trans. 93 (1997) 243–247.
[8] M. Naushad, Z.A. Alothman, M.R. Awual, M.M. Alam, G.E. Eldesoky, Ionics 21 (2015) 2237–2245.
[9] M. Natarajan, R.K. Wadi, H.C. Gaur, J. Chem. Eng. Data 35 (1990) 87–93.
[10] T.S. Banipal, G. Sehgal, Thermochim. Acta 262 (1995) 175–183.
[11] D.P. Kharakoz, J. Phys. Chem. 95 (1991) 5634–5642.
[12] T.V. Chalikian, A.P. Sarvazyan, K.J. Breslauer, J. Phys. Chem. 97 (1993) 13017–13025.
[13] M.S. Santosh, D. Krishna Bhat, A.S. Bhatt, J. Chem. Eng. Data 55 (2010) 4048–4053.
[14] A. Ali, A. Hyder, S. Sabir, D. Chand, A.K. Nain, J. Chem. Thermodyn. 38 (2006) 136–143.
[15] I. Gheorghe, C. Stoicescu, F. Sirbu, J. Mol. Liq. 218 (2016) 515–524.
[16] T.S. Banipal, J. Kaur, P.K. Banipal, J. Chem. Eng. Data 53 (2008) 1803–1816.
[17] C. Zhao, P. Ma, J. Li, J. Chem. Thermodyn. 37 (2005) 37–42.
[18] K. Zhuo, Q. Liu, Y. Yang, Q. Ren, J. Wang, J. Chem. Eng. Data 51 (2006) 919–927.
[19] S. Thirumaran, P. Inbam, Ind. J. Pure. Appl. Phys. 49 (2011) 451–459.
[20] M.A. Riyazuddeen, Usmani, Thermochim. Acta 527 (2012) 112–117.
[21] C.L. Liu, C.G. Ren, J. Chem. Eng. Data 54 (2009) 3296–3299.
[22] M. Naushad, Chem. Eng. J. 235 (2014) 100–108.
[23] M.A. Riyazuddeen, D. Usmani, J. Chem. Eng. Data 56 (2011) 3504–3509.
[24] C.L. Liu, L. Zhou, R.S. Lin, J. Solution. Chem. 39 (2010) 1253–1263.
[25] C.L. Liu, L. Zhou, L. Ma, R.S. Lin, J. Solut. Chem. 42 (2013) 1527–1579.
[26] L. Xu, C.R. Ding, R.S. Lin, J. Solut. Chem. 35 (2006) 191–200.
[27] H. Kumar, I. Behal, J. Mol. Liq. 219 (2016) 756–764.
[28] H. Kumar, M. Singla, R. Jindal, J. Mol. Liq. 208 (2015) 170–182.
[29] T.S. Banipal, D. Kaur, P.K. Banipal, G. Singh, J. Chem. Thermodyn. 39 (2007) 371–384.
[30] M.M. Duke, A.W. Hakin, R.M. Mckay, K.E. Preuss, Can. J. Chem. 72 (1994) 1489.
[31] H. Kumar, I. Behal, J. Chem. Eng. Data 61 (2016) 3740–3751.
[32] A. Pal, N. Chauhan, J. Chem. Thermodyn. 43 (2011) 140–146.
[33] S. Chauhan, K. Kumar, J. Chem. Eng. Data 59 (2014) 1375–1384.
[34] T.S. Banipal, D. Kaur, P.K. Banipal, J. Chem. Eng. Data 49 (2004) 1236–1246.
[35] H. Kumar, I. Behal, J. Chem. Eng. Data 62 (2017) 3138–3150.
[36] P.K. Banipal, N. Aggarwal, T.S. Banipal, J. Mol. Liq. 211 (2015) 78–89.
[37] H. Kumar, I. Behal, S. Siraswar, J. Chem. Eng. Data 64 (2019) 3772–3780.
[38] C. Xie, T. Zhang, X. Wang, B. Zhong, S. Tang, Fluid Phase Equilib. 474 (2018) 131–140.
[39] Z. Yang, J. Li, J. Luo, P. Wang, K. Zhou, Fluid Phase Equilib. 335 (2012) 60–63.
[40] T. He, J. Sun, W. Shen, Y. Ren, J. Chem. Thermodynamics 112 (2017) 31–42.
[41] C. Klofutar, J. Horvat, D. Rudan-Tasič, Acta Chim. Slov. 53 (2006) 274–283.
[42] F.J. Millero, Chem. ReV. 71 (1971) 147–176.
[43] Y. Marcus, G. Hefter, Chem. ReV. 104 (2004) 3405–3452.
[44] M.A. Cheema, S. Barbosa, P. Taboada, E. Castro, M. Siddiq, V.A. Mosquera, Chem. Phys. 328 (2006) 243–250.
[45] D.R. Torres, L.H. Blanco, F. Martinez, E.F. Vargas, J. Chem. Eng. Data 52 (2007) 1700–1703.
[46] R.W. Gurney, McGraw-Hill, New York, 1954..
[47] J.E. Desnoyers, M. Arel, G. Perron, C. Jolicoeur, J. Phys. Chem. 73 (1969) 3346–3351.
[48] G.R. Hedwig, J. Sol. Chem. 17 (1988) 383–397.
[49] M. Singla, H. Kumar, R. Jindal, J. Chem. Thermodyn. 76 (2014) 100–115.
[50] F.J. Millero, R.A. Horne (Eds.), Wiley-Interscience, New York, 1972, pp. 519–595..
[51] P.R. Misra, B. Das, M.L. Parmar, D.S. Banyal, Indian J. Chem. 44A (2005) 1582–1588.
[52] A.W. Hakin, M.M. Duke, L.L. Groft, J.L. Marty, M.L.K. Rushfeldt, Can. J. Chem. 73 (1995) 725–734.
[53] N. Aggarwal, M. Sharma, T.S. Banipal, P.K. Banipal, J. Chem. Eng. Data 64 (2019) 517–528.
[54] A.W. Hakin, M.M. Duke, J.L. Marty, K.E. Preuss, J. Chem. Soc., Faraday Trans. 90 (1994) 2027–2035.
[55] C.M. Romero, F. Negrete, Phys. Chem. Liq. 42 (2004) 261–267.
[56] H. Rodriguez, A. Soto, A. Acre, M.K. Khoshkbarchi, J. Sol. Chem. 32 (2003) 53–63.
[57] A. Soto, A. Acre, M.K. Khoshkbarchi, J. Sol. Chem. 33 (2004) 11–21.
[58] A. Pal, N. Chauhan, Thermochim. Acta 513 (2011) 68–74.
[59] A.K. Mishra, J.C. Ahluwalia, J. Phys. Chem. 88 (1984) 86–92.
[60] R. Bhat, N. Kishore, J.C. Ahluwalia, J. Chem. Soc. Faraday Trans. I (88) (1988) 2651–2665.
[61] J. Yan, J. Wang, H. Zhang, D. Liu, J. Sol. Chem. 27 (1988) 473–483.
[62] H. Kumar, A. Katal, P.K. Sharma, J. Chem. Eng. Data 65 (2020) 1473–1487.
[63] W.G. Mcmillan, J.E. Mayer, J. Chem. Phys. 13 (1945) 276–305.
[64] H.L. Friedman, C.V. Krishnan, J. Solution Chem. 2 (1973) 37–51.

JCT_2020_299